Dissertation

submitted to the

Combined Faculties for the Natural Sciences and for Mathematics

of the Ruperto-Carola Unviversity of Heidelberg, Germany

for the degree of
Doctor of Natural Sciences

presented by

Diplom-Physiker: Simon Gregor Schäfer
born in: Offenbach, Germany
Oral examination: 01.12.2004

Quintessence Cosmology

Quintessenz Kosmologie

Zusammenfassung

In dieser Arbeit diskutieren wir kosmologische Modelle in denen ein skalares Quintessenz Feld die dunkle Energie im Universum beschreibt. Nach einer kurzen Einführung in die bekannte Kosmologie erweitern wir unsere Analyse und diskutieren Störungsrechnung in der Allgemeinen Relativitätstheorie. Wir leiten 'Isocurvature' Anfangsbedingungen für die primordialen Fluktuationen her. Im Falle von 'tracking quintessence' gibt es keine zusätzliche Isocurvature Mode durch das Quintessenz Feld. Weiterhin diskutieren wir den Einfluss von 'früher Quintessenz' auf das CMB Spektrum und vergleichen dies mit den Daten des WMAP Satelliten. Schliesslich untersuchen wir die Folgen einer Veränderung der fundamentalen Konstanten auf die Vorhersagen der Urknall Nukleosynthese, wobei das Quintessenz Feld für die Zeitabhängigkeit der Koppelungskonstanten verantwortlich ist.

Quintessence Cosmology

Abstract

In this thesis we will analyze cosmological models containing a scalar field instead of a cosmological constant to account for the dark energy component of the universe. First, we will give a brief introduction to the background cosmology. We will then extend our analysis to perturbation theory in General Relativity. We determine possible isocurvature initial conditions for primordial perturbations. In tracking quintessence scenarios, no additional isocurvature mode is introduced by a quintessence field. After that, we discuss the influence of early quintessence energy density on the CMB spectrum and compare this to the first year WMAP data. Finally, we investigate the possible influence of a variation of the fundamental constants on the predictions of Big Bang Nucleosynthesis calculations. Quintessence comes into play as the driving field for the time evolution of the fundamental constants.

Contents

Chapter 1

Introduction

How to start the introduction of a subject like cosmology, which covers so many different fields of physics? Let's do it by imagining something very simple: It is a moonless night, we are sitting in the open and the sky is filled with millions of stars. Who could resist asking the simplest and most obvious questions? Where does all of this come from? What is the nature of the universe, the reason behind it, what are the laws that describe this beauty?

Cosmology tries to answer this question and describe the universe as we observe it today in a scientific language. In theoretical physics it sometimes happens that the beauty of nature is hidden within the equations but don't forget – it is nevertheless there.

We will demand the freedom of assigning the birthdate of modern cosmology to the formulation of the theory of general relativity by Einstein [1–3] at the beginning of the 20th century. Of course people have looked into and pondered about the nature of our universe for thousands of years. The observational means by which this happened did improve quite a lot with time but it was the geometrical description of gravitational interactions that formed our present understanding of the universe.

At the beginning of the 20th century people thought of the universe to be static. This is also apparent in the fact that Einstein wrote down his equations including a constant term allowing for such a static universe to be a solution of the equations. The first one to actually observe the contrary, namely that the universe was expanding, was Edwin Hubble in the 1920's. He found that all galaxies are drifting away from us with a velocity that is proportional to their distance. It is hard not to overestimate the importance of this observation, for that it paved the way for physicists to think of the universe to be evolving and dynamic in nature. From that moment on the static universe was history and scientists were asking questions as to how the universe came into being and what its fate will be. These question are part of the general quest in cosmology, that is to find a suitable description of our universe that will answer (most)

of our questions about the universe we live in.

The next milestone in the development of modern cosmology clearly was the (accidental) detection of the Cosmic Microwave Background (CMB) by Arno Penzias and Robert Wilson [4] in 1965, which had been predicted by George Gamow some years earlier. It seemed as if we had glimpsed at the very light of creation, the afterglow of the Big Bang! Suddenly we had a window into the very early universe and could test our hypothesis about the evolution of the universe against observations.

It was not much later that physicists realized that this remarkable observation cannot be explained by "simple" Big Bang cosmology because we cannot explain the observed isotropy of the CMB. This was the first of several discrepancies between theory and observation that would lead to a more sophisticated model of cosmology.

1.1 The Standard Cosmological Model

It is only in the past decade that physicists started started to think of a standard cosmological model. In the preceding years scientists tried to solve separate problems and the idea that it could be combined together to provide a consistent picture of our universe seemed far away. The cosmological "standard model" is not to compare with the standard model of particle physics. It rather is a collection of different mechanisms and processes that scientists believe must have been involved in the evolution of our universe. This model explains many of our observations but also leaves open questions.

Owing to the fact that we see the universe is expanding today, the standard model in cosmology assumes that at the beginning of the universe there must have been something comparable to the Big Bang, an initial singularity from which spacetime suddenly came into being and expanded since. This might have happened only once or the universe entails some kind of cyclic mechanism of Big Bang, expansion and then recollapsing into a singularity again.

After this act of creation the universe is governed by Planck-scale physics about which we now nothing at all. It would require the knowledge of a Theory of Everything (ToE) which we don't know. We are nevertheless sure that shortly after that epoch the process of inflation [5–7], driven by one or more inflaton fields, must have taken place. During this very brief moment the universe expands by at least 55-65 e-folds so that the particle horizon from the time of inflation is larger than our observable universe today. Hence the observable universe has been in causal contact and that is the reason why the Cosmic Microwave Background (CMB) we observe today is so extremely homogeneous and isotropic – it was a patch of the early universe that was in thermal equilibrium before inflation. As a side effect the curvature of spacetime, if there was one, is driven beyond our horizon and the universe appears to be flat.

Following this inflationary phase the inflaton field decays and produces particles and entropy. Further expansion now cools down the universe. As our universe contains mostly particles and no antiparticles something must have disturbed this equilibrium. We therefore need CP and baryon number violating processes in the standard model of particle physics so that the universe contains mostly particles after the electroweak phase transition. There are several different possible mechanism proposed to explain this phase transition but to rule out all but one of those scenarios is beyond our present knowledge. The same statement holds for the process of inflation.

The universe is still expanding and cooling down to a temperature where the first nuclei are not immediately torn apart, i.e. a temperature in the range of nuclear binding energies. This Big Bang Nucleosynthesis (BBN) is quite well understood, owing to the fact that one can do nuclear physics experiments in the laboratory and measure nuclear reaction cross-sections. This nucleosynthesis leads to the production of mainly deuterium, helium, lithium-7 and beryllium. The predicted abundances of helium, deuterium and lithium fit the measured abundances fairly well while the remaining uncertainties leave space for speculation. The higher elements like carbon, oxygen, nitrogen etc. are only synthesized in very small amounts and are mostly produced later in the interior of stars – and yes, it is true, we are all made up of stardust. The universe is still to hot for the nuclei to bind electrons and form atoms, therefore the mean free path of the photons is very short because of all the unbound electrons and the universe is opaque to photons.

Eventually the temperature drops below $\sim 0.4\text{eV}$ and the atoms recombine. The photons can now travel freely without being scattered. This is the "emission" of the Cosmic Microwave Background (CMB) radiation, containing much information about the universe at that time. As this radiation travels through space it gets more and more redshifted due to universal expansion but is still bearing the imprint of the fluctuations in the baryon photon plasma when it was emitted. In addition the radiation picks up traces of physical effects that change the pattern of fluctuations until it finally reaches us today and helps to improve our understanding of the early universe.

Following the last scattering of the CMB photons, nothing happens for a while, the universe is pretty dark until the first stars are formed. Driven by gravitational collapse the baryonic matter forms the first generation of stars which are so massive that they are very hot and have a very short lifetime. Their existence leads to a reionization of the universe which in turn leads to scattering of the CMB photons on the free electrons, an imprint which astronomers and cosmologists are able to determine in the CMB observations. Further gravitational collapse leads to the formation of galaxies and galaxy clusters out of the initial density fluctuations.

Finally the universe should (according to the theory) end up as we observe it today. Very clumpy with huge empty regions in it, lots of stars in lots of galaxies, no signs of

anti-matter and a surprisingly homogeneous and isotropic cosmic background radiation.

In the remarks above the "history" of the universe as understood by the standard cosmological model is sketched. But what are the open questions concerning the physics behind this? The ingredients came from the standard model of particle physics together with a theory of gravity. The most puzzling questions that remain to be explained in cosmology are the questions about the nature of dark matter and dark energy.

1.2 Dark Matter and Dark Energy

Many observations cannot be explained by the physics we know and therefore lead to the introduction of new concepts in physics. The first of such problems the astronomers discovered was that the rotational characteristics of galaxies were different from what they expected. If one looks edge on (or at a small angle) onto a galaxy one can see part of this galaxy rotating away and the other part rotating towards the observer. From the relative redshift one can infer the rotation velocity at different distances from the center and plot the result. If we think of the galaxy as a bunch of stars that orbit around the center we would expect (in a simplified case) the rotation velocity to drop of like $v \sim r^{-1/2}$. Instead we observe an almost constant rotation velocity extending into the halo of the galaxy – if Newtonian dynamics still hold there must be much more matter rotating than we can observe. This non-luminous matter is termed dark matter is seen in most galaxies and also in the rotation velocities of galaxies in galaxy clusters. When regarding the whole universe this dark matter is much more abundant than baryonic matter, it amounts to roughly 30 percent of the total energy and matter content of the universe ($\Omega_{dm} \approx 0.3$) whereas the baryons only contribute $\Omega_b \approx 0.05$. The question about the nature of dark matter has jet to be answered. Brown dwarfs, MACHOS and by now also neutrinos have been ruled out while particle physics still provide quite a lot of candidates including axions, axinos, other LSSP and many more. The quest continues and may be (!) solved once the LHC at CERN is fully operational.

The second big mystery in cosmology is that of dark energy. The isotropy of the CMB is the origin of a chain of arguments that lead to the postulation of this mysterious dark energy. When we look at the sky in different directions we look at CMB radiation that originated from parts of the universe that have never been in causal contact and could therefore not have established thermal equilibrium. Yet the radiation is so isotropic that it is inconceivable that this isotropy is not due to thermal equilibrium. The answer to this puzzle is provided by inflation. As mentioned above, we assume that at some very early time the universe must have undergone a period of inflationary expansion that blew up the universe so that our observable universe today originates from a patch of the universe that has been in thermal equilibrium before

inflation occurred. This mechanism also leads to the observable universe being flat (or close to it) because any curvature that it might have possessed has also been driven beyond our horizon. At a given expansion rate and a given size of the universe we can use the Friedmann equations to calculate the critical energy density that would be needed to make the universe flat. Summing up the tiny fraction of baryons and the dark energy we realize that the largest contribution towards $\Omega_{total} = 1$ must come from some homogeneously distributed dark energy with $\Omega_{de} = 0.6 - 0.7$. The simplest and most straight forward way to handle this dark energy would be to attribute it to some constant vacuum energy density, the cosmological constant Λ. [1] It fits the available data very good but it is – from a theoreticians point of view – not very satisfying.

Another model for the dark energy is the scalar quintessence field proposed by C. Wetterich [8] and Ratra and Peebles [9]. The quintessence scenario will be discussed in more detail later.

1.3 Structure of the Thesis

We will briefly introduce the basic concepts of cosmology in Chapter 2. That includes a short description of the Einstein equations and a discussion of the background cosmology. We will introduce the Friedmann equations and analyze them in some well-known cases. The basic parameters in cosmology are introduced. The problems of dark matter and dark energy are described and a summary of suggested solutions is given. Also, the idea of a quintessence field is explained and motivated and some examples of quintessence potentials are provided.

In Chapter 4 we will describe the most important observations concerning cosmology. This especially entails a description of the CMB and the various effects that can be described in the CMB spectrum. Also, recent supernovea, LSS and other observations are mentioned. Current constraints on cosmological parameters arising from those experiments are quoted.

After this introductory part (which will hold only few things the informed reader will not be familiar with) we will turn to perturbation theory in cosmology. In Chapter 5 the gauge problem is discussed and a gauge-invariant formalism is developed. The derivation follows the existing literature and is presented as a self contained chapter.

In Chapter 6 we explore perturbation theory to derive possible non-adiabatic initial conditions for the primordial perturbations. The analyzed universe contains baryons, cold dark matter, radiation, neutrinos and a quintessence field.

---

[1]As is common knowledge, Einstein wanted his equations of GR to allow for a static universe solution and therefore he already introduced a cosmological constant, though for a different reason than we do today.

After this we are going to take a closer look at the CMB spectrum. This is done in Chapter 7. The results of the first year WMAP data are interpreted in terms of a possible presence of dark energy at the level of a few percent at an earlier epoch rather than a k-dependent spectral index as proposed by the WMAP collaboration.

Finally, we will discuss the possible influence a change of the fundamental couplings has on the abundance predictions from Big Bang Nucleosynthesis. To do this a semi-analytical estimate for the primordial helium abundances is calculated. This work is found in Chapter 8.

The work presented in this thesis, especially the Chapters 6-8, was undertaken in close collaboration with Michael Doran, Christian M. Mueller and Christof Wetterich as can also be verified from the publications on the various subjects.

Chapter 2

Background Cosmology

Throughout this thesis we will work in units where $c = \hbar = 1$. For the metric we will use the convention $\eta = \mathrm{diag}(-1, +1, +1, +1)$. Latin indices denote space dimensions $i = 1..3$ whereas Greek indices run from $\mu = 0..3$. We use the subscript 'de' for dark energy in general, 'q' for quintessence and 'm' to denote matter (dark matter plus baryonic matter). A superscript ^{0} denotes quantities measured today.

2.1   Riemannian Geometry

This section is a short overview over the aspects of Riemannian geometry we need as well as an introduction to the Einstein field equations. All of it is well known to the reader and is just repeated for completeness.

For the theory of general relativity the most important question is how to handle the curved spacetime. Fortunately Einstein didn't have to come up with a theory himself but could rely on the work that was done in the 19th century by Georg Friedrich Bernhard Riemann (1826-1866). Instead of going into details we will just mention the important points. First, we will define the covariant differentiation (which assures that the derivative of a tensor of rank (n) is a tensor of rank $(n + 1)$) given as

$$\frac{DA^\mu}{dx^\nu} \equiv A^\mu_{;\nu} = \frac{\partial A^\mu}{\partial x^\nu} + \Gamma^\mu_{\lambda\,\nu} A^\lambda \tag{2.1}$$

where the Christoffel symbols are

$$\Gamma^\mu_{\lambda\,\nu} = \frac{1}{2} g^{\mu\,\kappa}(g_{\lambda\,\kappa},\nu + g_{\kappa\,\nu,\lambda} - g_{\lambda\,\nu,\kappa}). \tag{2.2}$$

According to variational principle particles moving in a curved space do so along geodesics, for which the defining equation reads

$$\frac{\mathrm{d}^2 x^\mu}{\mathrm{d}s^2} + \Gamma^\mu_{\lambda\,\kappa} \frac{\mathrm{d}x^\lambda}{\mathrm{d}s} \frac{\mathrm{d}x^\kappa}{\mathrm{d}s} = 0. \tag{2.3}$$

With the help of this equation we can now calculate the trajectory of a particle moving in a spacetime given a specific metric without telling us how to obtain this metric. The tensor describing the curvature of the manifold is the Riemann tensor $R^{\mu}{}_{\nu\kappa\lambda}$. If we contract two of the indices we obtain the Ricci tensor

$$R_{\mu\nu} = R^{\rho}{}_{\mu\rho\nu}. \tag{2.4}$$

Further contraction leads to the curvature scalar $R = g^{\mu\nu}R_{\mu\nu}$.

2.2   Einsteins Field Equation

The central idea in the theory of general relativity is that matter and energy influence the geometry of spacetime. Therefore we search for a field equation relating the energy momentum tensor to the geometry described by the Riemann tensor. The important question is what do the field equations look like? The Einstein Equation can be obtained from the action principle if one minimizes the action $S = S_{EH} + S_M$ with respect to the metric $g_{\mu\nu}$. The action contains the Einstein-Hilbert part S_{EH} describing gravity and the part from the normal matter fields S_M. They are given by

$$S_{EH} = -\frac{1}{16\pi G} \int \mathrm{d}^4 x \sqrt{-g}\,(R + 2\Lambda) \tag{2.5}$$

and

$$S_M = \int \mathrm{d}^4 x \sqrt{-g}\,\mathcal{L}_M \tag{2.6}$$

respectively. Calculating $\delta S/\delta g_{\mu\nu} = 0$ yields the Einstein Equation

$$G^{\mu}{}_{\nu} \equiv R^{\mu}{}_{\nu} - \frac{1}{2}\delta^{\mu}{}_{\nu}R = 8\pi G T^{\mu}{}_{\nu} + \delta^{\mu}{}_{\nu}\Lambda. \tag{2.7}$$

The equation contains a cosmological constant term Λ dating back to Einstein. We will discuss later why scientists nowadays reintroduced this constant term.

We could have also tried to simply write down the field equation and worry about the Lagrangian later. This may serve as a little motivation if one does not trust the action appearing so suddenly. So lets guess the vacuum field equation. For instance one could try $R^{\mu}{}_{\nu\kappa\lambda} = 0$ but it would imply that the spacetime in vacuum is always flat, i. e. no gravitational field. The better guess would be to choose $R_{\mu\nu} = 0$. This does not imply $R^{\mu}{}_{\nu\kappa\lambda} = 0$ and also delivers 10 equations for the 10 unknowns of $g_{\mu\nu}$. Extending this to the matter field equations we relate the curvature of spacetime to the energy momentum tensor $T_{\mu\nu}$. We could therefore write $R_{\mu\nu} = -8\pi G T_{\mu\nu}$. But energy and momentum are conserved and therefore $T^{\mu\nu}{}_{;\nu} = 0$, whereas $R^{\mu\nu}{}_{;\nu} \neq 0$. Instead we can try to find invariants that obey the above relation and quickly find one of the most simple ones, the Einstein tensor

$$G^{\mu}{}_{\nu} = R^{\mu}{}_{\nu} - \frac{1}{2}\delta^{\mu}{}_{\nu}R \tag{2.8}$$

with $G_{\mu\nu}{}^{;\nu} = 0$. It is very fortunate that the (man made) Einstein Hilbert action gives the same result for the field equation as we obtained by just guessing them.

2.3   FRW Metric and Friedmann Equations

We can now start looking for solutions of Eq.(2.7). This is not an easy task because the field equations are non-linear. The first solution was put forward by Schwarzschild in 1915 and it is a vacuum solution describing the metric around a spherically symmetric, static mass distribution – the well known Schwarzschild metric.

For the purpose of cosmology we invoke two assumptions in order to find a solution to Eq.(2.7), namely that the universe is homogeneous and isotropic on large scales and that it is expanding. This leads us to the Friedmann-Robertson-Walker metric

$$\mathrm{d}s^2 = c^2\mathrm{d}t^2 - a^2(t)\left[\frac{\mathrm{d}r^2}{1 - kr^2} + r^2(\mathrm{d}\theta^2 + \sin^2\theta\mathrm{d}\phi^2)\right], \qquad (2.9)$$

where the scale factor $a(t)$ plays the important role of leading to universal expansion of space and is related to the Hubble parameter via $H = \dot{a}/a$. The coordinates (t, r, θ, ϕ) are referred to as comoving coordinates, that means an observer initially at rest stays at rest and the time t is the proper time of an observer in that coordinate system. From this solution we can determine the dynamical equations of cosmology. In order to determine the left hand side of Eq. (2.7) we need to calculate the non-vanishing Christoffel symbols. Assuming the energy density of the universe is that of a perfect fluid, the energy momentum tensor reads

$$T^0{}_0 = -\rho, \;\; T^0{}_i = T^i{}_0 = 0 \;\; \text{and} \;\; T^i{}_j = p\delta^i{}_j. \qquad (2.10)$$

We therefore obtain

$$T^\mu{}_\nu = (\rho + p)u^\mu u_\nu + p\delta^\mu{}_\nu. \qquad (2.11)$$

Writing out the $0 - 0$ component of Einstein field equations yields

$$\left(\frac{\dot{a}}{a}\right)^2 + \frac{k}{a^2} = \frac{8\pi G}{3}\rho + \frac{\Lambda}{3}, \qquad (2.12)$$

and the $i - i$ component gives

$$2\frac{\ddot{a}}{a} + \left(\frac{\dot{a}}{a}\right) + \frac{k}{a^2} = -8\pi G\rho + \Lambda. \qquad (2.13)$$

These are the two Friedmann equations describing the dynamics of the background in a homogeneous, isotropic and expanding universe. In fact the energy density is comprised of the different particle species and radiation in the universe, i. e. $\rho = \sum_i \rho_i$. Usually one writes $\Omega_i = \rho_i/\rho_c$, where

$$\rho_c = 3H^2/8\pi G \qquad (2.14)$$

is the critical energy density. With the definition $\Omega_k = -k/H^2a^2$ we can rewrite Eq. (2.12) as

$$1 - \Omega_k = \sum_i \Omega_i = \Omega_{\text{total}}. \tag{2.15}$$

The Friedmann equations are usually quoted without the cosmological constant term and we will also drop it because it just corresponds to a contribution towards ρ with an equation of state $w = -1$.

The third equation follows from the conservation of energy and momentum $T_{\mu\nu}{}^{;\nu} = 0$ as

$$\dot\rho + 3(\rho + p)\frac{\dot a}{a} = 0. \tag{2.16}$$

Note that Eqns. (2.12), (2.13) and (2.16) are not independent of each other. The parameter k indicates the geometry/future expansion of the universe. Inspecting Eq. (2.12) we see that if $k < 0$ then $\dot a$ can never be zero, i. e. the expansion never stops. For $k > 0$, $\dot a$ can be zero at $k = \frac{8\pi G}{3}\rho a^2$. The limiting case $k = 0$ allows $\dot a$ to become zero as $a \to \infty$. Usually one assumes a rescaling of the coordinates so that k takes on the discrete values $k = -1, 0, +1$. These three different cases are termed open $(k = -1)$, flat $(k = 0)$ and closed $(k = +1)$ universes.

2.4 Evolution of a and ρ in a flat Universe

We can now investigate the dynamics of the universe for several so-called Friedmann models. In order to solve the equations we need to know the equation of state $w = p/\rho$ relating the energy density to the pressure. In a flat universe $(k = 0)$ we differentiate Eq. (2.12) with respect to time and combine it with Eq. (2.16). We then obtain

$$\ddot a = -\frac{4\pi G}{3}(1 + 3w)\rho a. \tag{2.17}$$

Again inserting this in Eq. (2.13) yields the relation

$$\frac{\dot\rho}{\rho} = -3(1 + w)\frac{\dot a}{a}, \tag{2.18}$$

i. e.

$$\rho \propto a^{-3(1+w)}. \tag{2.19}$$

Likewise, the behavior of a is given as

$$a \propto t^{2/3(1+w)} \tag{2.20}$$

Putting it in this form has the advantage that we can investigate the different scenarios according to the equation of state that is dominating the dynamics. For the radiation dominated universe we have $w = 1/3$ and accordingly $\rho \propto a^{-4}$, whereas for the matter

dominated universe the pressure and hence the equation of state is zero, leading to $\rho \propto a^{-3}$. The classical interpretation of this result is straight forward. The energy density of matter drops of with the cube of the length scale because space is expanding and the energy gets distributed over a bigger volume. For radiation, the redshift due to space expansion results in an additional factor $\propto a^{-1}$ depleting the energy density.

If in the other hand the cosmological constant dominates over matter and radiation we obtain the interesting result

$$a(t) = a_0 e^{\left(\frac{\Lambda}{3}\right)^{1/2} t}, \tag{2.21}$$

where $H = (8\pi G \rho_{vac}/3)^{1/2} = (\Lambda/3)^{1/2}$ and hence

$$a \sim e^{Ht}. \tag{2.22}$$

A constant vacuum energy density leads to the so-called Einstein-de Sitter phase in which the universe is exponentially expanding. It is the same mechanism that, according to the cosmological standard model, lead to inflation. Although the exact dynamics depend on the shape of the potential of the inflaton field the mechanism is similar. Shortly after the Big Bang the inflaton has a non-zero vacuum expectation value and therefore drives the universe in the de Sitter phase of exponential expansion. The late time behavior of our universe, if dominated by a cosmological constant, will also be de Sitter like.

A way of classifying accelerated expansion can be seen from Eq. (2.17). In a flat universe containing only matter ($w_m = 0$) and dark energy (w_{de}) we can find

$$-\frac{\ddot{a}}{\dot{a}} = 1 + 3 w_{\text{de}} \Omega_{\text{de}}. \tag{2.23}$$

For an accelerated expansion we require $\ddot{a}/\dot{a} > 0$ and hence we obtain

$$w_{\text{de}} \Omega_{\text{de}} < -\frac{1}{3} \tag{2.24}$$

as a condition for the universe to undergo accelerated expansion.

2.5 Cosmological Parameters and the Age of the Universe

Space is expanding and hence radiation being emitted and traveling through space gets redshifted. The redshift in wavelength is defined as

$$\frac{\lambda - \lambda_0}{\lambda} = z, \tag{2.25}$$

where λ is the observed wavelength and λ_0 is the wavelength measured in a laboratory. This relates to the scale factor a as

$$a^{-1} = 1 + z, \tag{2.26}$$

with the value of the scale factor today normalized to $a_0 = 1$. The deceleration parameter is defined as

$$q_0 = -\frac{\ddot{a}_0}{H_0^2 a_0}. \tag{2.27}$$

By integrating the Friedmann equation (2.12) and using the definition above we can find an expression for the age of the universe as

$$t_0 = H_0^{-1} \int_0^1 [1 - 2q_0 + 2q_0/x]^{-1/2} \mathrm{d}x, \tag{2.28}$$

which can be more conveniently written as

$$t_0 = H_0^{-1} \int_0^1 [1 - \Omega_m - \Omega_\Lambda + \Omega_m/x + \Omega_\Lambda x^2]^{-1/2} \mathrm{d}x. \tag{2.29}$$

In a flat universe, for a purely radiation dominated universe this would result in $t_0 = \frac{1}{2}H_0^{-1}$ while in a matter dominated universe would be given by $t_0 = \frac{2}{3}H_0^{-1}$.

The luminosity distance is defined as

$$d_L^2 = \frac{\mathcal{L}}{4\pi\mathcal{F}}, \tag{2.30}$$

where $\mathcal{L}$ is the absolute luminosity of an object and $\mathcal{F}$ is the measured flux. A more familiar form would be

$$d_L(z) = (1 + z) \int_0^z \frac{\mathrm{d}z'}{H(z')}. \tag{2.31}$$

In a matter dominated universe this can be written as

$$H_0 d_L = q_0^{-2} \left(zq_0 + (q_0 - 1) \left(\sqrt{2q_0 z + 1} - 1 \right) \right). \tag{2.32}$$

For small z we can expand Eq. (2.32) to recover Hubble's law

$$H_0 d_L = z + \frac{1}{2}(1 - q_0)z^2 + .. \quad . \tag{2.33}$$

Objects are receding faster from us observers the more distant they are. This observation lead Hubble to infer universal expansion and abandon the notion of a static universe.

Chapter 3

Dark Matter and Dark Energy

3.1 Dark Matter

That the universe contains some form of non-luminous matter was first discovered in 1933 by observing the dispersion velocities of the coma cluster [10]. This dark matter could also be detected by measuring the rotation curves of single galaxies, for which one example is shown in Figure 3.1. It was observed that the rotation curves of galaxies do not show the behavior expected from Newtonian dynamics, i.e. the rotation velocity does not drop off $v \sim r^{-1/2}$ but rather stays constant far beyond the optical radius of the galaxy. These observations confirmed that galaxies and galaxy clusters contain much more dark matter then luminous matter. So the question is: what can it be? One possible explanation to the nature of CDM is the existence of a huge abundance of massive compact halo objects (MACHO's) in the galactic halos. With the help of microlensing effects between the large magellanic cloud and us these postulated brown dwarfs or massive planets have been constraint to a number density which is by far not sufficient to explain the galactic rotation curves [12, 13]. Another serious problem with MACHO dark matter is that primordial abundance measurements and the theory of BBN predict $\Omega_b \approx 0.04$.

The alternative is to invoke particle physics to find elementary particles that can constitute the dark matter. Depending on the mass of the particle it is usually differentiated between hot dark matter (particles which are relativistic at decoupling with masses around $m_x \leq 30\text{eV}$) and cold dark matter (particles that are non-relativistic with masses above several GeV). Within this classification mixed dark matter scenarios are also possible and are investigated.

Many candidate particles have been suggested. The cold dark matter particle has to be very weakly interacting, that is why historically the neutrino (with unknown rest mass at that time) was a prominent dark matter candidate. We know that the formation of small scale structure is suppressed by hot dark matter like light neutrinos because
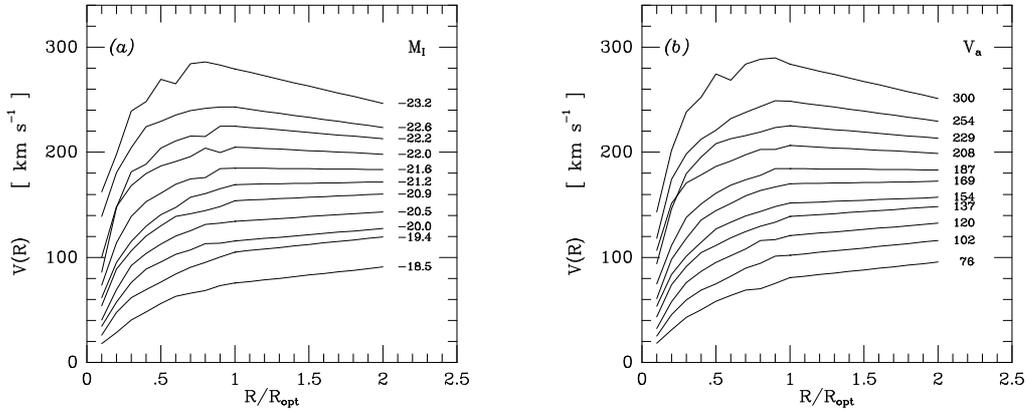
Figure 3.1: Rotation curves for a sample of spiral galaxies [11]. R_{opt} denotes the radius encompassing 83% of the total I-band luminosity and is comparable to the optical radius of the galaxy. M_I denotes the I-band absolute magnitude. One can clearly see effect of the dark matter halo which extends much farther than the luminous part of the galaxy. Figure taken from [11].

they are not pressureless, hence the hot dark matter scenario is seriously constraint by structure formation calculations. A variety of CDM particle candidates are presented in the literature. The existence of weakly interacting massive particles (WIMP's) was inferred, which merely is a description of the properties a CDM particle should have, namely sufficient weak interactions to have been able to avoid detection in modern particle detectors as well as enough mass to account for $\Omega_c \approx 0.3$.

One of the first proposed particles was the axion, which arises in the solution of the strong CP problem in particle physics [14]. Some of the more prominent possibilities arise from the supersymmetric extension of the standard model. If in supersymmetric theories R-parity is conserved the lightest supersymmetric particle (LSSP) is stable against decay and can therefore constitute the CDM. On the other hand, if it is not stable a lifetime of the Hubble time would be necessary for this particle to contribute significantly to Ω_c. As an example of the suggested CDM particles the axino, the superpartner of the axion, can fit the CDM constraints with a mass $m \approx 100\text{keV}$ and a reheating temperature of $10^6 K$ as has been shown in [15].

The DAMA collaboration has claimed [16] to have detected an annual modulation of the signal and attributed it to dark matter particles recoiling in the DAMA detector. They conclude that the neutralino mass lies in the range $30\text{GeV} \le m_x \le 130\text{GeV}$ at the 1-σ confidence level. This signal could not be detected in the recent experiments

like CDMS II [17] or EDELWEISS [18].

Direct upper limits for the WIMP mass cannot be given without the specification of a cross-section (which is model dependent). For current exclusion limits in the mass–cross-section plane see [18]. The question what the dark matter particle might be has not been answered yet.

In this work we will mostly ignore this lack of knowledge and assume that the dark matter is comprised of particles which constitute pressureless cold dark matter with an equation of state $w_{CDM} = 0$.

3.2 Dark Energy

As already mentioned in the introduction, the isotropy of the CMB poses a mayor theoretical problem which is solved by introducing the mechanism of inflation. One of the consequences of this model is that the universe is flat and hence its energy density exactly equals the critical energy density ρ_c today. Considering the amount of luminous matter that we can observe and adding the dark matter that we can deduce from observations there is still a fraction of $\Omega_{DE} \sim 0.6 - 0.7$ missing. Furthermore, observations of supernovae by the Hubble Space Telescope suggest that the universal expansion is accelerating in the recent history [19]. That is only possible if the dark energy component has a negative equation of state today and is dominating the energy density content of the universe (as was demonstrated with Eq. 2.24).

In some models the dark energy is identified with the aforementioned cosmological constant Λ. The theoretical implications of this are serious. We think of the vacuum energy as the zero point energy of some quantum theory of gravity it would be given by

$$\rho_\Lambda \propto \int_0^\infty \sqrt{k^2 + m^2}\, k^2 \mathrm{d}k. \tag{3.1}$$

This integral is ultraviolet divergent $\propto k^4$. To obtain a finite value we can regularize with a cutoff scale which in this case would be the Planck scale $\sim M_{\bar{P}}$. We therefore expect the energy density to be of order $\rho_\Lambda \sim M_{\bar{P}}^4$. This is roughly 120 orders of magnitude bigger than the measured value of ρ_Λ. It would require an absolute ridiculous amount of fine tuning in the theory to get such a small vacuum energy density. Having a lower cutoff scale like the QCD scale or some supersymmetry breaking scale would also not solve the issue but only shift it to a discrepancy of, say, 60 orders of magnitude.

Another question that is raising doubts about a cosmological constant is the so-called coincidence problem. Why does the cosmological constant become important only recently at the same epoch where structure formation takes place? It is extremely unlikely that a constant that is completely negligible in the past and will dominate the future of the universe is observed by us to be of the order of the matter contribution.

3.2.1 Possible Solutions to Dark Energy and Modifications of General Relativity

First of all we can try to explain the observed features that we described as dark energy with physical arguments within the theory of General Relativity. One of the first explanations proposed was a network of topological defects. They would exhibit a negative equation of state $w = -1/3$ [20] but are nowadays ruled out by observations because $w < -0.76$ at 95 % confidence level [19]. The same argument holds for domain walls which predict $w = -2/3$ [21] but are equally well ruled out.

The next step is to think about a modification or extension of the theory of General Relativity. Whether this modification is purely phenomenologic in nature or motivated by higher dimensional physics is of no importance as any justification would need to involve a more fundamental theory of nature. This overview over possible dark energy scenarios does not claim to be complete but covers the prominent scalar field theories and some other models.

3.2.2 Brans-Dicke Theories

Dating back to 1961, Brans and Dicke proposed a scalar field modification to GR [22]. The concept is to invoke a non-minimal coupling between a scalar field ϕ and gravity. We can write the Lagrangian for that theory as

$$\mathcal{L}_{BD} = \sqrt{-g} \left(\phi R - \frac{\omega}{\phi} \partial^\mu \phi \partial_\mu \phi - 2V(\phi) \right), \tag{3.2}$$

where ω is the Brans-Dicke parameter. The field ϕ can be regarded as the inverse of Newton's constant and hence this theory predicts a time dependence of the gravitational interaction strength.

By minimizing the action w.r.t the metric we can now find the modified Einstein equation. This altered Einstein equation leads to different Friedmann equations for a, ϕ and ω. We combine Eq. (3.2) with a FRW metric Eq. (2.9) and obtain [23]

$$H^2 + H\frac{\dot{\phi}}{\phi} - \frac{\omega}{6}\frac{\dot{\phi}^2}{\phi^2} - \frac{V}{3\phi} = \frac{\rho}{3\phi}, \tag{3.3}$$

$$2\frac{\ddot{a}}{a} + H^2 + \frac{\ddot{\phi}}{\phi} + 2H\frac{\dot{\phi}}{\phi} + \frac{\omega}{2}\frac{\dot{\phi}^2}{\phi^2} - \frac{V}{\phi} = -\frac{p}{\phi} \tag{3.4}$$

and

$$\ddot{\phi} + 3H\dot{\phi} = \frac{(\rho - 3p)}{2\omega + 3}(2V - \phi V'(\phi)). \tag{3.5}$$

Using the equations above one can now study the dynamics in Brans-Dicke theory

Eq. (3.2) is given in the Jordan frame where free falling test particles follow geodesics. For a more convenient representation in which the gravitational sector of

the action is written in the usual way we can Weyl scale the metric according to

$$g_{\mu\nu} = e^{\sigma/\sigma_*}\bar{g}_{\mu\nu}, \qquad e^{\sigma/\sigma_*} = 16\pi G\phi, \qquad \sigma_* = \sqrt{\frac{2\omega + 3}{16\pi G}}. \tag{3.6}$$

Now the the Lagrangian reads

$$\mathcal{L}_{BD} = \sqrt{-\bar{g}}\left(\frac{1}{16\pi G}\bar{R} - \frac{1}{2}\partial^\mu\sigma\partial_\mu\sigma - U(\sigma)\right), \tag{3.7}$$

where the potentials are related by

$$U(\sigma) = 2e^{-2\sigma/\sigma_*}V(\phi(\sigma)). \tag{3.8}$$

This scalar-tensor theory is the inspiration for most scalar field cosmologies as well as many other theories concerning the modification of gravity on large scales. It also bears a strong connection to coupled quintessence theories which we will mention later.

3.2.3 Quintessence

One of the promising attempts to extend standard GR to explain the fine tuning and coincidence problems is a minimally coupled scalar field φ called quintessence proposed by Wetterich [8] and Ratra and Peebles [9] in 1988. The energy density of this field is obviously time dependent and accounts for the dark energy. It was pointed out by Zlatev, Steinhard and Wang [24, 25] that a whole class of those models shows similar behavior, the so-called tracking quintessence models. The equation of state of the tracking quintessence will follow the behavior of the background equation of state while the energy density develops towards an attractor solution for a wide range of initial conditions. In those models the energy scale of the potential determines the epoch at which dark energy will dominate. If the potential starts with energies consistent with high energy physics the coincidence problem is solved because the present dark energy domination is achieved naturally. Fine tuning is also not necessary because the quintessence follows the evolution of the background while at late times the quintessence field dynamics depend on the form of the potential. The generically small value of the dark energy component today is then easily explained – it is so small because the universe is so old and only recently the quintessence field has begun to dominate the universe.

As with the other extensions of GR it is a phenomenological model because we are lacking the fundamental theory which could predict such a field. Hence we can only write down a Lagrangian and assume that this is the effective action, including all unknown quantum fluctuations. We can write down a Lagrangian for the quintessence field

$$\mathcal{L}_q = \sqrt{-g}\left(\frac{1}{2}\partial^\mu\varphi\partial_\mu\varphi + V(\varphi)\right), \tag{3.9}$$

where the potential $V(\varphi)$ distinguishes different quintessence models. The energy momentum tensor for the quintessence field can then be obtained as [8, 24, 25]

$$T^{\mu}_{\nu} = \varphi^{,\mu}\varphi_{,\nu} - \delta^{\mu}_{\nu}\left(\frac{1}{2}\varphi^{,\alpha}\varphi_{,\alpha} + V(\varphi)\right), \tag{3.10}$$

while the equation of state reads

$$w_q = \frac{\dot{\varphi}^2/2 - V(\varphi)}{\dot{\varphi}^2/2 + V(\varphi)} = \frac{T - V}{T + V}. \tag{3.11}$$

Here we can see that if the quintessence field varies slowly in time $\dot{\varphi}^2 \ll V$ its behavior is close that of a cosmological constant. The aforementioned tracking behavior can be expressed as a tracking condition

$$\frac{V'}{V} \approx \Omega_{\varphi}^{-1/2} \approx \frac{H}{\dot{\varphi}}. \tag{3.12}$$

The equation of motion for the quintessence field is given by the Klein-Gordon equation for φ

$$\ddot{\varphi} + 3H\dot{\varphi} + V'(\varphi) = 0, \tag{3.13}$$

where

$$H^2 = \frac{8\pi G}{3}\left(\rho_m + \rho_\gamma + \frac{1}{2}\dot{\varphi}^2 + V(\varphi)\right) \tag{3.14}$$

with ρ_m being the matter and ρ_γ the radiation energy density.

3.2.4 Quintessence Potentials

We will give a short account of the some popular quintessence models without the notion of completeness.

Inverse Power Law

One of the first and most simple potentials that have been proposed is the inverse power law potential (IPL) [9]

$$V(\varphi) = V_0\varphi^{-\alpha}. \tag{3.15}$$

Obviously this power law can be chosen to be as close to a cosmological constant as one wishes by adjusting the parameter α.

Exponential Potential

The exponential potential [26] is written in the form

$$V(\varphi) = V_0 \exp\left(-\frac{\alpha\varphi}{M_{\bar{P}}}\right), \tag{3.16}$$

where $M_{\bar{P}}$ is the reduced Planck mass. It the most simple form of potential but cannot make the transition from subdominant to dominant energy density component of the universe in late times. The equation of state is confined to $w_q^0 = 0$ today. Sahni and Wang proposed a model [27]

$$V(\varphi) = V_0(\cosh \lambda\varphi - 1)^p \tag{3.17}$$

This model interpolates from $V \propto e^{p\lambda\varphi}$ to $V \propto (\lambda\varphi)^{2p}$, thereby preserving some of the properties of the simpler exponential potential but allowing a different late time behavior.

SUGRA Models

Brax and Martin [28] have put forward a model that is a supergravity extension of the IPL potential

$$V(\varphi) = \frac{\Lambda^{4+\alpha}}{\varphi^\alpha} e^{\frac{\kappa}{2}\varphi^2}, \tag{3.18}$$

with $\kappa = M_P^{-2}$. The early evolution is similar to that of the unchanged ILP but at late times the exponential term allows this model to reach an equation of state w_q close to $w_q \approx -1$. As an example, for parameters $\alpha = 11$, $\Lambda \approx 10^{11} GeV$ and $\Omega_q = 0.7$ they find $w_q = -0.82$.

Also inspired by supergravity is the scalar field potential suggested by Barreiro et. al. [29, 30] which consists of two exponentials

$$V(\varphi) = M_P^4 \left(e^{\alpha\kappa(\varphi - A)} + e^{\beta\kappa(\varphi - b)} \right), \tag{3.19}$$

with A being a free parameter while B is constrained by the condition $M_P^4 e^{\beta B} \sim \rho_\varphi$. The authors emphasize that all parameters are of order Planck scale which makes this model more natural while still being able to give the observed dark energy behavior.

Albrecht and Skordis [31, 32] have analyzed a potential of the from

$$V(\varphi) = V_0[(\varphi - B)^2 + A]e^{-\lambda\varphi}. \tag{3.20}$$

The most general approach perhaps is presented by Ng et. al. [33] who studied a potential of the form

$$V(\varphi) \propto \varphi^\nu e^{\alpha\varphi^\beta}. \tag{3.21}$$

Leaping Kinetic Term

The most prominent question about the quintessence field is how can it make the transition from the tracking regime to become the dominant energy density component. For the most simple exponential potential this cannot be achieved because the equation of state for such simple models is $w_q^0 = 0$ today. We can assume more complex potentials
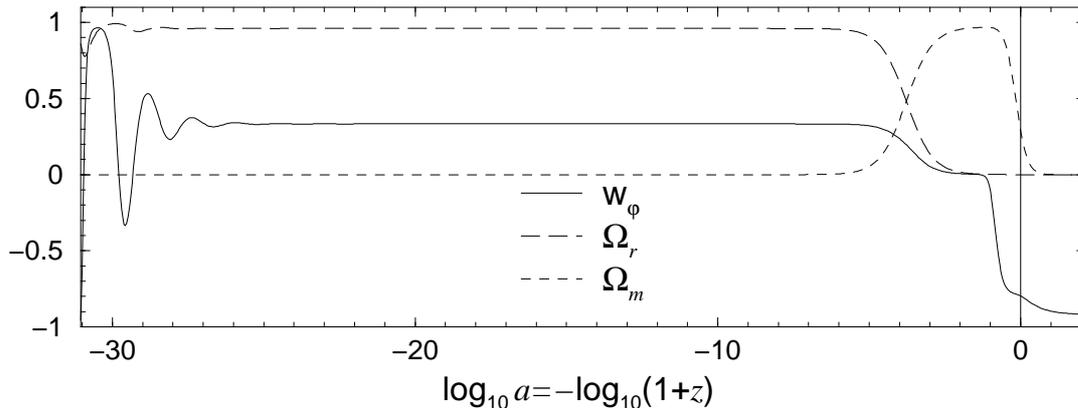
Figure 3.2: The evolution of the energy density of radiation (Ω_r) and matter (Ω_m) in a LKT quintessence model. Also shown is the equation of state of the quintessence field w_φ. Figure taken from [34].

(like some of the potentials mentioned above) in order to obtain a quintessence model which naturally predicts a negative equation of state to fit the observed w_q^0.

A more systematic way to address this issue is presented in [34]. The main aim of this approach is to present a theory of quintessence which does not contain any unnaturally small parameter to avoid the problem of fine tuning but still shows the features that are needed for a viable quintessence model. The Lagrangian for the quintessence field is written in the form

$$\mathcal{L}(\varphi) = \frac{1}{2}\partial^\mu\varphi\partial_\mu\varphi \; k^2(\varphi) - M_{\bar{P}}^4 e^{\varphi/M_{\bar{P}}}, \tag{3.22}$$

The φ-dependent kinetic term can be be put in a standard form with an appropriate change in the exponential (for details see [34]). This theory predicts early quintessence contribution towards $\Omega_{tot} = 1$ of size $\Omega_q = n_b k^2$. We therefore have an upper bound on $k(\varphi)$ during last scattering and structure formation. The contributions Ω_q^{ls} or Ω_q^{sf} are limited to the order of $\sim 10\%$ by observations. An example for $k(\varphi)$ would be

$$k(\varphi) = k_{min} + \tanh\left((\varphi - \varphi_1)/M_{\bar{P}}\right) + 1. \tag{3.23}$$

Here, k_{min} would have to be small enough not to violate the upper bound on Ω_q^{ls} and Ω_q^{sf} while the transition parameter φ_1 can be adjusted to give the right late time behavior. An example of the LKT quintessence is shown in Figure 3.2.4. Other transitions from the tracker phase to the dark energy dominated phase are possible including a smoother or more rapid change in $k(\varphi)$ [34].

The recent interest in the variation of the fundamental couplings has lead to model of quintessence where the quintessence field is identical with the scalar field which drives the time dependence of the fundamental couplings. This possibility has been

investigated in [35,36], where the quintessence model was termed crossover quintessence because of the crossover in the energy density from matter to a dark energy dominated universe and the crossover in the equation of state of quintessence from the tracking regime, where it is close to the equation of state of radiation $1/3$, to value $w_q^0 < 0$ consistent with observations. This crossover quintessence incorporates the change in α_{em} and the resulting changes in the predicted CMB spectrum in addition to being a LKT type quintessence.

3.2.5   Coupled Quintessence

In the above the quintessence field φ has no direct coupling to matter and interacts only indirect via gravity. However, there also exist models of quintessence in which the quintessence field is coupled to, for instance, dark matter and/or baryons [37]. Many of those coupled quintessence scenarios are conformally equivalent to Brans-Dicke type models with different potential terms [26]. The strength of a possible coupling is also limited by various experiments as can be seen in [26]. The generic difficulty with coupled quintessence models is that they have to guess both the coupling and the effective action (as all the actions quoted here are assumed to be the effective actions). It has been shown that the quantum corrections are of the order of the potential itself [38] and hence it is not very likely that by chance one picks the right value for the coupling given a specific effective action. It is therefore not assured that one analyzes a physically plausible potential-coupling configuration.

3.2.6   K-Essence

In most scalar field theories, model parameters have to be tuned to explain the coincidence of similar dark matter and dark energy contributions toward $\Omega_{\mathrm{tot}}^0 = 1$. To solve this problem a scalar field theory was proposed which has a non-linear kinetic term and thus exhibits new features in the dynamics. This k-essence termed scalar field [39] shows properties that are comparable to a tracking quintessence scenario. The k-essence field follows the equation of state of the background during radiation domination. The difference in tracking behavior shows itself at the epoch where the universe becomes matter dominated. Because the k-essence field is not able to mimic $w = 0$ it dynamically freezes to a small value. After a timescale typically close to the age of the universe it starts to dominate the energy density of the universe. In a dynamical relaxation process the equation of state changes from $w \approx -1$ to an asymptotic value between $0 < w < -1$ [39]. This scenario explains the coincidence problem at the cost of introducing a non-linear kinetic term in the Lagrangian. This kinetic term must be tuned to give the desired dynamics and it is therefore not obvious if this model entails

less parameter adjustment than a quintessence or Brans-Dicke model.

3.2.7 Higher Dimensions and Brane Cosmology

One can extend GR in many different ways. One possibility would be to invoke a spacetime with more than $d = 4$ dimensions. Those theories date back to Kaluza and Klein [40] who employed a 5-dimensional spacetime and were able to obtain GR as well as electromagnetism plus a scalar dilaton field by compactifying one of the space dimension. Today, brane world models with various geometries and spacetime dimensions are under investigation. Some of them do not serve to unify the different forces observed in nature but obtain descriptions of the 4-d gravitational field. In those models, the matter fields are localized on the brane (i.e. the 4 dimensional hypersurface we live in) while gravitation is a phenomenon permeating the full d dimensional bulk spacetime. The 4 dimensional metric is modified and hence the dynamics of our universe change. These brane world models and its parameters are chosen to predict the observed parameters and properties of our universe. Nevertheless, some features arise quite natural in these models. This huge and interesting field of research cannot be covered in a few introductory sentences and we therefore refer the reader to [41, 42] and references therein.

3.2.8 Even more models

Despite having described many different models to explain dark energy we have not covered the..

Chaplygin Gas

Among the many phenomenological theories to explain dark energy is an exotic fluid called Chaplygin gas with an equation of state [43]

$$p = -\frac{A}{\rho}. \tag{3.24}$$

It is motivated by higher dimensional physics and allows a supersymmetric extension. The potential to obtain such an equation of state reads [43]

$$V(\varphi) = \frac{1}{2}\sqrt{A}\left(\cosh 3\varphi + \frac{1}{\cosh 3\varphi}\right). \tag{3.25}$$

Phantom Energy

A model of dark energy with an equation of state $w < -1$ has also been proposed [44]. Such phantom energy termed models lack an explanation in the framework of GR but

are not excluded by the observations. In fact, some of the recent measurement seem to favor or at least allow an equation of state smaller than $w = -1$ [19]. The theoretical difficulties to explain an equation of state $w \leq -1$ are serious. An equation of state smaller than -1 will violate the strong energy condition, that is, the modulus of the pressure is greater than the rest energy and that seems to be a bit counter intuitive. Also, the perturbations in such a theory are not well behaved and allow tachyonic solutions. On the other hand it is to mention that before dark energy was seriously considered, a negative equation of state was also regarded not to be plausible.

Chapter 4

Current Observational Tests of Cosmology

Modern cosmology is not imaginable without the great achievements of observational astronomy. Since Hubble first observed the redshift of galaxies and Penzias and Wilson detected the CMB [4] the observational techniques improved enormously.

In this section we will give an account of the most important observations in cosmology, including their constraints on cosmological parameters.

4.1 The CMB Spectrum

Any cosmological model today is tested against a variety of different measurements and experimental data. One of the most important is the measurement of the temperature anisotropies of the CMB. The first measurement of the CMB spectrum was performed by the COBE satellite [45] with subsequent improvement with the ground based experiment MAXIMA [46] and DASI [47] and the balloon born experiment BOOMERANG [48]. The most up to date measurement of the CMB is provided by NASA's WMAP satellite [49, 50].

We will give a brief account for some of the features in the CMB spectrum that have been described qualitatively. In Chapter 7 we will make use of this when studying the effect of an early dark energy contribution on the CMB spectrum. A much more detailed discussions of the CMB, including minor effects which have been omitted here, can be found in [51, 52].

4.2   Primary Anisotropies

As the universe expands the temperature decreases while the content is in thermal equilibrium. The neutrinos drop out of the thermal equilibrium at $T \sim 1\mathrm{MeV}$ before the electron-positron annihilation takes place. Therefore, the temperature of the neutrinos is lower by a factor $T_\nu = (4/11)^{1/3}T$ because their temperature is not reheated. After Big Bang Nucleosynthesis, the temperature reaches value $T \sim 0.4\mathrm{eV}$ at which the electrons and protons recombine to form neutral hydrogen. From here on the photons can free stream, i.e. the universe is transparent. This event of last scattering or recombination is a very fast process because the density of the free electrons drops very sharply. It is therefore plausible to talk about this process as an event like moment in the universal history.

When we observe the CMB today we measure an almost perfect blackbody radiation – better than any blackbody we can measure in a laboratory. On top of this homogeneous radiation we are able to detect small deviations at the order of one part in 10^5. It is the pattern of acoustic oscillations in the photon baryon plasma before last scattering that leads to these tiny anisotropies of the CMB. Before decoupling, the differential optical depth is very large and hence the scattering between photons and electrons is very strong. The electrons in turn are coupled electrostatically to the baryons – together this forms the so-called tight coupling regime. Photons and baryons behave like a single fluid where the characteristic scale of the fluctuations is given by the sound horizon in the plasma.

The CMB plane wave that we observe is decomposed into spherical harmonics to visualize the 2-point correlation function of the anisotropies. We write the temperature anisotropy observed into direction $\mathbf{n}$ as [53]

$$\frac{\Delta T}{T}(\mathbf{n}) = \xi(\mathbf{n}). \tag{4.1}$$

This function is position and time dependent and we implicitly assume that it is valid today on earth. The decomposition into spherical harmonics given by

$$\xi(\mathbf{n}) = \sum_{\mathbf{l},\mathbf{m}} \mathbf{a_{l,m}} \mathbf{Y_l^m}(\mathbf{n}). \tag{4.2}$$

The 2-point correlation function is assumed to be independent of direction or orientation because of statistical homogeneity and isotropy, we can therefore write

$$\langle a_{l,m} a_{l',m'}^* \rangle = \delta_{ll'}\delta_{mm'}C_l. \tag{4.3}$$

We then obtain

$$\begin{aligned} \langle \xi(\mathbf{n})\xi(\mathbf{n'}) \rangle &= \sum_l C_l \sum_{m=-l}^{l} Y_l^m(\mathbf{n})(\mathbf{Y_l^m}(\mathbf{n'}))^* \\ &= \frac{1}{4\pi}\sum_l (2l+1)C_l P_l(\mu) \end{aligned} \tag{4.4}$$

where $P_l(\mu)$ are the Legendre polynomials and $\mu = \mathbf{n}.\mathbf{n}'$. We can Fourier transform this expression and obtain the C_l spectrum

$$C_l = 4\pi \int P(k)k^2 |\Delta_l(k, \tau_0)| \mathrm{d}k, \qquad (4.5)$$

where the $\Delta_l(k, \tau_0)$ are the coefficients of the Legendre series.

We can now interpret the observed 2-point correlation function in terms of physics that we expect to have taken place. Sound waves are propagating in the plasma and lead to compression and rarefaction phases. The odd peaks in the observed CMB spectrum correspond to the compression of the plasma and hence a temperature crest while the even peaks are due to rarefaction and a corresponding temperature trough.

One of the most straight forward deduction from the CMB spectrum is the curvature of the universe. By calculating the plasma sound speed we can predict the position of the first acoustic peak and conclude on the spatial geometry of the universe (inside our horizon). This is easily understood: with the first peak we observe an angular scale at the time of last scattering. This angular scale would seem to be smaller (or larger, respectively) than expected if the universe is closed (open) because of the convex (concave) bending of the light traveling towards us. Surprisingly, observations suggest that the universe is indeed flat [50].

Baryon Drag

The baryons are effectively pressureless but contribute towards the mass of the plasma. This alters the balance between gravitational infall and pressure and subsequently leads to a relative enhancement of compression peaks over rarefaction peaks. The measured difference of the first and second peak is therefore sensitive to the baryon density $\Omega_b h^2$. Because one also knows the number density of photons from the temperature of the CMB the relative height of the first acoustic peak compared to the second yields the baryon to photon ratio η, an important parameter concerning Big Bang Nucleosynthesis.

Sachs Wolfe Effect

The difference in the gravitational potential at the last scattering surface with resulting differences in photon energies, i. e. anisotropies, is called the Sachs-Wolfe effect [54]. It is one of the largest sources for anisotropies on large scales and contributes to the plateau at the low multipoles up to $l \approx 100$. It is those scales that a re larger than the horizon at decoupling. Its amplitude depends upon the primordial spectrum of density perturbations and agrees well with a scale invariant primordial spectrum.

4.3 Secondary Anisotropies

4.3.1 Gravitational Effects

The Integrated Sachs-Wolfe Effect

The time dependence of the gravitational potential along the path of the CMB photon has a large impact on the CMB. The early ISW is caused by the decay of the gravitational potential at horizon crossing if the universe was not completely matter dominated at last scattering. The effect is closer to the observer of the CMB and hence the same physical scale will arise at a larger scale than the same scale from the primary anisotropies.

The late ISW effect is due to the decay of gravitational potentials caused by the expansion of the universe. Photons which are in a potential while it decays pick up an effective redshift.

In addition, any effect that introduces a metric perturbation along the path of the photon will alter the CMB spectrum, for instance gravitational waves or topological defects.

The Sachs-Wolfe and ISW effect have the strongest influence in the low multipole region. It is important to note that the theoretical errors in this region is dominated by the cosmic variance limit. Due to the fact that we can observe only one realization of a CMB sky we have to invoke a sort of ergodic hypothesis: we assume that, for a given set of cosmological parameters, the average of a patch of our CMB sky, periodically extended to the whole sky, is equal to the average over many different realizations of the CMB sky for that set of parameters. This assumption breaks down for the large angular scales which results in large systematic error bars on those scales.

4.3.2 Scattering Effects

Sunjajev-Zel'dovich Effect

On their path, the CMB photons encounter hot clusters with a lot of free electrons. These clusters provide a different optical depth which causes preferential scattering [55]. The Doppler effect due to peculiar velocities is known as the kinematic SZ effect. Likewise, the Compton scattering off hot electrons alters the CMB signal, resulting in the thermal SZ effect. The cluster therefore sees not only the primary CMB quadrupole but two additional quadrupoles.

It is possible that future observations try to utilize this effect to extract more information about galaxy clusters from the CMB measurements, like for instance the transverse velocity of the cluster. Another interesting option is that the CMB quadrupole as seen by the cluster contains information about the last scattering surface at the clusters

position and could help to beat the cosmic variance limit [56, 57].

Reionization

The first stars that have been formed had a massive power output that led to a significant fraction of matter being reionized. The ionized intergalactic medium leads to scattering events between CMB photons and electrons. The intrinsic acoustic oscillation will be damped by this diffusion process. The reionization signal can be identified when the temperature polarization cross correlation is studied in the experimental data. Observations suggest that the reionization started at $z \approx 14$ [58]. If star formation is found to have set in very early it could be a challenging problem to inflation. The end of the reionization is believed to be around $z \approx 10$ [59], although indications suggest a more complex , non monotonic reionization history with significant reionization still being present at $z \approx 6$ [60].

Small angles

As decoupling is not an instantaneous process the surface of last scattering has a finite thickness. This leads to the so-called Silk damping at angular scales $l = 1000$. Gravitational lensing of the CMB photons by clusters and galaxies at small redshifts smoothes the CMB and further limits the accessible information at small angular scales.

4.3.3 WMAP and other CMB Experiments

The first year result from NASA's WMAP satellite [50] are of very good quality. The obtained data set extends up to $l \sim 800$ and the data sets of other experiments like ACBAR, CBI, [61–63] and VSA [64, 65] probing the higher l regions complement the CMB observations. The CMB map has to undergo a very rigid analysis to remove the apparent dipole caused by the relative movement of the earth with respect to the CMB rest frame. Also, the galactic foreground, bright sources like stars and potential SZ sources have to be removed from the data [66, 67]. As mentioned before, at large angular scales, i. e. in the low l regions, the experimental precision is limited by cosmic variance. Recently is was suggested [56, 57] to overcome this cosmic variance limit by observing the scattered CMB photons from distant galaxies and hence determining their CMB background to improve the statistics. Whether this will ever be experimentally possible is unknown, for the time being the cosmic variance contributes significantly to the uncertainties on large angular scales.

   The measurement errors for l between $10 < l < 400$ are very small and all cosmological model that are taken to be serious fit this part of the CMB spectrum very well. The higher l region is not as strongly constrained but the suppression of the higher peaks puts severe constraints on a model with a χ^2 comparable to the best fit model. The

	WMAP	WMAPext	WMAPext + 2dF	WMAPext + 2dF + Ly-α
A	0.9 ± 0.1	0.8 ± 0.1	0.8 ± 0.1	$0.75^{+0.08}_{-0.07}$
$\Omega_b h^2$	0.024 ± 0.001	0.023 ± 0.001	0.023 ± 0.001	0.0226 ± 0.0008
$\Omega_m h^2$	0.14 ± 0.02	0.13 ± 0.01	0.134 ± 0.006	0.133 ± 0.006
h	0.72 ± 0.05	0.73 ± 0.05	0.73 ± 0.03	0.72 ± 0.03
τ	$0.166^{+0.076}_{-0.071}$	$0.143^{+0.071}_{-0.062}$	$0.148^{+0.073}_{-0.071}$	$0.117^{+0.057}_{-0.053}$
n_s	0.99 ± 0.04	0.97 ± 0.03	0.97 ± 0.03	0.96 ± 0.02

Table 4.1: Best fit parameters for a ΛCDM model for the different data sets [50].

	WMAP	WMAPext	WMAPext + 2dF	WMAPext + 2dF + Ly-α
A	0.92 ± 0.12	0.9 ± 0.1	0.84 ± 0.09	$0.83^{+0.09}_{-0.08}$
$\Omega_b h^2$	0.023 ± 0.002	0.022 ± 0.001	0.022 ± 0.001	0.0224 ± 0.0009
$\Omega_m h^2$	0.14 ± 0.02	0.14 ± 0.01	0.136 ± 0.009	$0.135^{+0.008}_{-0.009}$
h	0.70 ± 0.05	0.71 ± 0.06	0.71 ± 0.04	$0.71^{+0.04}_{-0.03}$
τ	0.20 ± 0.07	0.20 ± 0.07	0.17 ± 0.06	0.17 ± 0.06
n_s	$0.93^{+0.07}_{-0.07}$	0.91 ± 0.06	$0.93^{+0.04}_{-0.05}$	0.93 ± 0.03
$\frac{\mathrm{d}n_s}{\mathrm{d}\ln k}$	-0.047 ± 0.04	-0.055 ± 0.038	$-0.031^{+0.023}_{-0.025}$	$-0.031^{+0.016}_{-0.017}$

Table 4.2: Best fit parameters for the running spectral index model as proposed by [50].

WMAP collaboration used two different cosmological models to fit the available experimental data. One cosmological model is a standard Λ CDM model while the other one is also a Λ CDM model but has the additional freedom to allow for a variation of the spectral index n_s with k, the so-called running spectral index model. Many inflationary models do not predict a running spectral index, which is why this possibility has not been given much attention prior to the WMAP proposal.

The WMAP collaboration performed a Markov Chain Monte Carlo simulation to determine the best fit parameters with the WMAP data only and an extended data set where the WMAP data was complemented with measurements of the higher l regions from the CBI [62, 63]and ACBAR [61] experiments. Furthermore, they included large scale structure data from the 2 degree Field Galaxy Redshift Survey (2dFGRS) [68] and the Lyman-alpha forest power spectrum constraints [69, 70]. The combined results for the different data sets for the best fit Λ CDM model can be found in Table 4.1, while the best fit parameters for the running spectral index model are shown in Table 4.2.

Further interesting information is obtained from the observations by measuring the polarization of the detected photons. The polarization is usually decomposed into E-

mode and B-mode polarization. Additional information can therefore be obtained from the cross correlation between temperature and polarization, the TE spectrum. A very interesting possibility of planned future CMB experiments is the observation of B-mode polarization [71, 72], which can be induced by tensor fluctuations, i.e. gravitational waves, and could therefore be a vital probe for their detection.

The WMAP satellite is still operating and hence the measurement accuracy is improving. Future CMB experiments like PLANCK [73, 74] should further improve this powerful cosmological probe.

4.4   Supernovae

One of the most accurate observations with significance in cosmology is the observation of supernova explosions of the type Ia. Assuming that those supernova can be distinguished from other types of supernovae by the shape of their lightcurve, and further assuming that those identified supernovae are equally bright we can use them as a standard candle and measure distances and redshifts of galaxies. With the Hubble Space Telescope (HST), SNeIa have been observed up to redshift $z \approx 1.6$ [19] with excellent accuracy.

The most recent SNeIa observations, enhanced by 16 high z SNeIa from the HST, provide good evidence that the universe has made transition from decelerated to accelerated expansion at around $z \sim 0.5$ [19] (See Fig. 4.1). This is concluded from the fact that the observed supernovae appear dimmer than predicted and hence the distance is larger than expected from decelerated expansion. This conclusion holds until an alternative explanation for this apparent faintness can be found.

The experiment suggests that the universal expansion changed from decelerating to accelerated expansion at $z = 0.43 \pm 0.13$. The best fit flat ΛCDM model for the SNeIa data alone predicts $\Omega_M = 0.29^{+0.05}_{-0.03}$. Including large scale structure data and a static dark energy component, the best fit model has an equation of state today given by $w_q^0 = -1.02^{+0.13}_{-0.19}$. The only dark energy models that exhibit $w_q^0 < -1$ are the phantom energy models [44]. The data is nowhere near to be able to exclude $w_q^0 \geq -1$ and hence the hint for such an exotic equation of state is not conclusive, it rather seems that measurements are homing in on $w = -1$. With the present accuracy, the supernovae observations are one of the most powerful tools in modern cosmology and are best suited for determining w_q^0. The foreseeable end of the HST project will be a major blow for the efforts to determine w^0.
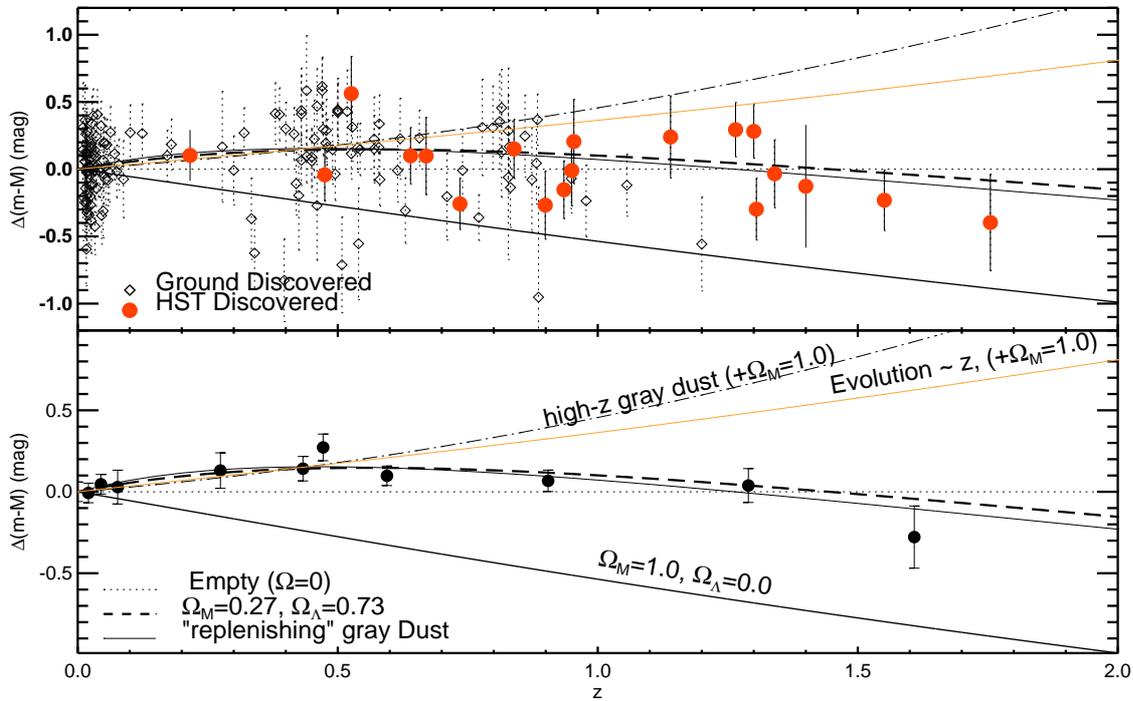
Figure 4.1: This figure shows the present supernova data including the new HST supernovae (full cicles). Figure taken from Riess et al. [19]

4.5 Galaxy Surveys

The distribution of matter in the universe is one of key the predictions of any cosmological model. There are several ways to observe this large scale structure [75, 76].

One way of doing it is to observe hundreds of thousands of galaxies and determine their position and redshift. The sky surveys with the largest number of observed galaxies are the 2 degree field galaxy redshift survey (2dfGRS) [75] and the Sloan Digital Sky Survey (SDSS) [77]. Both provide data for reconstructing the matter power spectrum down to scales of a galaxy, $k \sim 0.1 Mpc^{-1}$. At this scale the matter fluctuations become nonlinear and the predictions from theory have to be interpreted with care. The result is usually quoted in terms of σ_8, that is the amplitude of matter fluctuations at the scale of 8Mpc. The latest results of the large scale structure observations are those of the SDSS collaboration and are shown in Fig. 4.2 together with a best fit model. When performing galaxy surveys, the derived power spectrum has to be multiplied with a biasing factor to correct for the systematics that are introduced by the fact that we do not observe the dark matter distribution directly but are limited to observe the
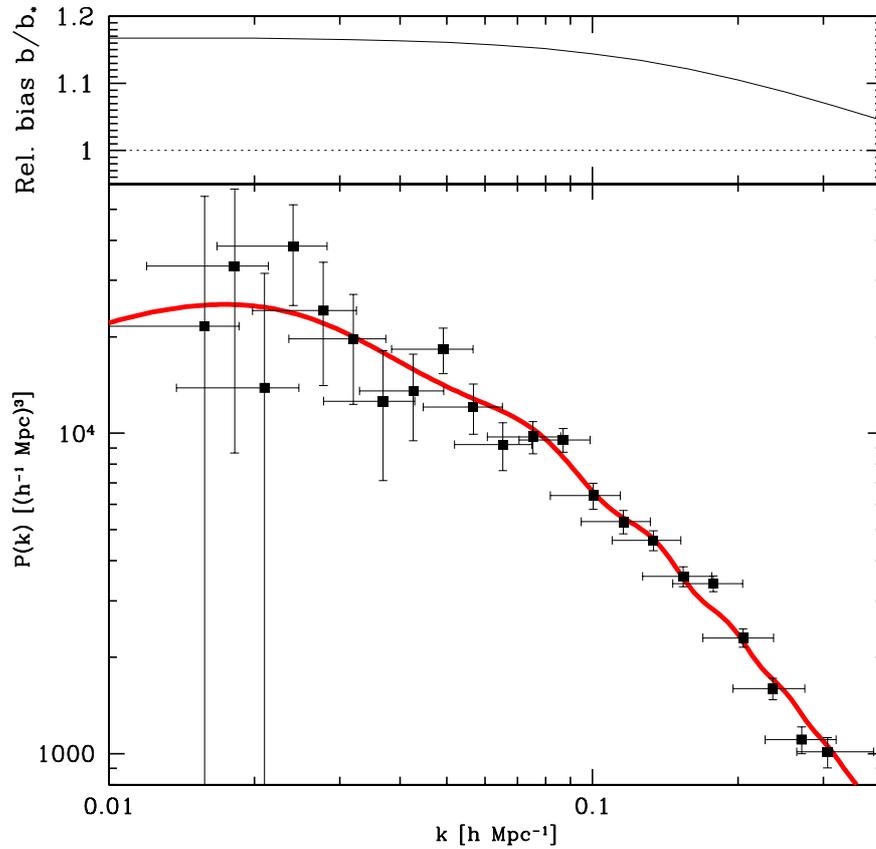
Figure 4.2: The matter power spectrum as measured by SDSS [77]. The luminosity dependent clustering leads to a scale dependent bias, which is removed from the spectrum by dividing by the square of the shown bias. The overall calibration error is 4% and not included in the shown errorbars. Figure taken from Tegmark et.al. [77].

distribution of luminous baryonic matter (i.e. galaxies). Also, a selection effect due to the faintness of distant galaxies cannot be excluded.

4.6 Gravitational Lensing

A more recent development in observational techniques is the gravitational lensing effect. Light from distant sources is distorted by a mass distribution that lies between the source and the observer. This effect can be used to study the mass distribution that is causing the effect.

Of special importance to cosmology is weak gravitational lensing [78] where not a

single gravitational lens is studied but a small part of the sky. The distortions of many distant and faint galaxies that are observed can be translated into a dark matter mass distribution (for a review of the theory of weak lensing see for instance Bartelmann and Schneider [79]). Weak lensing has the particularly nice feature that it probes the dark matter distribution directly without the need for introducing a bias factor or accounting for selection effects. Another advantage is that this method probes scales up to the non-linear region of the power spectrum. This new tool can help to break parameter degeneracies and to determine the equation of state of dark energy w_{de}^0.

As with other measurements it is the question what data and priors to include to determine cosmological parameters, for instance Hoekstra $et\ al.$ [80] derive a bound $\sigma_8 = 0.46^{+0.05}_{-0.07}\,\Omega_m^{-0.50}$ by using gaussian priors for the source redshift distribution. Slightly different values are obtained by using other priors or fixing some parameters, for instance Ω_m, to values obtained from other experiments. In the future it also seems possible to deduce the actual 3-d dark matter distribution from this type of measurements [81].

4.7   Lyman alpha Forrest

Observations of the Lyman-alpha forest from the spectrum of distant quasars provide information about intergalactic hydrogen clouds leaving their imprints in form of absorption lines in the quasar spectra. The absorption spectra are translated into a matter power spectrum with the help of elaborate numerical codes (for instance the Gadget code [82]) simulating the hydrogen clouds. The matter power spectrum has to be interpreted carefully. The calibration of the power spectrum is debated because a biasing factor for this kind of measurement seems plausible [83]. Also, the data touches the non-linear part of the power spectrum where the linear approximations introduce larger errors. The most recent results are obtained by McDonald et. al. [84] who have used the SDSS [77] spectra to obtain their power spectrum from the Lyman-alpha forrest. Before them, the other groups have used a smaller sample of spectra to generate a matter power spectrum, for instance Croft et. al. [69] and Kim et. al. [85].

4.8   Big Bang Nucleosynthesis

Big Bang Nucleosynthesis predicts the primordial abundances of the light elements based on calculations of the nuclear reactions. One important parameter that enters those calculations is the baryon to photon ratio η. We can therefore deduce the value of η from the observations of element abundances and compare this value to the η value obtained from the CMB measurements. It is very fortunate that we are able to

compare two very different fields of physics via this parameter. Recent measurements of the primordial helium abundance and calculation of the required η yield $\eta = 3.4^{+0.7}_{-0.6}$ and $\eta = 4.0^{+1.1}_{-0.5}$ [86] while η determined from WMAP reads $\eta = 6.14 \pm 0.25$ [50]. This discrepancy is significant at first sight but one could argue that the possible systematic error in the observational determination of the primordial helium abundance is able to accommodate the two different results. Nevertheless, this mismatch of two independent measurements is the motivation for the BBN analysis performed in Chapter 8. BBN is also very sensitive to the number of neutrino species and has in the past provided constraints in this respect.

4.9   Combining Measurements

To break parameter degeneracies and tighten error bars it is helpful to combine different measurements and perform a Monte Carlo search for the best fit cosmological model in the huge parameter space. We have done so in our analysis of the WMAP data as presented in Chapter 7 where we had to use the same data sets as the WMAP collaboration to allow for a comparison between the different cosmological models. More recent measurements of tremendous importance, in addition to those mentioned above, are the new HST supernovea, the SDSS large scale strucure data and the VSA CMB data for higher l regions. Many observations are still in progress and new data is available almost every month. For instance, a combined study of different data sets has been performed by Tegmark et.al. [77] and shown in Figure 4.3. The CMB constraints on the power spectrum are obtained from the BOOMERANG, MAXIMA, DASI, CBI, ACBAR, VSA and WMAP data. The lensing data is taken from Hoeckstra et. al. [80] while the Ly-alpha data is the one from Croft et.al. [69] which has been reanalyzed by Gnedin & Hamilton [70].

4.10   Remark on the Anthropic Principle

We would also like to comment on an argument which is often fielded in the discussions about the origin and nature of our universe. The anthropic principle can be explained by stating it in form of the following question:

Is it possible that some of the seemingly strange or unlikely properties of the universe are necessary for the universe to be able develop life or even intelligent life? Is this the reason why we are observing the universe as it is today?

We don't want to repeat the discussion at this point but briefly comment. The question is legitimate to ask. However, the problem with the answer is that science, by now, knows very little about the evolution of intelligent life, its abundance or necessary
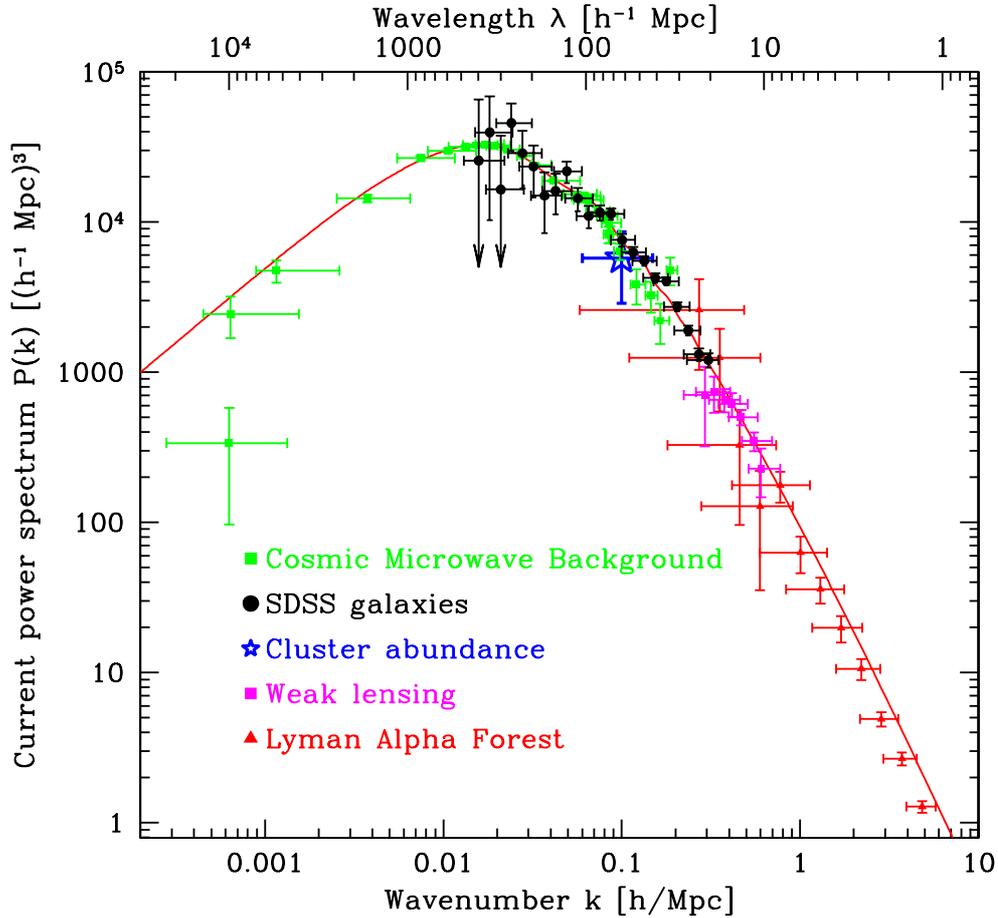
Figure 4.3: This power spectrum combines different measurements. This figure is for a ΛCDM model with a scale invariant spectrum, $\Omega_m = 0.28$, $h = 0.72$, $\Omega_b = 0.044$ and optical depth $\tau = 0.17$. The aforementioned bias is set to $b_* = 0.92$ for the SDSS results. Figure taken from Tegmark et al. [77].

conditions for its creation. We can therefore not conclude on any properties of the universe based on this idea. Hence we think that conclusions drawn based on the anthropic principle are nothing more than speculation. At the moment it does not seem possible to derive meaningful bounds on the properties of the universe by employing the anthropic principle.

Chapter 5

Gauge-invariant Perturbation Theory

When studying small perturbations in cosmology we we are confronted with the gauge problem. We want to map the 'real' manifold in which the unperturbed metric is given onto a manifold of the background metric. This involves defining a way to obtain the averaged background metric $\bar{g}_{\mu\nu}$ and the averaged energy momentum tensor $\bar{T}_{\mu\nu}$ from the unperturbed quantities $g_{\mu\nu}$ and $T_{\mu\nu}$. This averaging procedure is not uniquely defined and some authors claim that inhomogeneities induce a backreaction effect that is responsible for the negative equation of state today and hence the backreaction lies at the center of the dark energy problem. We argue instead that two different averaging procedures contain errors of the order of the metric perturbations itself which we will assume to be part of the metric perturbation. We are encouraged in this assumption by recent work [87] that shows that the corrections are negligible on subhorizon scales.

The second difficulty is the following: Because the mapping of 'real' metric onto the background is invariant under diffeomorphisms the perturbations are not uniquely defined. The different possible mapping schemes are termed 'gauges'. A sensible approach would be to choose the gauge in the most easy way, i.e. choose the condition so that the resulting equations have the most simple form. Another possibility is to employ a physical argument why we choose a certain gauge condition. In the literature the most commonly used gauges are the synchronous gauge and the newtonian or longitudinal gauge [88]. In the synchronous gauge we put ourselves in on hypersurfaces of synchronized time which stay synchronized as we evolve the perturbations. It corresponds to the rest frame of the freely falling observer, e. g. the cold dark matter rest frame. This gauge is not fixed in the sense that it defines a coordinate system as a reference. Instead of preferring a certain set of observers we can completely fix the coordinate system. This is done in the newtonian or longitudinal gauge. It corresponds to zero-shear hypersurfaces and the dynamics are Newtonian on sub horizon scales.

Both gauges have their justification and are, among many others, widely used in the literature. Nevertheless, there are good reasons why we think that a gauge-invariant approach is useful. Comparing results obtained with different gauge conditions is tedious and one has to be careful not to include artificial gauge modes in the analysis when using the synchronous gauge [52]. We therefore decided to perform our perturbation analysis in gauge-invariant variables which can be easily put in the form of a specific gauge by employing a gauge condition. We can be sure not to include gauge modes in out discussion as well as being able to compare the results with different groups. In this chapter we want to derive a set of equations that describe the perturbations of all particle species and radiation. Furthermore, we also derive the gauge-invariant quintessence field perturbation. This set of equation can then be used to solve for the eigenmodes of the system of equation and is the basis for our discussion of initial conditions for the CMB in Chapter 6.

5.1 Metric Perturbations

Now that we study perturbation theory we will denote background quantities with a bar. We also change the notation from comoving time t to conformal time $d\tau = dt/a$. A dot will now and in the following denote the derivative with respect to conformal time τ and we define

$$\mathcal{H} \equiv \frac{\dot{a}(\tau)}{a(\tau)}, \quad H = \frac{\dot{a}(\tau)}{a^2(\tau)}. \tag{5.1}$$

First, we summarize the gauge-invariant approach of Bardeen, Kodama and Sasaki and Durrer [53, 89, 90]. Perturbing a homogenous Friedman universe, one classifies fluctuations according to their transformation properties with respect to the rotation group. In flat spacetime, we may expand the perturbation variables in terms of harmonic functions [90]. With $Q_{,i} = \partial Q/\partial x^i$ one defines

$$Q_i(\boldsymbol{k}, \boldsymbol{x}) \equiv -k^{-1}Q(\boldsymbol{k}, \boldsymbol{x})_{,i} \tag{5.2}$$

and

$$Q_{ij}(\boldsymbol{k}, \boldsymbol{x}) \equiv k^{-2}Q(\boldsymbol{k}, \boldsymbol{x})_{,ij} + \frac{1}{3}\delta_{ij}Q(\boldsymbol{k}, \boldsymbol{x}), \tag{5.3}$$

where the $Q(\boldsymbol{k}, \boldsymbol{x})$ are eigenfunctions of the Laplace-operator, $\nabla^2 Q_k(\boldsymbol{x}) = -k^2 Q_k(\boldsymbol{x})$ and in spatially flat universes $Q = \exp(i\boldsymbol{k}\boldsymbol{x})$. As modes with different $\boldsymbol{k}$ decouple in linear theory, we will not display the $\boldsymbol{k}$-dependence of Q in the following. [1] The scalar parts of vector and tensor fields can then be written as

$$B_i = BQ_i \tag{5.4}$$

---

[1]The mode mixing in higher order perturbation theory is the major problem in 2nd order perturbation theory .

and

$$H_{ij} = H_L Q \delta_{ij} + H_T Q_{ij}. \tag{5.5}$$

respectively.

Of course one could also write down the vector and tensor perturbations in cosmology. In this work, we are only interested in scalar fluctuations because scalar quintessence will not influence vector or tensor modes. We decompose the metric into background and perturbation according to

$$ds^2 = g_{\mu\nu} dx^\mu dx^\nu \equiv (\bar{g}_{\mu\nu} + a^2 h_{\mu\nu}) dx^\mu dx^\nu. \tag{5.6}$$

With $h_{\mu\nu} dx^\mu dx^\nu$ given by

$$h_{\mu\nu} dx^\mu dx^\nu = -2A d\tau^2 - 2B_i d\tau dx i + 2H_{ij} dx^i dx^j \tag{5.7}$$

we can write down a general ansatz for a line element for a perturbed Robertson-Walker metric as

$$ds^2 = a(\tau)^2 [-(1+2A) d\tau^2 - 2B_i d\tau dx^i + (\delta_{ij} + 2H_{ij}) dx^i dx^j]. \tag{5.8}$$

In the scalar case B_i and H_{ij} are given by equations (5.4) and (5.5). The gauge transformation of a tensor T is given by [53, 89–92]

$$\tilde{T}(x) = T(x) - L_\epsilon \bar{T}, \tag{5.9}$$

where L_ϵ is the Lie derivative in direction ϵ. The transformation vector ϵ can be decomposed as

$$\tilde{\tau} = \tau + T(\tau) Q(\boldsymbol{x}), \tag{5.10}$$

$$\tilde{x}^i = x^i + L(\tau) Q^i(\boldsymbol{x}), \tag{5.11}$$

where L and T are arbitrary functions of τ. The transformation properties of the metric perturbations are given by [89, 92]

$$\tilde{A} = A - \mathcal{H}T - \dot{T}, \tag{5.12}$$

$$\tilde{B} = B + \dot{L} + kT, \tag{5.13}$$

$$\tilde{H}_L = H_L - \mathcal{H}T - \frac{k}{3}L, \tag{5.14}$$

$$\tilde{H}_T = H_T + kL. \tag{5.15}$$

The functions L and T can be used to eliminate two of the metric perturbations. The above mentioned most popular choices are $A = B = 0$ for the synchronous gauge and $B = H_T = 0$ for the longitudinal gauge.

From equations (5.12)-(5.15) one can construct the gauge-invariant Bardeen potentials [89]

$$\Psi = A - \mathcal{H}k^{-1}\sigma - k^{-1}\dot{\sigma}, \qquad (5.16)$$

$$\Phi = H_L + \frac{1}{3}H_T - \mathcal{H}k^{-1}\sigma, \qquad (5.17)$$

with $\sigma \equiv k^{-1}\dot{H}_T - B$. It is worthwhile to note that in longitudinal gauge, for which $B = H_T = \sigma = 0$, the perturbed metric takes on the simple form

$$ds^2_{(long.)} = a(\tau)^2\big[-(1 + 2\Psi\,Q)d\tau^2 + (1 + 2\Phi\,Q)\delta_{ij}dx^i dx^j\big]. \qquad (5.18)$$

With $\mathrm{M}_{\bar{P}} \equiv (8\pi G)^{-1/2}$ denoting the reduced Planck mass, Einstein's equation reads

$$T^\mu_{\ \nu} = \mathrm{M}^2_{\bar{P}}\left(R^\mu_{\ \nu} - \frac{1}{2}\delta^\mu_{\ \nu}R \right), \qquad (5.19)$$

where the energy momentum tensor of a perfect fluid is given by

$$T^\mu_{\ \nu} = p\delta^\mu_{\ \nu} + (\rho + p)u^\mu u_\nu + \pi^\mu_{\ \nu}. \qquad (5.20)$$

The covariant 4-velocity is written down as

$$u_i = a[v(\tau) - B]\,Q_i, \qquad (5.21)$$

where the spacial velocity is $v_i = vQ_i$. We define the energy density contrast δ by

$$\rho = \bar{\rho}\,(1 + \delta(\tau))Q, \qquad (5.22)$$

the spatial trace by

$$p\,\delta^i_{\ j} = \bar{p}(\tau)(1 + \pi_L(\tau)Q)\,\delta^i_{\ j} \qquad (5.23)$$

and the traceless part by

$$\pi^i_{\ j} = \bar{p}\,\Pi\,Q^i_{\ j}. \qquad (5.24)$$

The π_L is interpreted as the isotropic pressure perturbation while Π is the anisotropic stress perturbation. Putting these definitions together we obtain the components of the energy momentum tensor as

$$\begin{aligned}
T^0_{\ 0} &= -\bar{\rho}(1 + \delta(\tau)Q), & (5.25)\\
T^i_{\ 0} &= -\bar{\rho}(1 + w)\,v\,Q^i, & (5.26)\\
T^0_{\ i} &= \bar{\rho}\,(1 + w)\,(v - B)\,Q_i, & (5.27)\\
T^i_{\ j} &= \bar{p}\,\big[(1 + \pi_L Q)\,\delta^i_{\ j} + \Pi Q^i_{\ j}\big]. & (5.28)
\end{aligned}$$

Given the gauge-transformation properties of δ, v and π_L [53, 89–92], one can construct the corresponding gauge-invariant quantities for the energy density contrast Δ, the

velocity V and the entropy perturbation Γ. These are given by

$$\Delta = \delta + 3(1+w)\left(H_L + \frac{1}{3}H_T\right), \tag{5.29}$$

$$V = v - k^{-1}\dot{H}_T, \tag{5.30}$$

$$\Gamma = \pi_L - \frac{c_s^2}{w}\delta. \tag{5.31}$$

Here, $c_s^2 \equiv \partial\bar{p}/\partial\bar{\rho}$ is the adiabatic sound speed. Note that there exists no unique definition for the gauge-invariant energy density perturbation.

From the conservation of the zero component of the energy momentum tensor $\nabla_\mu \bar{T}^\mu{}_0 = 0$ we obtain

$$\frac{\dot{\bar{\rho}}_\alpha}{\bar{\rho}_\alpha} = -3(1+w_\alpha)\,\mathcal{H}, \tag{5.32}$$

where $w = \bar{p}/\bar{\rho}$ is the equation of state of the particular species.

The perturbed metric allows us to calculate the Christoffel symbols which in turn allow us to determine the Riemann and the Ricci tensor. After some algebra this calculation then obtains the perturbed part of the Einstein tensor as

$$\delta G^0{}_0 = \frac{2}{a^2}\left[3\mathcal{H}^2 A - \mathcal{H}kB - 3\mathcal{H}\dot{H}_L - k^2(H_L + \frac{H_T}{3})\right]Q, \tag{5.33}$$

$$\delta G^i{}_0 = \frac{2}{a^2}\left[(\dot{\mathcal{H}} - \mathcal{H}^2)B - k\mathcal{H}A + k(\dot{H}_L + \frac{\dot{H}_T}{3})\right]Q^i, \tag{5.34}$$

$$\delta G^0{}_j = \frac{2}{a^2}\left[k\mathcal{H}A - k(\dot{H}_L + \frac{\dot{H}_T}{3})\right]Q_j, \tag{5.35}$$

$$\begin{aligned}
\delta G^i{}_j = &\frac{2}{a^2}[(2\frac{\ddot{a}}{a} + 3\mathcal{H}^2)A + \mathcal{H}\dot{A} - \frac{k^2}{3}A - \frac{k}{3}(\dot{B} + 2\mathcal{H}B) \\
&- a^{-1}\frac{\mathrm{d}}{\mathrm{d}\tau}(a\dot{H}_L) - \mathcal{H}\dot{H}_L - \frac{k^2}{3}(H_L + \frac{H_T}{3})]\delta^i{}_j Q \\
&+ \frac{1}{a^2}[-k^2 A - k(\dot{B} + \mathcal{H}B) + a^{-1}\frac{\mathrm{d}}{\mathrm{d}\tau}(a\dot{H}_T) \\
&+ \mathcal{H}(\dot{H}_T - kB) - k^2(H_L + \frac{H_T}{3})]Q^i{}_j.
\end{aligned} \tag{5.36}$$

The perturbed Friedmann equations in gauge-invariant variables are then obtained by relating $\delta G^\mu{}_\nu$ to the energy momentum tensor [53, 89–92]. The dynamic equations for Δ, V and Π then read

$$a^2\bar{\rho}\Delta = 2\,\mathrm{M}_{\bar{P}}^2\,k^2\Phi - 3a^2\bar{\rho}(1+w)\left(\mathcal{H}k^{-1}V - \Phi\right), \tag{5.37}$$

$$a^2(\bar{\rho} + \bar{p})V = 2\,\mathrm{M}_{\bar{P}}^2\,k\left(\mathcal{H}\Psi - \dot{\Phi}\right), \tag{5.38}$$

$$a^2\bar{p}\,\Pi = -\mathrm{M}_{\bar{P}}^2\,k^2(\Phi + \Psi). \tag{5.39}$$

In the above, it is understood that the quantities Δ, V and Π are the sum of the contributions of all species α. Using $\dot{w} = (c_s^2 - w)\dot{\bar{\rho}}/\bar{\rho}$ and (5.32) we get from $T^\mu{}_{0;\mu} = 0$

Symbol	Meaning	Equation
Ω_{species}	fraction of total energy density	n.a.
$\Omega^0_{\text{species}}$	fraction of total energy density today	n.a.
a	scale factor of the universe	n.a.
τ	conformal time: $\mathrm{d}\tau = \mathrm{d}t/a$	n.a.
k	wavenumber of mode	n.a.
x	$k\tau$	n.a.
$\cdot$	derivative w.r.t conformal time	n.a.
$'$	derivative w.r.t. $x\frac{\mathrm{d}}{\mathrm{d}x}$	n.a.
$\mathcal{H}$	$\dot{a}/a$	n.a.
Δ	gauge-inv. density contrast (Δ_g of [90])	(5.29)
V	gauge-invariant velocity	(5.30)
Π	shear	(5.28)
$\tilde{V}$	reduced velocity: $\tilde{V} = x^{-1}V$	n.a.
$\tilde{\Pi}$	reduced shear: $\tilde{\Pi} = x^{-2}\Pi$	n.a.

Table 5.1: Symbols and their meanings.

that

$$\dot{\Delta} + 3(c_s^2 - w)\mathcal{H}\Delta + kV(1 + w) + 3\mathcal{H}w\Gamma = 0, \tag{5.40}$$

and from $T^{\mu}_{i;\mu} = 0$

$$\dot{V} = \mathcal{H}(3c_s^2 - 1)V + k[\Psi - 3c_s^2\Phi] + \frac{c_s^2 k}{1 + w}\Delta + \frac{wk}{1 + w}\left[\Gamma - \frac{2}{3}\Pi\right]. \tag{5.41}$$

5.2 Gauge-invariant Quintessence Perturbations

The scalar quintessence field is decomposed into a background and fluctuation part according to $\varphi(\tau, \boldsymbol{x}) = \bar{\varphi}(\tau) + \chi(\tau, \boldsymbol{x})$. The fluctuation can be promoted to a gauge-invariant quantity by defining the gauge-invariant quintessence field fluctuation $X \equiv \chi - \dot{\bar{\varphi}}k^{-1}\sigma$. The field dynamics is governed by the Klein-Gordon equation. For the background, it reads

$$\ddot{\bar{\varphi}} = -2\mathcal{H}\dot{\bar{\varphi}} - a^2 V'(\varphi), \tag{5.42}$$

while the perturbation obeys the equation of motion

$$\ddot{X} = \dot{\bar{\varphi}}(\dot{\Psi} - 3\dot{\Phi}) - 2a^2 V'(\varphi)\Psi - (a^2 V''(\varphi) + k^2)X - 2\mathcal{H}\dot{X}. \tag{5.43}$$

From the energy momentum tensor for the quintessence field

$$T^{\mu}_{\nu} = \varphi^{,\mu}\varphi_{,\nu} - \delta^{\mu}_{\nu}\left(\frac{1}{2}\varphi^{,\alpha}\varphi_{,\alpha} + V(\varphi)\right), \tag{5.44}$$

using $\varphi = \bar{\varphi} + X$ and the longitudinal gauge metric, one gets

$$\delta T^0{}_0{}^{(lon.)} = \left[a^{-2} \left(\dot{\bar{\varphi}}^2 \, \Phi - \dot{X}\dot{\bar{\varphi}} \right) - V'(\varphi)X \right] Q \tag{5.45}$$

$$\delta T^i{}_0{}^{(lon.)} = -a^{-2} \, k\, \dot{\bar{\varphi}}\, X\, Q^i. \tag{5.46}$$

Using the definition of Δ, equation (5.29) in longitudinal gauge and $\bar{\rho}_q + \bar{p}_q = a^{-2}\dot{\bar{\varphi}}^2$ one can read off from equation (5.45) the gauge-invariant expression

$$\Delta_q = (1 + w_q) \left[3\Phi - \Psi + \dot{X}\dot{\bar{\varphi}}^{-1} \right] + XV'(\varphi)\bar{\rho}_q^{(-1)}. \tag{5.47}$$

In the same manner, one gets from equation (5.46) and the fact that $v^{(long.)} = V$ the relation

$$V_q = k\dot{\bar{\varphi}}^{-1}X. \tag{5.48}$$

Taking the time derivative of equations (5.47) and (5.48) and using the equation of motion (5.43), one obtains the evolution equations

$$\dot{\Delta}_q = (1 + w_q) \left[\frac{2a^2V'(\varphi)}{\dot{\bar{\varphi}}} \left(\frac{\Delta_q}{1 + w_q} - 3\Phi \right) + \left(\frac{6a\dot{a}V'(\varphi)}{k\dot{\bar{\varphi}}} - k \right) V_q \right] + \frac{\dot{w}_q \Delta_q}{1 + w_q} \tag{5.49}$$

and

$$\dot{V}_q = k \left[\frac{\Delta_q}{1 + w_q} - 3\Phi + \Psi \right] + 2\mathcal{H}V_q. \tag{5.50}$$

Equation (5.49) depends on the specific quintessence model through V' and $\dot{\bar{\varphi}}$.

We can try to put Equation 5.49 in a more simple form by simplifying the behavior of w_q. This can be achieved by considering tracking quintessence models [8,9,25] for which the equation of state of the quintessence field w_q is nearly constant during radiation domination. We will use this vanishing of $\dot{w}_q$ in the following to derive relations to simplify equation (5.49). Considering $a^{-2}\dot{\bar{\varphi}}^2 = (1+w_q)\rho_\varphi$ it follows using the Friedman equation $3a^{-2}\mathrm{M}_{\bar{P}}^2\mathcal{H}^2 = \rho$ that

$$\dot{\bar{\varphi}} = [3(1 + w_q)\Omega_q]^{\frac{1}{2}}\mathrm{M}_{\bar{P}}\mathcal{H}, \tag{5.51}$$

and hence

$$\frac{\ddot{\bar{\varphi}}}{\dot{\bar{\varphi}}} = \frac{\mathrm{d}}{\mathrm{d}\tau} \ln \dot{\bar{\varphi}} = \frac{1}{2}\frac{\dot{\Omega}_q}{\Omega_q} + \frac{\dot{\mathcal{H}}}{\mathcal{H}}, \tag{5.52}$$

where we have neglected a term involving $\dot{w}_q$. We will in the following assume that at early times, the universe expands as if radiation dominated. In this case, $\mathcal{H} = \tau^{-1}$ and inserting the above equation (5.52) into the equation of motion (5.42), one finds

$$\frac{a^2V'}{\dot{\bar{\varphi}}} = -\frac{3(1 - w_q)}{2\,\tau}. \tag{5.53}$$

Using this relation (5.53), the evolution equation for Δ_q becomes

$$\dot{\Delta}_q = 3(w_q - 1)\frac{k}{x}\left[\Delta_q - 3(1 + w_q)\Phi + \left\{ 3 - \frac{x^2}{3(w_q - 1)} \right\} (1 + w_q)\tilde{V}_q \right], \tag{5.54}$$

whereas the one for the velocity remains almost unaltered while we move to the reduced velocity $\tilde{V}_q$:

$$\dot{\tilde{V}}_q = \frac{k}{x} \left[\frac{\Delta_q}{1 + w_q} - 3\Phi + \Psi \right] + \tau^{-1} \tilde{V}_q. \tag{5.55}$$

Note that Γ_q does not usually vanish. Instead, we obtain

$$w_q \Gamma_q = (1 - c_{s(q)}^2) \left[\Delta_q - 3(1 + w_q)\Phi + 3\frac{\dot{a}}{a}(1 + w_q)\frac{V_q}{k} \right] \tag{5.56}$$

with the sound speed of quintessence given by

$$c_{s(q)}^2 = \dot{\bar{p}}_q / \dot{\bar{\rho}}_q = w_q - \frac{1}{3}\frac{a}{\dot{a}}\frac{\dot{w}_q}{1 + w_q} \tag{5.57}$$

5.3   Matter and Radiation

Setting $w = c_s^2 = \Gamma = 0$ in equations (5.40) and (5.41), we obtain the cold dark matter evolution equations

$$\dot{\Delta}_c = -kx\tilde{V}_c, \tag{5.58}$$

$$\dot{\tilde{V}}_c = \frac{k}{x}(-\tilde{V}_c + \Psi). \tag{5.59}$$

The multipole expansion of the neutrino distribution function [88, 93] can be truncated beyond the quadrupole at early times. In terms of density, velocity and shear, it is given by [92, 93]

$$\dot{\Delta}_\nu = -\frac{4}{3}kx\tilde{V}_\nu, \tag{5.60}$$

$$\dot{\tilde{V}}_\nu = \frac{k}{x}\left(\frac{1}{4}\Delta_\nu - \tilde{V}_\nu - \frac{1}{6}x^2\tilde{\Pi}_\nu + \Psi - \Phi \right), \tag{5.61}$$

$$\dot{\tilde{\Pi}}_\nu = \frac{k}{x}\left(\frac{8}{5}\tilde{V}_\nu - 2\tilde{\Pi}_\nu \right). \tag{5.62}$$

Deep in the radiation dominated era, for which the initial conditions here are derived, Compton scattering tightly couples photons and baryons [90, 94]. The coupling leads to $V_b = V_\gamma$ and the evolution equations become [90]

$$\dot{\Delta}_\gamma = -\frac{4}{3}kx\tilde{V}_\gamma, \tag{5.63}$$

$$\dot{\tilde{V}}_\gamma = \frac{k}{x}\left(\frac{1}{4}\Delta_\gamma - \tilde{V}_\gamma + \Psi - \Phi \right), \tag{5.64}$$

$$\dot{\Delta}_b = -k\,x\,\tilde{V}_\gamma. \tag{5.65}$$

As the photon quadrupole and all higher photon multipoles are suppressed during tight coupling, it follows that Φ is given from Einstein's equation by

$$\Phi = -\Psi - \Omega_\nu \tilde{\Pi}_\nu, \tag{5.66}$$

Quantity	Scaling behaviour
$\dot{\varphi}$	$\propto \tau^{-(1+3w_q)/2}$
V'	$\propto \tau^{-(7+3w_q)/2}$
V''	$\propto \tau^{-4}$
$\Delta_q^{\text{adiab.}}$	$const.$
$X_{\text{adiab.}}$	$\propto \tau^{(1-3w_q)/2}$

Table 5.2: Tracking quintessence in the radiation era: Scaling handbook.

where we have used the Friedmann equation. Finally, the Poisson equation (5.37) in terms of the various species is

$$
\Psi = -\frac{\sum\limits_{\alpha=c,b,\gamma,\nu,q} \Omega_\alpha(\Delta_\alpha + 3(1 + w_\alpha)\tilde{V}_\alpha)}{\sum\limits_{\alpha=c,b,\gamma,\nu,q} 3(1 + w_\alpha)\Omega_\alpha + \frac{2x^2}{3}} - \Omega_\nu \tilde{\Pi}_\nu, \tag{5.67}
$$

where the index α runs over all species. Rewriting the evolution equations (5.58) - (5.65) in terms of $\mathrm{d}/\mathrm{d}\ln x$ and replacing Φ by means of (5.66), one arrives at (6.2)-(6.11).

Chapter 6

Initial conditions for the CMB

6.1 Why bother with non-adiabaticity?

The initial density fluctuation that lead to the CMB anisotropies are usually assumed to be adiabatic fluctuations. This is because the most popular inflationary models predict adiabatic fluctuations [95–97]. More elaborate models lead to an admixture of adiabatic and isocurvature fluctuations [98, 99]. Isocurvature perturbations are perturbations in the local equation of state and arise in various inflationary models like, for instance, multi field inflation.

The time evolution of adiabatic and non-adiabatic fluctuations is well understood for a universe composed of radiation, baryons, cold dark matter (CDM) and neutrinos [88]. In the context of quintessence [8, 9, 100], the behavior of the field fluctuation has been studied in several works [101–105]. Initial conditions have been proposed in [106] for the case of negligible quintessence contribution in the early universe. We will now conduct a systematic treatment of initial conditions for quintessence models which differs from that of [106] in approach and interpretation.

6.2 A Description of the Analysis

Our basic setting assumes that small deviations from homogeneity are generated during a very early stage of the big bang, typically an inflationary epoch. During the following radiation dominated period the wavelength of the relevant fluctuations is far outside the horizon. Apart from this, we will not use any further constraint on the primordial fluctuations. Only the spectra of a certain number of "dominant" modes can possibly influence events such as emission of the CMB and its anisotropies since the other modes decay. The information about these dominant modes therefore constitutes the initial conditions for practical purposes. Primordial information beyond the dominant modes

is effectively lost and not observable. The detailed time of specification of the initial conditions is therefore irrelevant as long as it is much shorter than the time of matter-radiation equality.

During the period relevant for the discussion of the initial conditions the universe is radiation dominated. However, our approach allows for the presence of scalar fields which evolve like radiation at early times or are subdominant. Consequently, our results hold for a wide class of quintessence models, including those with non-negligible Ω_q at early times [107]. In fact, we only use a "tracking" property [25] for the background of homogenous quintessence, namely that its equation of state $w_q = p_q/\rho_q$ is almost constant and determined only by the energy densities of the radiation and matter components. The parameters w_q and $\Omega_q = 1 - \Omega_m - \Omega_\nu - \Omega_\gamma$ will therefore be the only parameters of the quintessence model that influence the early time evolution of small fluctuations. This makes our analysis model independent to a large extent.

In the previous Chapter 5 we derived the perturbation equations in a gauge-invariant formalism. This allows us to formulate the evolution equations for the perturbation variables as a first order differential matrix equation:

$$\frac{\mathrm{d}}{\mathrm{d}\ln x} \boldsymbol{U} = A(x)\boldsymbol{U}, \qquad (6.1)$$

where the vector $\boldsymbol{U}$ contains all perturbation variables and the matrix $A(x)$ encodes the evolution equations. In doing so, we relate the problem of finding initial conditions and dominant modes to the familiar language of eigenvalues and eigenvectors. This formulation makes "mode-accounting" transparent by counting the degeneracy of the largest eigenvalue. We find four dominant modes that remain regular at early times. For physical reasons, we choose a basis using adiabatic, CDM Isocurvature, Baryon Isocurvature and Neutrino Isocurvature initial conditions. As we will show, adiabaticity between CDM, baryons and photons implies adiabaticity of quintessence. It therefore exists no pure quintessence isocurvature mode. In addition, using the matrix formulation reveals facets of the modes that otherwise remain obscured.

In contrast to earlier work, we find it more appropriate to specify the initial conditions and time evolution of the quintessence field in terms of the gauge-invariant density contrast and velocity, thus unifying the language for all species. As anticipated, the quintessence density perturbation remains constant at super-horizon scales for adiabatic initial conditions. In contrast to this, the field fluctuation follows a simple power law in conformal time that only depends on the quintessence equation of state.

6.3 The Perturbation Equations

In Chapter 5 we derived the perturbation equations by following the gauge-invariant approach as devised by Bardeen [89]. It turns out that the evolution is best described as

a function of $x \equiv k\tau$, where τ is the conformal time and k the comoving wavenumber of the mode. We assume that at early times, the universe expands as if radiation dominated. This assumption is well justified for small Ω_q at early times, as well as for potentials that are essentially exponentials at the time of interest, regardless of Ω_q. The assumption is certainly not justified for models in which quintessence is dominating the universe at early times with equation of state $w_q \neq 1/3$. For such (slightly exotic) models, the following steps would need to be modified.

Assuming tracking quintessence we obtain the following set of equations [1]:

$$\Delta'_c = -x^2 \tilde{V}_c, \tag{6.2}$$

$$\tilde{V}'_c = -2\tilde{V}_c + \Psi, \tag{6.3}$$

$$\Delta'_\gamma = -\frac{4}{3} x^2 \tilde{V}_\gamma, \tag{6.4}$$

$$\tilde{V}'_\gamma = \frac{1}{4}\Delta_\gamma - \tilde{V}_\gamma + \Omega_\nu \tilde{\Pi}_\nu + 2\Psi, \tag{6.5}$$

$$\Delta'_b = -x^2 \tilde{V}_\gamma, \tag{6.6}$$

$$\Delta'_\nu = -\frac{4}{3} x^2 \tilde{V}_\nu, \tag{6.7}$$

$$\tilde{V}'_\nu = \frac{1}{4}\Delta_\nu - \tilde{V}_\nu - \frac{1}{6} x^2 \tilde{\Pi}_\nu + \Omega_\nu \tilde{\Pi}_\nu + 2\Psi, \tag{6.8}$$

$$\tilde{\Pi}'_\nu = \frac{8}{5} \tilde{V}_\nu - 2\tilde{\Pi}_\nu, \tag{6.9}$$

$$\Delta'_q = 3(w_q - 1)\left[\Delta_q + 3(1 + w_q)\left\{\Psi + \Omega_\nu \tilde{\Pi}_\nu\right\}\right.$$
$$\left. + \left\{3 - \frac{x^2}{3(w_q - 1)}\right\}(1 + w_q)\tilde{V}_q\right], \tag{6.10}$$

$$\tilde{V}'_q = 3\Omega_\nu \tilde{\Pi}_\nu + \frac{\Delta_q}{1 + w_q} + \tilde{V}_q + 4\Psi, \tag{6.11}$$

with the gauge-invariant Newtonian potential Ψ given by

$$\Psi = -\frac{\displaystyle\sum_{\alpha=c,b,\gamma,\nu,q} \Omega_\alpha(\Delta_\alpha + 3(1 + w_\alpha)\tilde{V}_\alpha)}{\displaystyle\sum_{\alpha=c,b,\gamma,\nu,q} 3(1 + w_\alpha)\Omega_\alpha + \frac{2x^2}{3}} - \Omega_\nu \tilde{\Pi}_\nu. \tag{6.12}$$

We denote the derivative $\mathrm{d}/\mathrm{d}\ln x$ with a prime. The gauge-invariant energy density contrasts Δ_α, the velocities $\tilde{V}_\alpha$ and the shear $\tilde{\Pi}_\nu$ are the ones found in the literature [53, 89, 90], except that we factor out powers of x from the velocity and shear defining $\tilde{V} \equiv V/x$ and $\tilde{\Pi}_\nu \equiv x^{-2}\Pi_\nu$. This factoring out leads to the particularly simple form of the system of equations for $x \ll 1$. It does, however, exclude modes with diverging Ψ at early times such as a neutrino velocity mode [108]. The index α runs over the

---

[1]Without assuming tracking quintessence one would have to use Eqns. (5.49) and (5.50) instead.

five species in our equations, namely cold dark matter, baryons, photons, neutrinos and quintessence, denoted with the subscript q. We assume tight coupling between photons and baryons. The equation of state $w = \bar{p}/\bar{\rho}$ takes on the values $w_c = w_b = 0$, $w_\gamma = w_\nu = 1/3$ and w_q is left as a free parameter. Equations (6.2), (6.4), (6.6) and (6.7) can be regarded as continuity relations between the density fluctuations and the velocity. We obtain equations (6.10) and (6.11) from the perturbed Klein-Gordon equation of the quintessence scalar field expressed in terms of Δ_q and V_q, the energy density and velocity perturbations as defined in Chapter 5.

6.4   Matrix Formulation and Dominant Modes

Conceptually, it is convenient to note that the above set of equations can be concisely written in matrix form according to Equation (6.1) where the perturbation vector is defined as

$$\boldsymbol{U}^T \equiv (\Delta_c, \, \tilde{V}_c, \, \Delta_\gamma, \, \tilde{V}_\gamma, \, \Delta_b, \, \Delta_\nu, \, \tilde{V}_\nu, \, \tilde{\Pi}_\nu, \, \Delta_q, \, \tilde{V}_q). \tag{6.13}$$

The matrix $A(x)$ can easily be read off from equations (6.2)-(6.11). This enables us to discuss the problem of specifying initial conditions in a systematic way.

The initial conditions are specified for modes well outside the horizon, i.e. $x \ll 1$. In this case, the r.h.s. of equations (6.2), (6.4), (6.6) and (6.7) can be neglected, provided $\tilde{V}_\alpha$ does not diverge $\propto x^{-2}$ or faster for $x^2 \to 0$. The evolution matrix $A(x)$ loses any explicit x dependence for $x^2 \to 0$. Yet, it still depends on x via terms involving Ω_c, Ω_b and Ω_q.

To analyze this remaining time dependence we can distinguish two cases.

The first case it an equation of state $w_q = 1/3$ for quintessence. The term containing Ω_q is then constant (tracking quintessence). In leading order, the matrix A becomes therefore x-independent for very early times. In fact, the general solution to Equation (6.1) in the (ideal) case of a truly constant A would be

$$\boldsymbol{U}(x) = \sum_i c_i \left(\frac{x}{x_0}\right)^{\lambda_i} \boldsymbol{U}^{(i)}, \tag{6.14}$$

where $\boldsymbol{U}^{(i)}$ are the eigenvectors of A with eigenvalue λ_i and the time independent coefficients c_i specify the initial contribution of $\boldsymbol{U}^{(i)}$ towards a general perturbation $\boldsymbol{U}$. As time progresses, components corresponding to the largest eigenvalues λ_i will dominate. Compared to these "dominant" modes, initial contributions in the direction of eigenvectors $\boldsymbol{U}^{(i)}$ with smaller $\text{Re}(\lambda_i)$ decay. It therefore suffices to specify the initial contribution c_i for the dominant modes, if one is not interested in very early time behavior shortly after inflation. In our case, the characteristic polynomial of $A(x)$ indeed has a fourfold degenerate eigenvalue $\lambda = 0$ in the limit $x^2 \to 0$, independent

of Ω_c, Ω_b and Ω_q.[2] While it is not feasible to obtain the remaining six eigenvalues by analytic means, we have checked numerically for a wide range of Ω_γ, Ω_ν, Ω_b, Ω_c, Ω_q and w_q that the remaining eigenvalues have indeed negative real parts and contributions from the corresponding eigenvectors towards a general perturbation $\boldsymbol{U}$ will therefore decay according to Equation (6.14). We can improve the analytic description of the dominant modes by taking corrections $\propto x$ into account.

As $\Omega_c \propto \Omega_b \propto x$, it is appropriate to split $A(x)$ according to the scaling with x,

$$A(x) = A_0 + x\, A_1, \tag{6.15}$$

where A_0 and A_1 are constant and $x\, A_1$ contains the small, time-dependent corrections from terms involving Ω_c and Ω_b. We may also write[3] the eigenvectors as a series in x,

$$\boldsymbol{U}(x) = \boldsymbol{U}_0 + x\, \boldsymbol{U}_1. \tag{6.16}$$

Inserting Equations (6.15)-(6.16) in Equation (6.1), we get

$$A_0\, \boldsymbol{U}_0 = 0, \tag{6.17}$$

and

$$\boldsymbol{U}_1 = -(A_0 - \mathbb{1})^{-1} A_1 \boldsymbol{U}_0. \tag{6.18}$$

The second possible case we want to discuss corresponds to $w_q < 1/3$, while we assume the background expands radiation dominated. In this case, $\Omega_q \propto \tau^{(1-3w_q)}$ and we can split the matrix in three parts according to their scaling with x:

$$A(x) = A_0 + x\, A_1 + x^{(1-3w_q)}\, A_q. \tag{6.19}$$

Again, Equation (6.1) will lead to a solution vector of the form

$$\boldsymbol{U}(x) = \boldsymbol{U}_0 + x\, \boldsymbol{U}_1 + x^{(1-3w_q)}\, \boldsymbol{U}_q. \tag{6.20}$$

Substituting this into Equation (6.1) and keeping only leading orders in x, we get

$$A_0\, \boldsymbol{U}_0 \;=\; 0, \tag{6.21}$$
$$A_1\, \boldsymbol{U}_0 + A_0\, \boldsymbol{U}_1 \;=\; \boldsymbol{U}_1, \tag{6.22}$$
$$A_q\, \boldsymbol{U}_0 + A_0\, \boldsymbol{U}_q \;=\; (1 - 3w_q)\, \boldsymbol{U}_q. \tag{6.23}$$

While the conclusion regarding $\boldsymbol{U}_0$ and $\boldsymbol{U}_1$ are still the same as in the case for constant Ω_q, we see that quintessence may introduce a correction

$$\boldsymbol{U}_q = -\left[A_0 - (1 - 3w_q)\mathbb{1}\right]^{-1} A_q\, \boldsymbol{U}_0. \tag{6.24}$$

---

[2]For $w_q = 1$ we find another eigenvalue with $\lambda = 0$. We will ignore this special case in what follows.

[3]This form is not an ansatz, but dictated by Equation (6.1), once the dependence of $A(x)$ on x is given.

This contribution $x^{(1-3w_q)}\,\boldsymbol{U}_q$ could in principle dominate over $x\,\boldsymbol{U}_1$ for $w_q > 0$, $\Omega_q > \Omega_c$. However, as we will see shortly, the contribution is only of interest for the CDM Isocurvature and Baryon Isocurvature modes, as it is otherwise negligible compared to the constant order. Yet for CDM Isocurvature and Baryon Isocurvature,

$$A_q\,\boldsymbol{U}_0 = 0 \qquad\qquad (6.25)$$

and hence

$$\boldsymbol{U}_q = 0 \qquad\qquad (6.26)$$

for CDM Isocurvature and Baryon Isocurvature modes. One order higher in x there may be a contribution which we neglect.

Finally, we briefly discuss the case of vanishing $\boldsymbol{U}_0$. This only concerns possible subdominant modes. Equation (6.22) then yields $A_0\,\boldsymbol{U}_1 = \boldsymbol{U}_1$, i.e. $\boldsymbol{U}_1$ is an eigenvector of A_0 with eigenvalue $\lambda = 1$. As A_0 does not have such an eigenvector, we are led to conclude that Equation (6.1) does not have a regular solution involving $\boldsymbol{U}_1$, if $\boldsymbol{U}_0 = 0$. Turning to Equation (6.23), we similarly conclude that $\boldsymbol{U}_q$ needs to be a eigenvector of A_0 with $\lambda = (1 - 3w_q)$ for vanishing $\boldsymbol{U}_0$. For $w_q < 1/3$ this is once again excluded and for $w_q = 1/3$, we just regain the results stated above.

Equation (6.18) is easy to solve, once $\boldsymbol{U}_0$ has been determined. We see from Equation (6.17) that to constant order the solutions of Equation (6.1) are indeed given by eigenvectors to the eigenvalue $\lambda = 0$. We should emphasize that the vectors $\boldsymbol{U}_0$ do not evolve in time if their corresponding eigenvalues are $\lambda = 0$. Thus, the perturbations remain constant in the super-horizon regime during radiation domination in this approximation. If we include the next-to-leading order contribution to $\mathbf{U}$, the eigenvectors do evolve and we can no longer apply Eq. (6.14). These corrections are, however, small as long as we are deep in the radiation dominated era due to the small contributions of baryons, radiation and quintessence during this era. Given a set of initial conditions in the form of coefficients for the four dominating modes at $z_{initial}$ we can find the perturbations at some later time (provided the modes are still super-horizon sized and we have radiation domination). In leading order, the coefficients will remain the same while in next-to-leading order we can use the evolution of $\mathbf{U}$ to compute the coefficients for $z < z_{initial}$. If initial conditions are specified with accuracy of next-to-leading order one therefore has to specify $z_{initial}$ as well. In leading order this is unnecessary for z in a wide range long before last scattering.

6.5   Constraint Equations to Leading Order

Equation (6.17) is equivalent to setting the l.h.s. of Equations (6.2)-(6.11) equal to zero and using $\Omega_c = \Omega_b = x^2 = 0$. Then Equations (6.2), (6.4), (6.6) and (6.7) are

automatically satisfied (provided $\tilde{V}_\alpha$ does not diverge $\propto x^{-2}$ or faster), and Equations (6.3),(6.5),(6.8)-(6.11) yield non-trivial constraints for the components of $\boldsymbol{U}_0$:

$$2\tilde{V}_c - \Psi = 0, \tag{6.27}$$

$$1/4\Delta_\gamma - \tilde{V}_\gamma + \Omega_\nu\tilde{\Pi}_\nu + 2\Psi = 0, \tag{6.28}$$

$$1/4\Delta_\nu - \tilde{V}_\nu + \Omega_\nu\tilde{\Pi}_\nu + 2\Psi = 0, \tag{6.29}$$

$$8/5\tilde{V}_\nu - 2\tilde{\Pi}_\nu = 0, \tag{6.30}$$

$$3\Omega_\nu\tilde{\Pi}_\nu + \Delta_q/(1+w_q) + 3\tilde{V}_q + 3\Psi = 0, \tag{6.31}$$

$$3\Omega_\nu\tilde{\Pi}_\nu + \Delta_q/(1+w_q) + \tilde{V}_q + 4\Psi = 0. \tag{6.32}$$

In the above, all quantities are considered only to constant order. (we have omitted the subscript '0' for notational convenience.) In particular, there is no contribution of CDM and baryons to Ψ at constant order. Note that, apart from w_q, no model-specific parameters occur in any of these equations so the modes will be independent of the type of quintessence as long as the scalar field is in a regime with approximately constant w_q. We note that for w_q substantially smaller than $1/3$ the quintessence fraction Ω_q changes with time. By the assumption that the universe expands as if radiation dominated, the quintessence contribution would however be small in this case and its contribution to Ψ can be neglected.

We mention that for $w_q = 1/3$, quintessence evolves the same way as radiation, therefore Ω_q does not change in this case. If $w_q = -1/3$, quintessence has the same influence on the scale factor a as a curvature term in an open universe. However, the geometry is still flat and one can distinguish an open universe from this quintessence model by measuring the position of the first acoustic peak in the CMB.

6.6   The Modes in Detail

6.6.1   Classifying the Modes

While any basis for the subspace spanned by the eigenvectors with eigenvalue $\lambda = 0$ can be used to specify the initial conditions, it is still worthwhile to use a basis that is physically meaningful. Following the existing literature, we use the gauge-invariant entropy perturbation [90]

$$S_{\alpha:\beta} = \frac{\Delta_\alpha}{1+w_\alpha} - \frac{\Delta_\beta}{1+w_\beta}, \tag{6.33}$$

between two species α and β, as well as the gauge-invariant curvature perturbation on hyper-surfaces of uniform energy density of species α [96,98,109]

$$\zeta_\alpha = \left(H_L + \frac{1}{3}H_T\right) + \frac{\delta\rho_\alpha}{3(1+w_\alpha)\bar{\rho}_\alpha}, \tag{6.34}$$

in order to classify the physical modes. On slices of uniform total energy density, the curvature perturbation is correspondingly

$$\zeta_{tot} = \left(H_L + \frac{1}{3} H_T \right) + \frac{\sum_\alpha \delta\rho_\alpha}{\sum_\alpha 3(1 + w_\alpha)\bar\rho_\alpha}. \tag{6.35}$$

In our variables, these expressions take on the manifestly gauge-invariant form

$$\zeta_\alpha = \frac{\Delta_\alpha}{3(1 + w_\alpha)} \ , \quad \zeta_{tot} = \frac{\sum_\alpha \Delta_\alpha \Omega_\alpha}{\sum_\alpha 3(1 + w_\alpha)\Omega_\alpha}. \tag{6.36}$$

If $\zeta_{tot} = 0$, energy density perturbations do not generate curvature. It is therefore clear that such a perturbation is a perturbation in the local equation of state. One should note that the definition of ζ_{tot} is different from that of [91]:

$$\zeta_{MFB} = \frac{2}{3} \frac{\mathcal{H}^{-1}\dot\Psi + \Psi}{(1 + w)} + \Psi. \tag{6.37}$$

However, one may verify that this quantity coincides with ζ_{tot} in the super-horizon limit for a flat universe [110].

6.6.2 The Adiabatic Mode

The first (rather intuitive) perturbations one would try to find are adiabatic perturbations, which are specified by the adiabaticity conditions $S_{\alpha:\beta} = 0$ for all pairs of components. In our case, this results in eleven constraints[4] for the ten components of $\boldsymbol{U}_0$. It is a priori not clear that this has a solution so we will not include quintessence in the adiabaticity requirement. Requiring adiabaticity between CDM, baryons, neutrinos and radiation,

$$\Delta_\nu = \Delta_\gamma = \frac{4}{3}\Delta_c = \frac{4}{3}\Delta_b, \tag{6.38}$$

and using the six constraint Equations (6.27)-(6.32), we obtain

$$\begin{pmatrix} \Delta_c \\ \tilde{V}_c \\ \Delta_\gamma \\ \tilde{V}_\gamma \\ \Delta_b \\ \Delta_\nu \\ \tilde{V}_\nu \\ \tilde{\Pi}_\nu \\ \Delta_q \\ \tilde{V}_q \end{pmatrix}_{\text{adiabatic}} = C \begin{pmatrix} 3/4 \\ (-5/4)\,\mathcal{P} \\ 1 \\ (-5/4)\,\mathcal{P} \\ 3/4 \\ 1 \\ (-5/4)\,\mathcal{P} \\ -\mathcal{P} \\ 3(1 + w_q)/4 \\ (-5/4)\,\mathcal{P} \end{pmatrix}, \tag{6.39}$$

---

[4]Without requiring quintessence to be adiabatic, we have six constraints from equations (6.27)-(6.32) plus three constraints from Eq. (6.38) plus one constraint from the overall normalization, which is fixed by choosing a specific value for Δ_γ.

where $\mathcal{P} = (15 + 4\Omega_\nu)^{-1}$ and C is an arbitrary constant. From $\Delta_q/\Delta_\gamma = 3(1 + w_q)/4$ we conclude that quintessence is automatically adiabatic if CDM, baryons, neutrinos and radiation are adiabatic, independent of the quintessence model for as long as we are in the tracking regime. As all components are non-vanishing, we do not quote the next to leading order contributions from $x\,\boldsymbol{U}_1$.

6.6.3 Neutrino Isocurvature

Having found the adiabatic vector, one could specify three additional linearly independent vectors satisfying the constraint Equations (6.27)-(6.32). This would complete the basis. It is, however, appropriate to choose modes that may be generated by physical processes. These modes are in general not orthogonal but span the eigenspace of $\lambda = 0$. Modes that may be generated by physical processes are isocurvature modes. A given mode is an isocurvature mode, if the gauge-invariant curvature perturbation ζ_{tot} vanishes, i.e. $\zeta_{tot} = 0$. In order to distinguish different isocurvature modes from one another, we require that the other species are adiabatic with respect to each other, i. e. $S_{\alpha:\beta} = 0$ except for quintessence and one species σ, which has non-vanishing $S_{\sigma:\gamma}$.

Let us first consider the neutrino isocurvature mode. For this, we require that CDM, baryons and radiation are adiabatic, while $S_{\nu:\gamma} \neq 0$ and that the gauge-invariant curvature perturbation vanishes:

$$\zeta_{tot} = 0, \quad \Delta_c = \Delta_b = \frac{3}{4}\Delta_\gamma. \tag{6.40}$$

Using this and Equations (6.27)-(6.32) leads to

$$\begin{pmatrix} \Delta_c \\ \tilde{V}_c \\ \Delta_\gamma \\ \tilde{V}_\gamma \\ \Delta_b \\ \Delta_\nu \\ \tilde{V}_\nu \\ \tilde{\Pi}_\nu \\ \Delta_q \\ \tilde{V}_q \end{pmatrix}_{\text{neutrino iso.}} = C \begin{pmatrix} 3/4 \\ \Omega_\gamma \mathcal{P} \\ 1 \\ \left(\Omega_\gamma + \Omega_\nu + \frac{15}{4}\right)\mathcal{P} \\ 3/4 \\ -\Omega_\gamma/\Omega_\nu \\ -\frac{15}{4}\mathcal{P}\,\Omega_\gamma/\Omega_\nu \\ -3\,\mathcal{P}\,\Omega_\gamma/\Omega_\nu \\ 0 \\ \Omega_\gamma \mathcal{P} \end{pmatrix}. \tag{6.41}$$

It is important to note that we did not require quintessence to be adiabatic. One can see from the neutrino isocurvature vector that $\Delta_q = 0$, and as a consequence quintessence is not adiabatic with respect to either neutrinos, radiation, baryons or CDM. Hence, we could just as well have labeled this vector "quintessence isocurvature". We cannot require adiabaticity between neutrinos, CDM, baryons and radiation and hope to obtain

a "pure" quintessence isocurvature vector since, as we have seen in the discussion of the adiabatic mode, these requirements lead to quintessence being adiabatic as well.

6.6.4   CDM Isocurvature and Baryon Isocurvature

The CDM isocurvature mode is characterized by $S_{c:\gamma} \neq 0$, $\zeta_{tot} = 0$ and adiabaticity between photons, neutrinos and baryons:

$$\zeta_{tot} = 0, \quad \Delta_\gamma = \Delta_\nu = \frac{4}{3}\Delta_b. \tag{6.42}$$

Using this and Equations (6.27)-(6.32) yields

$$\boldsymbol{U}_0^T(\text{CDM iso.}) = (1, 0, 0, 0, 0, 0, 0, 0, 0, 0). \tag{6.43}$$

This vector fulfills $\zeta_{tot} = 0 + \mathcal{O}(\Omega_c)$, which is in line with our approximation since $\Omega_c \ll 1$. Similarly, for the Baryon Isocurvature mode, we require $S_{b:\gamma} \neq 0$, $\zeta_{tot} = 0$ and adiabaticity between photons, neutrinos and baryons. The resulting vector reads

$$\boldsymbol{U}_0^T(\text{baryon iso.}) = (0, 0, 0, 0, 1, 0, 0, 0, 0, 0). \tag{6.44}$$

As all but one of the components of $\boldsymbol{U}_0$ are vanishing for CDM Isocurvature and Baryon Isocurvature, we use Equation (6.18) to obtain the next to constant order solution for CDM Isocurvature

$$\begin{pmatrix} \Delta_c \\ \tilde{V}_c \\ \Delta_\gamma \\ \tilde{V}_\gamma \\ \Delta_b \\ \Delta_\nu \\ \tilde{V}_\nu \\ \tilde{\Pi}_\nu \\ \Delta_q \\ \tilde{V}_q \end{pmatrix}_{\text{CDM iso.}} = C \begin{pmatrix} 1 \\ \Omega_c(4\Omega_\nu - 15)\mathcal{U}/12 \\ 0 \\ -(15/4)\Omega_c\mathcal{U} \\ 0 \\ 0 \\ -(15/4)\Omega_c\mathcal{U} \\ -2\Omega_c\mathcal{U} \\ \Omega_c(15 + 2\Omega_\nu)(1 + w_q)\mathcal{U} \\ \Omega_c\mathcal{U}\mathcal{V} \end{pmatrix}, \tag{6.45}$$

where $\mathcal{U} = (30 + 4\Omega_\nu)^{-1}$ and $\mathcal{V} = [105 - 45w_q + 4\Omega_\nu(3w_q - 1)]/[36(w_q - 1)]$. Similarly,

we find for Baryon Isocurvature

$$
\begin{pmatrix}
\Delta_c \\
\tilde{V}_c \\
\Delta_\gamma \\
\tilde{V}_\gamma \\
\Delta_b \\
\Delta_\nu \\
\tilde{V}_\nu \\
\tilde{\Pi}_\nu \\
\Delta_q \\
\tilde{V}_q
\end{pmatrix}_{\text{baryon iso.}}
= C
\begin{pmatrix}
0 \\
\Omega_b(4\Omega_\nu - 15)\mathcal{U}/12 \\
0 \\
-(15/4)\Omega_b\mathcal{U} \\
1 \\
0 \\
-(15/4)\Omega_b\mathcal{U} \\
-2\Omega_b\mathcal{U} \\
\Omega_b(15 + 2\Omega_\nu)(1 + w_q)\mathcal{U} \\
\Omega_b\mathcal{U}\mathcal{V}
\end{pmatrix}.
\tag{6.46}
$$

Note that these vectors are not constant since Ω_b and Ω_c both evolve in time. We observe that the corrections to U are indeed proportional to Ω_c or Ω_b as expected. This result holds for all tracking quintessence models with $w_q = 1/3$ or $w_q \leq 0$ during the radiation dominated period. For intermediate values $0 < w_q < 1/3$ the deviation from the leading behavior scales $\propto x^\alpha$, $\alpha < 1$. Obviously, the adiabatic, CDM Isocurvature, Baryon Isocurvature and neutrino isocurvature vectors U_0 are linearly independent. We have therefore identified four modes corresponding to the fourfold degenerate eigenvalue zero of $A(x)$. These four vectors span the subspace of dominant modes in the super-horizon limit, and there are no more linearly independent vectors that satisfy the constraints (6.27) - (6.32). Arbitrary initial perturbations may therefore be represented by projecting a perturbation vector U at initial time into the subspace spanned by the four aforementioned vectors, as this is the part of the initial perturbations which will dominate as time progresses.

Figure 6.1 demonstrates that the early time behavior is well described by our analytic formulae. It also includes the comparison of the field fluctuation X as derived in Appendix A for completeness. The analytic results agree very well with the simulation for early times, when the mode is outside the horizon. In the lower graph, we plot the equation of state w_q. The quintessence model used is parameterized by an equation of state $w_q(a) = -0.95 + 0.75(1 - a)$, leading to $w_q(\text{early}) = -0.2$ and according to (A3), $X \propto \tau^{0.8}$. This differs from reference [106]. [5]

We see that including quintessence does not add a new dominant mode. The two additional modes added by the fluctuations of the scalar field are both subdominant and decay with negative eigenvalue λ_i. This is due to the fact that none of the perturbation equations for quintessence equate to zero in the superhorizon limit. This holds for

---

[5] In [106] it is stated that the quintessence fluctuation in Newtonian gauge scales $\propto \tau^2$ for adiabatic initial conditions. This does not agree with our results in Appendix. Actually, equation (101) of [106] includes a factor φ_{t0}, which, interpreted as a dynamical quantity $d\varphi/dt$ (and not fixed at some initial time t_0), leads to a power law in τ which is then consistent with our result for the field perturbation.
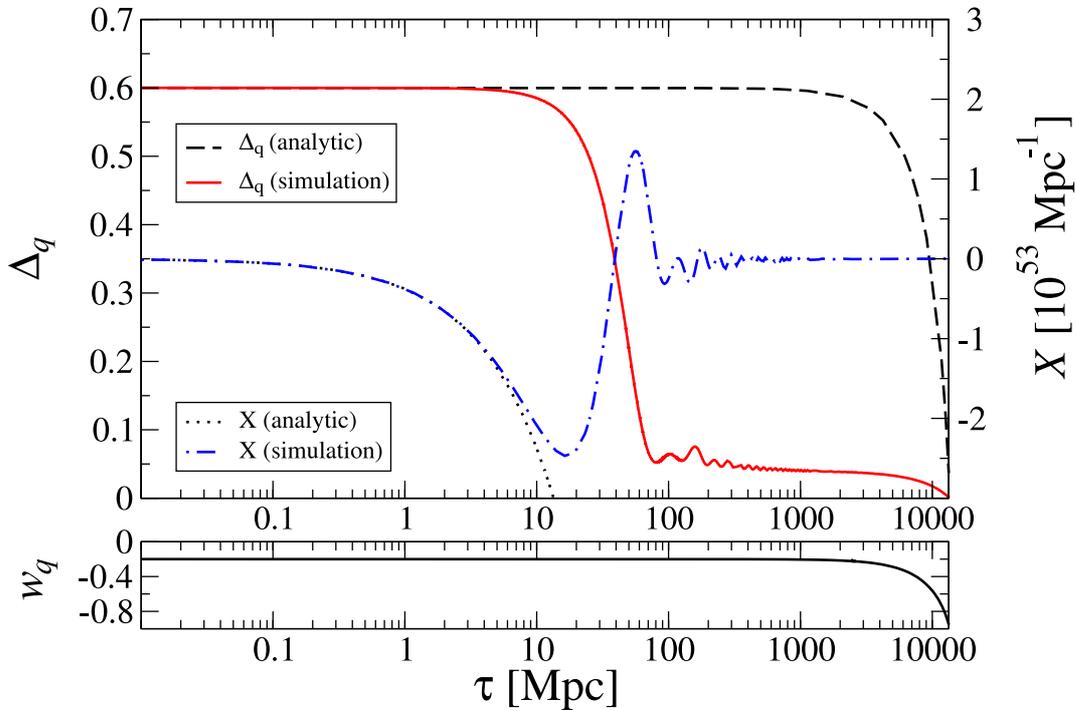
Figure 6.1: Gauge-invariant energy density perturbation Δ_q and quintessence field fluctuation X as simulated (straight and dashed-dotted lines), compared to the analytic solution of Equations (6.39) and (A3) (dashed and dotted lines) as a function of conformal time τ for adiabatic initial conditions. Radiation and matter equality corresponds to $\tau = 109$Mpc. Shown is the mode for $k = 0.1\,\mathrm{Mpc}^{-1}$ and the cosmological parameters have been $\Omega_b^0 h^2 = 0.022$, $h = 0.7$, $\Omega_m^0 = 0.3$, $\Omega_q^0 = 0.7$.

non-tracking quintessence models as well. Let us investigate this in detail. For all the other fluid components, $\Delta_a' = 0$ in the super-horizon limit, but for quintessence we get from Eq. (5.40) that $\Delta_q' = -3(c_{s(q)}^2 - w_q)\Delta_q - 3w_q\Gamma_q$. For tracking quintessence, we obtain from equation (5.57) that $c_{s(q)}^2 = w_q$ and we find

$$\Delta_q' = -3w_q\Gamma_q \tag{6.47}$$

Since Γ_q does not vanish except for $w_q = 1$ (see Eq. (5.56)), this does not equate to zero. [6] Hence, due to the non-vanishing entropy perturbation of quintessence there is no additional dominant mode. [7]

---

[6]Note that $w_q = 0$ does not lead to $\Delta_q' = 0$.

[7]We have not yet investigated the relationship between decaying quintessence modes and the back-
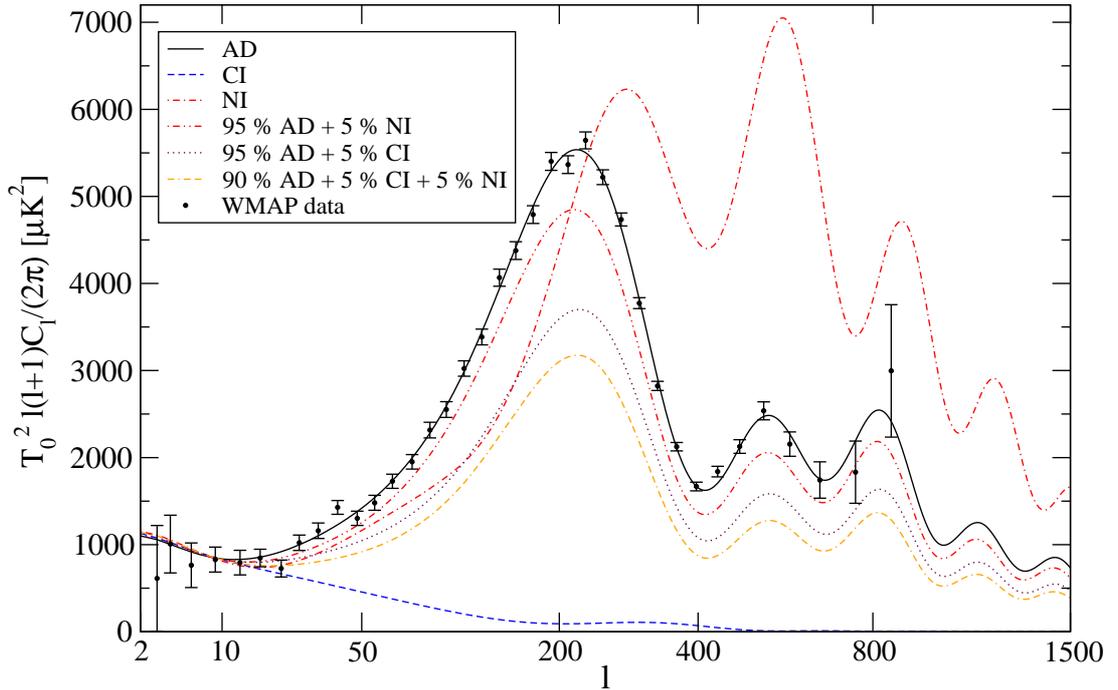
Figure 6.2: CMB Temperature spectra as a function of multipole l in an early quintessence cosmology. The pure adiabatic (AD), CDM isocurvature (CI), neutrino isocurvature (NI) mode and three different combinations of these dominant modes are plotted. For comparison with experimental data we also give the WMAP measurements of the CMB [50]. The spectrum of the pure Baryon Isocurvature mode is essentially identical to that of the pure CDM Isocurvature mode. All spectra have been normalized to the same power at $l = 10$.

6.7 Isocurvature Initial Conditions and the CMB

We illustrate the influence of different initial conditions on the CMB with an example. For an analysis of experimental data and a possible isocurvature contribution to the CMB we refer the reader to [111–113]. Here, we merely wish to show the qualitative features of the different modes. We use a modified version of CMBEASY [92,114] to compute CMB spectra corresponding to different initial conditions for an early quintessence model which will be shown in Chapter 7 to fit the WMAP data very well [107]. The exact values of the parameters can be found in Table 7.1. We set the spectral index of the isocurvature modes identical to the spectral index of the pure adiabatic mode, $n_s = 0.99$. The resulting spectra are plotted in Fig. 6.2.

The spectrum of the pure CDM isocurvature mode decays quickly when going to small scales as has been found in previous works [115–117]. The neutrino isocurvature mode

---

ground evolution.

shows prominent peaks at higher multipoles than the adiabatic mode with different peak ratios. For the mixed initial conditions with only small isocurvature contribution, the shape of the curve remains more or less the same. A small admixture of isocurvature fluctuations leads to a decrease of power at larger multipoles if the overall normalization is fixed at $l = 10$. Comparison with the WMAP data in the same figure shows that non-adiabatic initial perturbations are strongly constrained. Clearly, pure isocurvature initial conditions are inconsistent with CMB observations.

We have not performed a full scale Markov Chain Monte Carlo simulation with varying initial conditions to find the best fit model allowing for the inclusion of isocurvature perturbations. This would introduce new degrees of freedom to allow for a better fit to the experimental data. Wether the gain in χ^2 would be significant to clearly point towards a primordial spectrum containing isocurvature contributions remains to be determined.

6.8   Remarks on Isocurvature Initial Conditions

We have investigated perturbations in a radiation-dominated universe containing quintessence, CDM, neutrinos, radiation and baryons in the tight coupling limit. The perturbation evolution has been expressed as a differential equation involving a matrix acting on a vector comprised of the perturbation variables. This formulation leads to a systematic determination of the initial conditions. In particular, we find that due to the presence of tracking scalar quintessence no additional dominant mode is introduced. This fact is beautifully transparent in the matrix language. Indeed, contributions of higher order in $x \equiv k\tau$ towards a perturbation vector $\boldsymbol{U}$ can easily be determined by solving a simple matrix equation once the constant part of $\boldsymbol{U}$ has been determined.

In total, we find four dominant modes and choose them as adiabatic, CDM Isocurvature, Baryon Isocurvature and Neutrino Isocurvature. For the Neutrino Isocurvature mode, quintessence automatically is forced to non-adiabaticity. Hence, we could have as well labeled the Neutrino Isocurvature mode as quintessence isocurvature. To demonstrate the influence on the cosmic microwave background anisotropy spectrum, we have calculated spectra for all modes. Clearly, non-adiabatic contributions are severely constrained by the data. A detailed study may provide ways to put additional constraints on quintessence models or reveal details about the initial perturbations after inflation.

Early Quintessence and the CMB

Recently performed high precision measurements of the CMB by the WMAP satellite [49, 50, 58, 118–120] open the possibility to test and compare different cosmological models with unprecedented accuracy. Due to this improvement in available data it is possible to tighten the constraints on various cosmological parameters. Combining the different cosmological probes like CMB, LSS and SNe Ia observations it seems possible to falsify some cosmological models based on those new data sets.

Here, we will now present an analysis of the first year WMAP data.

7.1   WMAP Results

The WMAP collaboration has analyzed the WMAP first year data in different ways. The underlying cosmological model that was used to calculate the resulting CMB spectrum was a ΛCDM model with adiabatic power-law primordial density fluctuations, i.e.

$$|\delta_k|^2 \propto k^{n_s}. \tag{7.1}$$

The second model against which the experimental data was tested was a ΛCDM model with a k-dependant spectral index, the so-called running spectral index model. None of those two models had a dynamical dark energy component. We will now present an analysis with a leaping kinetic term (LKT) quintessence scenario with a constant spectral index close to one which is able to fit the data equally well.

The WMAP team used different data sets to complement the WMAP measurement. For the higher l region of the CMB spectrum (where WMAP did not take data) they additionally used the CBI [62,63] and ACBAR [61] measurements. The matter power spectrum obtained from the WMAP spectrum was supplemented with the large scale structure (LSS) data from the 2dFGRS [68] and the LSS estimate from the Ly-alpha data from Croft et. al. [69]. The WMAP collaboration presents the best fit cosmological

model for the WMAP data alone, for WMAP and the other CMB experiments, a model with further constraints from the matter power spectrum from 2dFGRS and finally a model also including also the Ly-alpha datapoints (for details see [50]).

For the two different models the cosmological parameters obtained from various data sets have already been quoted in Tables 4.3.3 and 4.3.3.

7.2 Early Quintessence

The WMAP team analyzed the available data with the help of a ΛCDM model. We will extend this analysis to quintessence models and explicitly investigate the claimed k-dependent spectral index. In the basic quintessence scenario, the dark energy enters only at late times, as required for cosmic acceleration. In a more realistic picture, the late appearance of the quintessence may not be the whole story. As has been mentioned in Chapter 2, scalar field models of quintessence with global attractor solutions [8, 9, 24, 25] have been shown to "track" the dominant component of the cosmological fluid. One consequence is that just after inflation, the universe may contain a non-negligible fraction of the cosmic energy density. Through subsequent epochs, the quintessence energy density ρ_q lags behind the dominant component of the cosmological fluid with a slowly varying Ω_q, and an equation-of-state $w_q \equiv p_q/\rho_q$ which is nearly constant. The field energy tracks the background until the current epoch, when the quintessence energy density crosses and overtakes the matter density. A non-negligible fraction of dark energy at last scattering, $\Omega_q^{(ls)}$, and during structure formation, $\Omega_q^{(sf)}$, then arises quite naturally. From the observational viewpoint, detection of any trace of "early quintessence" would give us a tremendous clue as to the physics of dark energy.

We will focus on "early quintessence", characterized by non-negligible values $\Omega_q^{(ls)}$, $\Omega_q^{(sf)} \lesssim 0.05$. Typical scalar field models exhibit an exponential form of the scalar potential in the range of the field relevant for early cosmology, with special features in the potential or kinetic term in the range governing the present epoch [31, 34, 36, 121–123]. These LKT quintessence explicitly allows for a non-negligible fraction of dark energy at last scattering or structure formation.

Our attention is drawn toward these models due to the claims of suppressed power on small scales in the combined WMAP / CMB / large scale structure data set. We are motivated precisely by the fact that the most prominent influence of a small amount of early dark energy is a suppression of the growth of dark matter fluctuations [124, 125]. As we discuss, this influence can help to make the fluctuation amplitude extracted from galaxy catalogues or the Ly-α forest compatible with a relatively high amplitude CMB anisotropy.

The effect of early quintessence on the mass fluctuation power spectrum can be

understood simply as a suppression of the growth function for dark matter and baryonic fluctuations. Just as fluctuation growth is suppressed at late times with the onset of dark energy, so is the growth of linear modes slowed at early times due to non-negligible $\Omega_{\mathrm{q}}^{(\mathrm{ls})}$, $\Omega_{\mathrm{q}}^{(\mathrm{sf})}$. We can directly examine the effect on the mass power spectrum by comparing the σ_8 values of an early quintessence model with a Λ model having the same amount of present-day dark energy. Fixing the amplitude of the CMB fluctuations over a range of angular multipoles corresponding to $k \approx (8\,\mathrm{Mpc})^{-1}$, then

$$\frac{\sigma_8(Q)}{\sigma_8(\Lambda)} = (a_{eq})^{3\Omega_{\mathrm{q}}^{(\mathrm{sf})}/5}(1 - \Omega_{\mathrm{q}}^{(0)})^{-(1+\tilde{w}^{-1})/5}\sqrt{\frac{\tau_0(Q)}{\tau_0(\Lambda)}}. \tag{7.2}$$

The dominant effect is the first factor with $a_{eq} = \Omega_r/\Omega_m \approx 1/3230$. This factor accounts for the slower growth of the cold dark matter fluctuations. The other kinematical factors involve a suitably averaged quintessence equation-of-state in the recent epoch, $\tilde{w}$ [126–128], and the present conformal time τ_0 for the quintessence and Λ models. We emphasize that Equation (7.2) results in a uniform suppression of the cold dark matter amplitudes for all modes that have entered the horizon since z_{eq}.

Now we turn to consider the implications of the CMB for quintessence. The temperature anisotropy power spectrum, from the plateau through the first two peaks, now has been measured with new accuracy. In the context of a spatially-flat Λ model, this would tell us the Hubble constant, h, matter and baryon densities, Ω_{m} and Ω_{b}, very precisely. For the case of quintessence, a degeneracy exists amongst these parameters, and the influence of the equation-of-state can play off the Hubble constant to achieve an otherwise indistinguishable anisotropy pattern out to small angular scales [127]. Clearly, the CMB sky is consistent with a small amount of early quintessence in addition to $\Omega_{\mathrm{q}}^{(0)}$ insofar as the angular-diameter distance to the last scattering surface is preserved. As a means of proof by example, we identify a set of models in Table 7.1 with observationally indistinguishable CMB patterns, *i.e.* identical peak positions, but differing amounts of $\Omega_{\mathrm{q}}^{(\mathrm{ls})}$, $\Omega_{\mathrm{q}}^{(\mathrm{sf})}$, shown as Models (A,B) in Figure 7.1. Model (C) is WMAP's best fit ΛCDM and Model (D) the best fit for an extended data set with ΛCDM and running spectral index [50]. Our methodology, therefore, is to use the CMB data to guide our search for compatible quintessence models, rather than carrying out an exhaustive survey of parameter space. We choose models with present-day equation-of-state $w_{\mathrm{q}}^{(0)} \lesssim -0.9$ so as to focus attention on the early rather than late quintessence behavior, as compared to a Λ model. Because a significant parameter degeneracy between the primordial scalar spectral index n_s and the optical depth to last scattering τ persists in the WMAP data, we explore different combinations of n_s, τ.

In Fig.7.2 we compare the prediction of our models for the matter power spectrum with data extracted from galaxy catalogues (e.g. 2dFGRS [68, 129, 130] or the Ly-α forest [69, 70]). In view of the uncertainties from bias and nonlinearities, the agreement is good for all models (A-D).
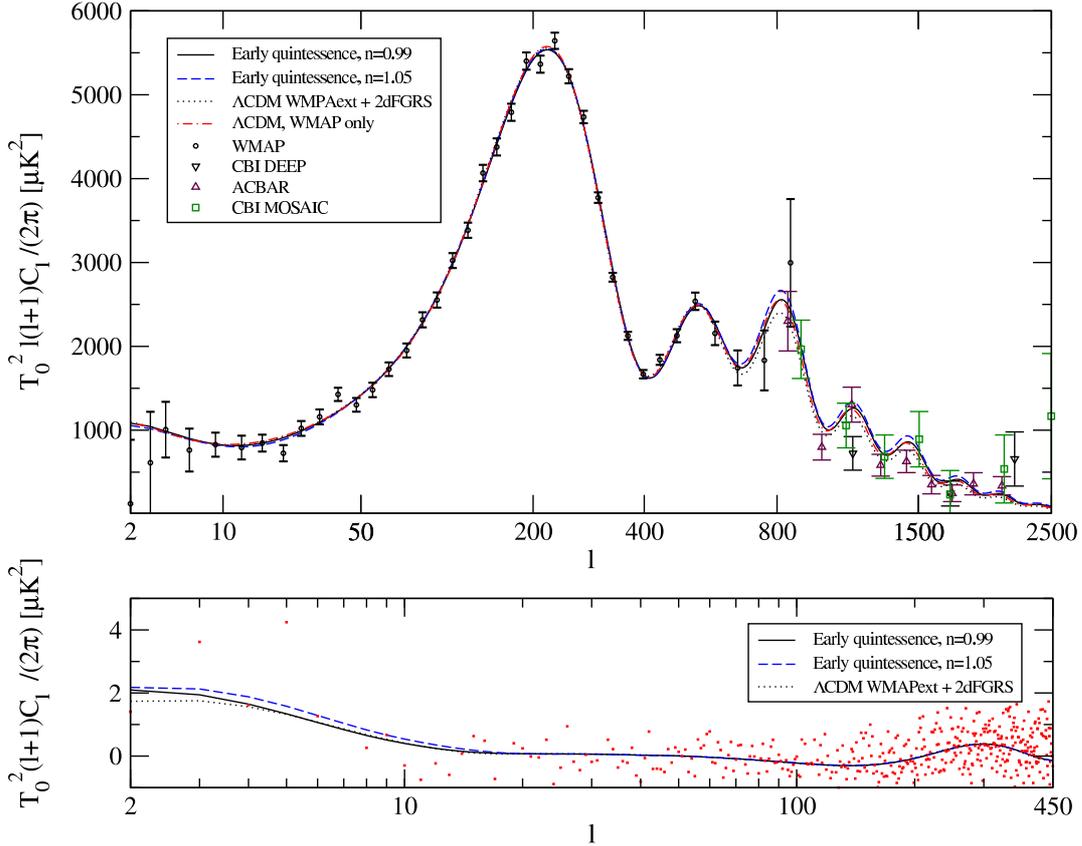
Figure 7.1: Temperature (TT) and Polarization (TE) as a function of multipole l. The WMAP data [58, 118] are plotted alongside two early quintessence models with $n_s = 0.99$ and $n_s = 1.05$ (see Table 7.1 for the other cosmological parameters). For comparison, we plot WMAP-normalized spectra for the best fit ΛCDM model (no Ly-α data) with constant spectral index $n = 0.97$ of [50], as well as the best fit ΛCDM model with running spectral index $n_s = 0.93$, $\mathrm{d}n_s/\mathrm{d}\ln k = -0.031$. At large l we plot the CBI [62, 63] and ACBAR [61] measurements.

Table 7.1: Models and parameters

	A	B	C	D
$\Omega_q^{(sf)}$	0.03	0.05	0	0
$\Omega_q^{(ls)}$	0.03	0.05	0	0
$w_q^{(0)}$	-0.91	-0.95	-1	-1
n_s	0.99	1.05	0.97	0.93
h	0.65	0.70	0.68	0.71
$\Omega_m h^2$	0.15	0.16	0.15	0.135
$\Omega_b h^2$	0.024	0.025	0.023	0.0224
τ	0.17	0.26	0.1	0.17
σ_8	0.81	0.87	0.87	0.85
χ^2_{eff}/ν	1432/1342	1432/1342	1430/1342	1432/1342

Increasing the spectral index to $n_s > 1$ induces more power for the fluctuation spectrum on small scales relative to large. We remark that this enhancement of small-scale power can be balanced by an increase in $\Omega_q^{(sf)}$. Typically, for σ_8 to remain constant a 10% increase of n_s is compensated by a 5% increase of $\Omega_q^{(sf)}$. Consequently we find a degeneracy in the $n_s - \Omega_q^{(sf)}$ plane for σ_8. (See Fig. 3d of [124].) The degeneracy may be broken once data for much larger k is included, such as the Ly-α forest. Whereas $\Omega_q^{(sf)}$ leads to a uniform decrease of all mass fluctuations with $k/h > 0.064\,\mathrm{Mpc}^{-1}$ by a constant factor, the increase of the small scale matter fluctuations due to n_s depends on scale $\propto k^{n_s}$.

An increase of n_s also influences the detailed CMB spectrum in a number of ways. First, the spectral index influences the precise location of the first peak in angular momentum space l_1. Parametrizing the location of the peaks as [131]

$$l_m = l_A(m - \varphi_m), \tag{7.3}$$

one observes that the shift φ_1 decreases by 4.7% if n_s increases by 10%. Keeping the well-measured position of l_1 fixed [120], this results in a decrease of l_A by 5%. As a consequence, the location of the second and third peak are shifted by $\Delta l_2 \approx 19$, $\Delta l_3 \approx 38$ towards smaller l. Again, this effect can (partly) be compensated by an increase of $\Omega_q^{(ls)}$ according to [132]

$$\varphi_1 \approx [1 - 0.466(n_s - 1)][0.2604 + 0.291\Omega_q^{(ls)}]. \tag{7.4}$$

Second, increasing n_s lowers the amplitude ratio between the second and first peak. This can to be compensated by a larger fraction of baryons $\Omega_b h^2$. Third, larger n_s adds power to the CMB spectrum at large l, or a lower relative power at low l. To the extent
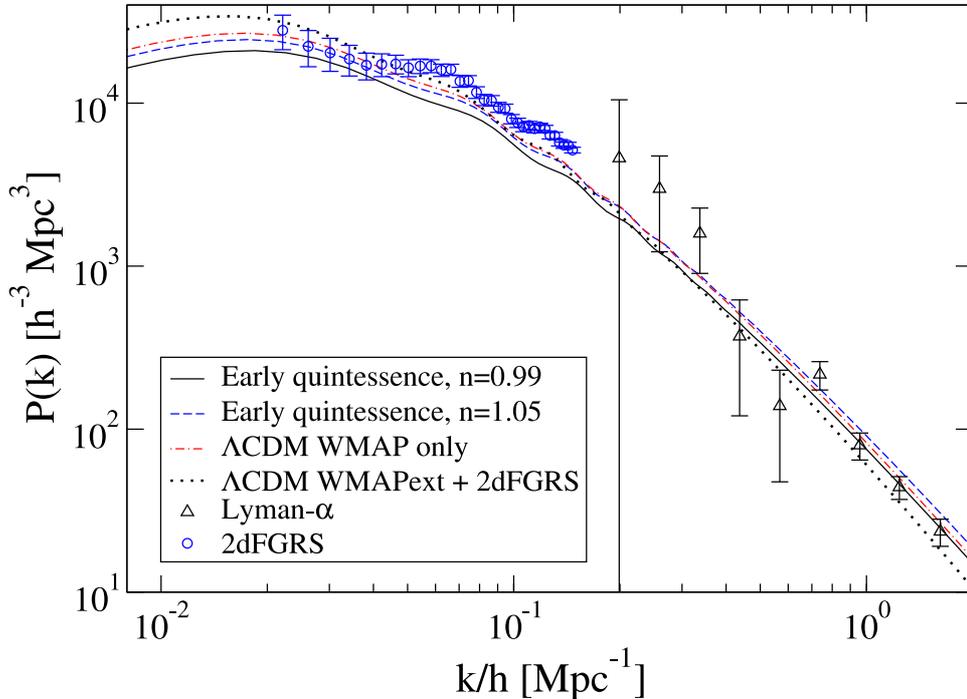
Figure 7.2: The cold dark matter power spectrum today as a function of k/h. We plot the linear spectrum for two early quintessence models with spectral indices $n_s = 0.99$ and $n_s = 1.05$ (see Table 7.1 for the other cosmological parameters). Also shown is the best fit Λ model with running spectral index $n_s = 0.93$, $dn_s/d\ln k = -0.031$ of [50], normalized to WMAP (no Ly-α data). The 2dFGRS [68,129,130] and Ly-α [69,70] data have been evolved to $z = 0$, although we have not convolved our theoretical data with the experimental window functions. The galaxy power spectrum has a bias compared to theoretical predictions which is not included in the figure.

that WMAP and COBE [133,134] observe a lack of power on large scales, $l \lesssim 10$, then a blue tilt is beneficial, as a 10% gain in n_s lowers the quadrupole relative to $l = 40$ by a factor of ~ 1.8, more in line with observations.

In the extended WMAP parameter analysis, combining CMB with non-CMB cosmological constraints, the running k-dependence in n_s is shown to lower the matter power spectrum at σ_8 and smaller scales, as well as reduce the small-angle CMB fluctuation power, without touching the region of l measured by WMAP [50]. In the case of early quintessence, the CMB power spectrum on small angular scales is only mildly lowered. However, the matter fluctuations turn out to be smaller for a given CMB amplitude.

The net effect is a shift of the CMB power extrapolated from structure formation data towards larger values.

We have computed the spectra in Figures 7.1, 7.2 using CMBEASY [92] for a class of "leaping kinetic term quintessence" [34] models with early quintessence. The main features depend only on two parameters besides the present fraction of dark energy $\Omega_q^{(0)}$ and the present equation of state $w_q^{(0)}$, namely the fraction of dark energy at last scattering, $\Omega_q^{(ls)}$, and during structure formation, $\Omega_q^{(sf)}$.

7.3   Parametrization

In order to facilitate comparison with other effects of quintessence – for example the Hubble diagram $H(z)$ for supernovae – we present a useful parametrization of quintessence [36, 122, 123] rather than detailed models. For $a > a_{eq}$ and $x \equiv \ln a = -\ln(1+z)$ we consider a quadratic approximation for the averaged equation-of-state $(x_{ls} \approx -\ln(1100))$

$$
\begin{aligned}
\overline{w}_q(x) &= -\frac{1}{x} \int_x^0 dx' w_q(x') \\
&= w_q^{(0)} + (\overline{w}_q^{(ls)} - w_q^{(0)})\frac{x}{x_{ls}} + Ax(x - x_{ls}).
\end{aligned}
\tag{7.5}
$$

The time-dependent average equation of state $\overline{w}_q(x)$ is directly connected to the time history of the fraction in dark energy $\Omega_q(x)$ according to

$$
\frac{\Omega_q(x)}{1 - \Omega_q(x)} = \frac{\Omega_q^{(0)}(1 + a_{eq})}{1 - \Omega_q^{(0)}} \frac{\exp(-3x\overline{w}_q(x))}{1 + a_{eq}\exp(-x)}
\tag{7.6}
$$

which connects $\overline{w}_q^{(ls)}$ to $\Omega_q^{(ls)}$. The parameter A is related to the average fraction of dark energy during structure formation $(a_{tr} \approx 1/3)$

$$
\Omega_q^{(sf)} = \int_{\ln a_{eq}}^{\ln a_{tr}} \frac{\Omega_q(a)\,d\ln a}{\ln(a_{tr}/a_{eq})}.
\tag{7.7}
$$

The parameters describing our models are (A): $\overline{w}_q^{(ls)} = -0.188$, $A = -0.0091$; (B): $\overline{w}_q^{(ls)} = -0.172$, $A = -0.015$. The Hubble expansion has a simple expression in terms of $\overline{w}_q(x)$

$$
\begin{aligned}
H^2(z) &= H_0^2 \Bigg[\Omega_q^{(0)}(1 + z)^{3(1+\overline{w}_q(x))} + \\
&\qquad \Omega_m^{(0)}\Big((1 + z)^3 + a_{eq}(1 + z)^4\Big) \Bigg].
\end{aligned}
\tag{7.8}
$$

Our models (A) and (B) are consistent with all present bounds for $H(z)$, including type 1a supernovae [128, 135–138].

To summarize, we have demonstrated that models of early quintessence are compatible with the presently available data for a constant spectral index of primordial density perturbations. Parameter degeneracies in the angular-diameter distance to last scattering are consistent with a small abundance of early quintessence. In turn, the presence of early quintessence results in a reduction in the spectrum of matter fluctuations on small scales, which may have significant consequences for the interpretation of combined CMB and large scale structure data. Increasing the spectral index as a means to understand the lack of very large scale power in the CMB can be compensated in part by increasing the amount of early quintessence. We look ahead toward on-going and future tests which afford tighter measurements of small scale CMB and matter power spectra. A precision measurement of the position and height of the third peak could be extremely helpful for determining the fraction of early quintessence.

Chapter 8

BBN and the Variation of the Fundamental Constants

We have already briefly mentioned the cosmological epoch at which hydrogen, helium and in small amounts deuterium, lithium and beryllium have been formed via nuclear reactions. Big Bang Nucleosynthesis is believed to be understood quite well. The process starts with a given number density of protons and neutrons and an ever decreasing temperature. As the the temperature drops the energy will reach a value below the binding energy of deuterium which will then be formed due to nuclear reactions. After that, tritium, helium-3 etc. can be synthesized. The various different nuclear reactions are strongly temperature dependent and to calculate the exact abundances needs accurate knowledge of the reaction rates and an elaborate numerical code. In principle this should suffice to give an exact prediction for the abundances of the light elements in the universe. Comparing the BBN predictions with the observed abundances establishes a powerful link between cosmology and nuclear physics. The baryon to photon ratio η is determined in this fashion and can be compared to the η that is deduced from the most up to date CMB experiment.

The WMAP [50] value for η reads $\eta = 6.14 \pm 0.25 \times 10^{-10}$ resulting in a prediction for the helium abundance $Y_{\mathrm{He}} = 0.2484^{+0.0004}_{-0.0005}$ [139]. Measurements of the helium abundance yield various values in the range $Y_{\mathrm{He}} = 0.2421 \pm 0.0021$, $Y_{\mathrm{He}} = 0.2444 \pm 0.0020$ [86] and $Y_{\mathrm{He}} = 0.238 \pm 0.002 \pm 0.005$ [140]. Furthermore, the abundances of deuterium and lithium-7 are much more delicate to determine from observation and bear much larger errors. This disagreement between two different determinations of Y_{He} (or η, if we deduce the one from the other) with two independent and yet seemingly accurate methods has attracted our interest.

Recently, a detection of a change in the fine structure constant α_{em} over cosmological time scales [141] has been reported. The observed absorption spectra of distant quasars showed evidence that the strength of the electromagnetic interaction and hence the

atomic energy levels had changed with time. The deduced bound on the variation of α_{em} is $\Delta\alpha_{em}/\alpha_{em} = -1.1 \pm 0.4 \times 10^{-5}$ [141]. There are several different methods and observations to detect a variation of the fundamental constants. Most of them will naturally just yield upper bounds on $\Delta\alpha_{em}/\alpha_{em}$. Amongst those experiments is the Oklo natural reactor [142, 143] and the rhenium to osmium decay measurements [144]. Both of these measurements strongly constrain a possible variation of α but only up to small redshift values. A change of the fundamental couplings at BBN ($z \sim 10^5$) is not strongly constrained by the measurements mentioned before. Although the evidence in favor of a variation of α_{em} is not convincing and the only direct detection via quasar absorption lines could not be verified [145–148] we will nevertheless spend some time to investigate the effects a change of the fundamental couplings will have on the predictions of Big Bang Nucleosynthesis.

In order to do this we need to calculate the BBN abundances as a function of the parameters that will change when we assume a variation of the fundamental couplings. Furthermore, in contrast to earlier investigations, we do not change the electromagnetic coupling and leave the others constant. We employ a simple grand unified theory scheme in which the variations of the couplings will be interdependent. This model seems more plausible to us than changing a single and not independent parameter in the model. Once we have derived the primordial abundances they will be stated as functions of the 'nuclear physics parameters' X_i

$$X_i = (M_{\bar{P}},\ \alpha_{em},\ \langle\phi\rangle,\ m_e,\ \tau_n,\ Q,\ B_d). \tag{8.1}$$

Here, $\langle\phi\rangle$ is the Higgs field vev, τ_n is the neutron lifetime, Q is the proton-neutron mass difference and B_d is the binding energy of the deuteron. These parameters will be related to the six dimensionless fundamental particle physics parameters G_k

$$G_k = (M_{\bar{P}}/\Lambda_{QCD},\ \alpha_{em},\ \langle\phi\rangle/\Lambda_{QCD},\ m_e/\Lambda_{QCD},\ m_q/\Lambda_{QCD},\ \Delta m/\Lambda_{QCD}). \tag{8.2}$$

We scale all quantities with respect to Λ_{QCD} which is the strong interaction scale. The reduced Planck mass $M_{\bar{P}}$ sets the gravitational interaction strength and the Higgs vev $\langle\phi\rangle$ is the weak scale. The quark masses enter this description via $m_q = (m_u + m_d)/2$ and $\Delta m = m_d - m_u$.

Because we do not use a full numerical simulation but a semi-analytical approximation we will restrict ourselves to analyze the helium abundance and leave the determination of deuterium and lithium abundances for future investigations.

8.1   Linearization

When we think of a change in the fundamental couplings we assume that this change between the time of BBN and today is very small. We therefore assume that we can

linearize this change in the different parameters G_k according to

$$\frac{\Delta Y_{\text{He}}}{Y_{\text{He}}} = \frac{Y_{\text{He}}(G + \Delta G) - Y_{\text{He}}}{Y_{\text{He}}} = \sum_k c_k^{(G)} \frac{\Delta G_k}{G_k}, \qquad (8.3)$$

where Y_{He} denotes the helium abundance in terms of mass fraction. As emphasized before this investigation is done to include the dependencies among the different G_k.

Because a nuclear physics calculation will involve the nuclear physics parameters X_i rather than the fundamental couplings the BBN estimmate will yield a result

$$\frac{\Delta Y_{\text{He}}}{Y_{\text{He}}} = \sum_i c_i^{(X)} \frac{\Delta X_i}{X_i}. \qquad (8.4)$$

We therefore need to relate both parameter sets to each. This is done via

$$\frac{\Delta X_i}{X_i} = \sum_k f_{ik} \frac{\Delta G_k}{G_k}, \qquad (8.5)$$

with

$$f_{ik} = \frac{\partial \, ln X_i}{\partial \, ln G_k}. \qquad (8.6)$$

Once the coefficients $c_i^{(X)}$ have been approximated from nuclear physics and the matrix f_{ik} has been determined the coefficients $c_k^{(G)}$ follow according to

$$c_k^{(G)} = \sum_i c_i^{(X)} f_{ik}. \qquad (8.7)$$

8.2 Analytic estimate for the primordial helium abundance

We will now analytically estimate the helium abundance dependent on the parameters X_i. Our approach to simplifying this problem is the same as that of Esmailzadeh, Starkman and Dimopoulos [149] and we will also use their form of short notation. It abbreviates the reaction

$$\alpha + \beta \rightarrow \gamma + \delta \qquad (8.8)$$

as $[\alpha\beta\gamma\delta]$ and will be used in the following discussion.

Before BBN, the universe contains protons and neutrons which are in thermal equilibrium. The reaction rate for converting neutrons into protons is given by [150]

$$\Gamma_{n \rightarrow p} = A \int dx \; x^2 \left(1 - \frac{m_e^2}{(Q + x)^2} \right)^{\frac{1}{2}} (Q + x)^2 (1 + e^{(x/T)})^{-1} (1 + e^{-(Q+x)/T})^{-1}. \quad (8.9)$$

The integral runs from $-\infty$ to $+\infty$ with an energy gap between $-Q - m_e$ and $-Q + m_e$ with Q being the proton neutron mass difference. Here $A \sim \langle \phi \rangle^{-4}$ is the 4 point

transition probability in Fermi-theory which depends on the axial and vector couplings c_V and c_A. For simplicity we will work with constant c_V and c_A.

We now need to define a criteria for which this reaction becomes small and one can regard the abundances of protons and neutrons to be fixed, i.e. a freeze out condition. There certainly exist some freedom of choice for this condition and we will assume that it happens when the Hubble expansion is comparable to the reaction rate. This defines a freeze out temperature

$$\Gamma_{n \to p}(T_n^*) = b \, H(T_n^*), \tag{8.10}$$

where the parameter b is put in to alter the freeze out temperature T_n^* slightly. We adjust b so that our helium abundance estimate (Y_{He}) is close to the prediction of a fully numerical study. This reflects the fact that we approximate a BBN calculation. The factor b must be set to $b = 1.22$ for our calculation to yield the numerically determined Y_{He} value. To solve Eq.(8.10) we also need the Friedmann equation

$$H^2 = \frac{\rho}{3M_{\bar{P}}^2} \tag{8.11}$$

and the energy density

$$\rho = g_* \frac{\pi^2}{30} T^4. \tag{8.12}$$

The effective number of massless degrees of freedom g_* (those with $m \ll T$) is given by

$$g_* = \sum_{i=bosons} \left(\frac{T_i}{T}\right) + \frac{7}{8} \sum_{i=fermions} \left(\frac{T_i}{T}\right). \tag{8.13}$$

At the temperature range we are considering ($\sim 1\text{MeV}$) we have to include the three neutrino species, electron and positron and the two photon polarizations. This yields a value of $g_* = 10.75$. Given T_n^* we can now determine the freeze out concentration of neutrons via

$$Y_n^* = \frac{1}{1 + e^{Q/T_n^*}}. \tag{8.14}$$

After this freeze out, the neutrons will decay according to

$$Y_n(t) = Y_n^* e^{t/\tau_n} \tag{8.15}$$

until they take part in the nuclear reactions and become bound in helium, deuterium or tritium. At the end of BBN, by far most neutrons are bound in helium and we are therefore justified to assume that the neutrons decay until the helium production rate dominates over the neutron decay. This defines a time t_f for free neutron decay

$$2\dot{Y}_{\text{He}}(t_f) = -\dot{Y}_n(t_f). \tag{8.16}$$

The final ^{4}He abundance is then estimated by

$$Y_{\text{He}} = \frac{1}{2} Y_n(t_f) = \frac{1}{2} Y_n^* e^{-(t_f/\tau_n)}. \tag{8.17}$$

It depends on the couplings via Q, T_n^*, τ_n and t_f. In turn, T_n^* depends on $A \sim \langle \phi \rangle^{-4}$, Q, m_e and $M_{\bar{P}}$ via Eqs. (8.9), (8.10) and (8.11). To determine the time t_f we use the fact that the dominant process for helium production is [151]
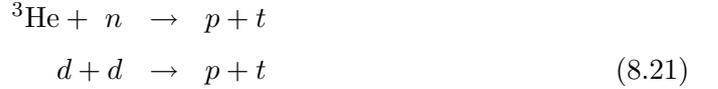
$$d + t \rightarrow {}^4\text{He} + n, \tag{8.18}$$

while we neglect the subdominant processes. Using the abbreviation introduced above the condition for t_f reads

$$2Y_\text{d}Y_\text{t}[dtn\alpha] = \frac{1}{\tau_n}Y_\text{n}^* e^{-t_f/\tau_n}. \tag{8.19}$$

As the time for free neutron decay depends on the abundances of deuterium (Y_d) and tritium (Y_t) we also need to determine those. Because we are in the temperature range around $\sim 1\text{MeV}$ the deuterium abundance is in equilibrium with the neutron and proton abundance ($Y_\text{p} \approx 1 - Y_\text{n}$) and given by the Saha equation [152]

$$Y_\text{d} = 8.15 \left(\frac{T}{m_n} \right)^{3/2} \eta \; e^{B_d/T} \; Y_n Y_p. \tag{8.20}$$

For the tritium abundance we need to consider the processes

$$\begin{aligned}
{}^3\text{He} + n &\rightarrow p + t \\
d + d &\rightarrow p + t
\end{aligned} \tag{8.21}$$

creating and

$$t + d \rightarrow {}^4\text{He} + n \tag{8.22}$$

annihilating tritium. Other reactions are subdominant by at least 2 orders of magnitude (as can be verified from [151]) and are therefore neglected. Close to thermal equilibrium the fixed point condition [149] leads us to an equation for Y_t of the form:

$$Y_\text{t} = \frac{Y_\text{n} \, Y_3 \, [n3pt] + Y_\text{d} \, Y_\text{d} \, [ddpt]}{Y_\text{d} \, [dtn\alpha]}. \tag{8.23}$$

To solve for Y_t the ${}^3\text{He}$ abundance is also required. The reactions involved are

$$\begin{aligned}
p + d &\rightarrow {}^3\text{He} + \gamma, \tag{8.24} \\
d + d &\rightarrow {}^3\text{He} + n, \tag{8.25} \\
d + {}^3\text{He} &\rightarrow p + {}^4\text{He}, \tag{8.26} \\
n + {}^3\text{He} &\rightarrow p + t. \tag{8.27}
\end{aligned}$$

Near the equilibrium the fixed point condition leads to

$$Y_3 = \frac{Y_\text{d} \, Y_\text{p}[pd3\gamma] + Y_\text{d} \, Y_\text{d}[ddn3]}{Y_\text{d} \, [d3p\alpha] + Y_\text{n} \, [n3pt]}. \tag{8.28}$$

We now have sufficient information to determine t_f and hence solve the equations above for the helium abundance Y_{He}. The equations ar not analytically solvable so we will need to solve them numerically.

What remains is to specify how we have incorporated the change of the parameters X_i into this estimate. Because we will rescale the model so that the strong scale Λ_{QCD} is kept fixed we don't need to consider changes in the reaction rates due to changes in the strong scale but only those due to a change in α_{em}. The dependence of the nuclear reaction rates on α_{em} has been studied by Bergström, Iguri and Rubinstein (BIR) [153] and was extended by Nollett and Lopez [154]. For standard reaction rates, we use the data of the NACRE compilation [155] where available, otherwise we use those of Smith, Kawano and Malaney (SKM) [151]. For the process $^{3}\text{He}(n, p)t$ we use the fit of Cyburt, Fields and Olive [156].

We assume a linear dependence of $\Delta Y_{\text{He}}/Y_{\text{He}}$ on the involved parameters. We have therefore investigated small changes in a single parameter while we keep the others fixed. This will yield the linear dependence of Y_{He} on the different parameters. The result of this numerical approximation in given in Table 8.1.

variable	$M_{\bar{P}}$	α_{em}	$\langle\phi\rangle$	m_e	τ_n	Q	B_D
coeff.	-0.81	-0.043	2.4	0.024	0.24	-1.8	0.53

Table 8.1: Coefficients $c_i^{(X)}$ for nuclear physics parameters

8.3 The Relation of the Fundamental Couplings to the Parameters X_i

What is left to be determined is the relation between the parameters

$$X_i = (M_{\bar{P}},\ \alpha_{em},\ \langle\phi\rangle,\ m_e,\ \tau_n,\ Q,\ B_d) \tag{8.29}$$

and the fundamental couplings

$$G_k = (M_{\bar{P}}/\Lambda_{QCD},\ \alpha_{em},\ \langle\phi\rangle/\Lambda_{QCD}m_e/\Lambda_{QCD},\ m_q/\Lambda_{QCD},\ \Delta m/\Lambda_{QCD}). \tag{8.30}$$

It is obvious that the matrix f_{ik} obeys the relation $f_{ik} = \delta_{ik}$ for $i = 1..4$ because the parameters are identical. Inspecting the list of parameters X_i, it is convenient to first determine the dependence of Q on the fundamental couplings because we will need this dependence to specify τ_n. To parametrize the $\Delta Q/Q$ in terms of the G_k we will use the formula provided by Gasser and Leutwyler [157] which reads

$$Q = \left[-0.76\left(1 + \frac{\Delta\alpha_{em}}{\alpha_{em}}\right) + 2.05\left(1 + \frac{\Delta(\Delta m)}{\Delta m}\right)\right] \text{ MeV} . \tag{8.31}$$

The binding energy of deuterium depends on the Higgs vev $\langle\phi\rangle$ and on the quarks masses via m_q and Δm. Assuming only small changes and hence a linear dependence on those parameters we keep one parameter fixed and vary the other.

To model the electromagnetic part we use the fit of Pudliner et al. [158] while for the dependence on $m_\pi \propto m_q^{1/2}$ we adopt the linear fit of Yoo [159]. This leads us to

$$B_d = B_d^0 \left[(r+1) - r\frac{m_\pi}{m_\pi^0}\right] - 0.018\frac{\Delta\alpha_{em}}{\alpha_{em}} \text{ MeV} , \qquad (8.32)$$

where r is a parameter that varies between 6 and 10 and $B_d^0 = 2.225$ MeV is the deuteron binding energy as measured in the laboratory today. Next, we need the change in the neutron lifetime in terms of a variation of the fundamental parameters. The most straight forward relation is those of the neutron lifetime and the weak scale $\tau_n \propto G_F^{-2} \propto \langle\phi\rangle^4$. What needs to be taken into account as well is the change in the phase space volume for free neutron decay

$$f = \int_{m_e}^{Q} dq \ q^2(Q-q)^2(1 - \frac{m_e^2}{q^2})^{1/2}. \qquad (8.33)$$

This phase space integral also depends on Q and hence we obtain additional terms from α_{em} and Δm leading to

$$\frac{\Delta\tau_n}{\tau_n} = 3.86\frac{\Delta\alpha_{em}}{\alpha_{em}} + 4\frac{\Delta\langle\phi\rangle}{\langle\phi\rangle} + 1.52\frac{\Delta m_e}{m_e} - 10.4\frac{\Delta(\Delta m)}{\Delta m}. \qquad (8.34)$$

The information given above is now sufficient to write down the matrix f_{ik} which is provided in Table 8.2. We do not claim to have included every possible effect but did take those into considerations which have the largest effect. If a zero is the matrix element there is no dependence at all, if a the entry is left empty the effect is to be neglected. Once we have determined f_{ik} we can calculate the relative change in Y_{He} if one varies the fundamental couplings G_k. This result is stated in Table 8.3.

8.4   Example

We have emphasized that we perform this investigation because the impact of a variation of the fundamental constants will not only be restrict to one parameter, for instance α_{em}. The underlying grand unified theory (GUT) will predict an interdependence of the relevant fundamental couplings. We want to demonstrate this with the help of a simple example. It is possible to specify many different plausible GUT models and we will choose one that renders the analysis relatively simple.

The scalar field χ that drives the time evolution of the fundamental couplings can be identified with the scalar field that accounts for the observed dark energy of the universe today [8,160]. This would imply that in a phenomenological approach we can

Table 8.2: The matrix entries f_{ik}, corresponding to the coefficients relating relative changes in G_k to relative changes in X_i.

parameter [1]	$M_{\bar{P}}$	α_{em}	$\langle\phi\rangle$	m_e	m_q	Δm
$M_{\bar{P}}$	1	0	0	0	0	0
α_{em}	0	1	0	0	0	0
$\langle\phi\rangle$	0	0	1	0	0	0
m_e	0	0	0	1	0	0
τ_n	0	3.86	4	1.52	-	-10.4
Q	0	-0.59	-	-	-	1.59
B_d	0	-0.0081	-	-	$-r/2$	-

Table 8.3: Coefficients $c_k^{(G)}$ for fundamental couplings

variable	$M_{\bar{P}}$	α_{em}	$\langle\phi\rangle$	m_e	m_q	Δm
coeff.	-0.81	1.94	3.36	0.389	-1.59	-5.358

calculate the field evolution and determine the variation of the fundamental couplings at the different epochs for which observational bounds exist, e.g. QSO absorption lines, the Oklo natural reactor bound and laboratory observations today. In this short example we will instead just study the era BBN without the relation to the other epochs, we therefore just need to assume that this field had a different value at the BBN epoch compared to today. The evolution of this cosmon field χ does not influence this example.

A detailed study of the dependencies of the fundamental couplings on a scalar field has been presented in [35, 36]. The calculation to one loop order yields [35]

$$\alpha_s^{-1}(M_W) = \frac{4\pi Z_F(\chi)}{\bar{g}^2} + \frac{7}{2\pi}\ln\zeta_w(\chi), \tag{8.35}$$

$$\alpha_w^{-1}(M_W) = \frac{4\pi Z_F(\chi)}{\bar{g}^2} + \frac{5}{3\pi}\ln\zeta_w(\chi), \tag{8.36}$$

$$\alpha_{em}^{-1}(M_W) = \frac{32\pi Z_F(\chi)}{3\bar{g}^2} - \frac{5}{3\pi}\ln\zeta_w(\chi), \tag{8.37}$$

where the W-Boson mass is $M_W(\chi) = \zeta_w(\chi)\,\chi$ and $Z_F(\chi)$ determines the renormalized grand unified gauge coupling ($g_R^2 = \bar{g}^2/Z_F$, $\bar{g}$ fixed). We normalize χ such that $M_{GUT}(\chi) = \chi$. The frame in which we work will be that of a constant strong interactions so that the reaction rates do not change for our helium abundance estimate. Note that such a frame can always be found via a Weyl scaling and will lead to a time

dependent reduced Planck mass $M_{\bar{P}}$. We also define that the ratio

$$\frac{M_{\bar{P}}(\chi)}{M_{GUT}(\chi)} = \frac{f}{\sqrt{6}} \tag{8.38}$$

is constant. From [35] we use the relations for the Planck scale

$$\ln \frac{M_{\bar{P}}}{m_n} = -\frac{2}{9} \ln \zeta_w + \ln f + \frac{8\pi Z_F}{9\bar{g}^2} \tag{8.39}$$

and the weak scale

$$\frac{\partial \ln M_W/m_n}{\partial \ln \chi} = \frac{7}{9} \frac{\partial \ln \zeta_W}{\partial \ln \chi} + \frac{8\pi^2}{9\bar{g}^2} \frac{\partial \ln Z_F}{\partial \ln \chi}. \tag{8.40}$$

We are now able to specify a particularly simple scenario in which we also keep the weak scale fixed w.r.t the strong scale, i.e.

$$\frac{\partial \ln M_W/m_n}{\partial \ln \chi} = 0. \tag{8.41}$$

Using $\delta(1/\alpha) = -\Delta\alpha/\alpha^2$, a short calculation then yields

$$\frac{\Delta\alpha_{em}(M_W)}{\alpha_{em}^2(M_W)} = -\frac{88\pi}{7} \frac{\Delta Z_F}{\bar{g}^2}. \tag{8.42}$$

From Eq. 8.39 we obtain

$$\frac{\Delta M_{\bar{P}}/\Lambda_{QCD}}{M_{\bar{P}}/\Lambda_{QCD}} = -\frac{\pi}{11} \frac{\Delta\alpha_{em}(M_W)}{\alpha_{em}^2(M_W)}. \tag{8.43}$$

The other G_k parameters are determined as follows. Because we fixed the weak scale we have $\Delta\langle\phi\rangle/\langle\phi\rangle = 0$, while for the others we neglect the variations in the Yukawa couplings and hence obtain

$$\frac{\Delta m_e}{m_e} = \frac{\Delta(\Delta m)}{\Delta m} = \frac{\Delta m_q}{m_q} = \frac{\Delta\langle\phi\rangle}{\langle\phi\rangle}. \tag{8.44}$$

The running of the coupling α_{em} below M_W is given by

$$\alpha_{em}(\mu)^{-1} = \alpha_{em}(M_W)^{-1} + \frac{2}{3\pi} \sum_i Q_i^2 \ln \frac{M_W}{\mu}, \tag{8.45}$$

where the charges Q_i of particles with masses in the range μ to M_W is given by five quarks in three colours plus three leptons

$$\sum_i Q_i^2 = 3 \times (8/9 + 3/9) + 3. \tag{8.46}$$

In this simple example we have $\Delta\alpha_{em}^{-1}(m_e) = \Delta\alpha_{em}^{-1}(M_W)$ and the only unknown parameter that remains is the unified gauge coupling Z_F. Because the GUT coupling is arbitrary and would serve to define the model we can equally well choose the parameter to be α_{em}. In this case we can specify what the change in α_{em} needs to be for the helium abundance to agree with the observed value $Y_{\text{He}} \approx 0.24$. We obtain

$$\frac{\Delta\alpha_{em}(m_e)}{\alpha_{em}(m_e)} = -1.0 \times 10^{-3}. \tag{8.47}$$

8.5   Remarks

The semi-analytic estimate presented here does not replace the need to study BBN with fully numerical codes. The main advantage of the presented analysis is the modular design which allows for easy improvements of the estimate without the need to change the whole calculation. This might be of interest to scientists who do not have the full numerical BBN code to test their hypothesis but want to estimate the specific effect on the BBN abundance predictions. For instance, it is easy to incorporate new results and estimates for the dependence of Y_{He} on the X_i without the need to alter the matrix f_{ik}. Likewise, if changes or improvements on the level of the fundamental couplings need to be implemented one needs to change the entries in the matrix f_{ik} without the need to change the helium abundance estimate. Last but not least, the specific GUT model is also disconnected from the different parts of the analysis. One can therefore easily test the predictions of a different GUT model by calculating the $c_k^{(G)}$ for that model and using the rest of the analysis as provided here.

Chapter 9

Conclusions

What is the present state of modern cosmology? The standard cosmological model explains most of the features we observe very well, although in a phenomenological way. The existence of both dark matter and dark energy is supported by an abundance of very accurate measurements. Despite the many proposed theories, the nature of dark matter and dark energy still remain obscured. Various possible dark matter explanations have been suggested, none of which could be verified by present experiments. The dark energy problem also remains unsolved, partly because possible models are not easily distinguished by experiments. Determining the equation of state of dark energy today and an accurate measurement of the dark matter power spectrum seem to be the most promising tools to further improve the constraints.

Other areas of cosmology and astrophysics are making progress but are still quite far from being fully understood. The ultra high energy cosmic rays are puzzling in nature and a proper computer simulation of structure formation, predicting the parameters we observe, is not yet possible. Nevertheless, the picture about the evolution of our universe is sketched with some parts of it still missing but many parts being put in the right place. Parametrizing our lack of knowledge with the help of dark matter and dark energy at least serves to give a name to the things in cosmology we really don't understand.

Trying to shed light on the open issues in cosmology, we presented work on several research topics involving quintessence as the dark energy component [107, 161, 162].

The discussion of the gauge problem followed the existing literature [53, 89, 90]. Based on this treatment we derived the perturbation equations for the energy density contrast and the velocity fields in a radiation dominated universe containing CDM, baryons, radiation, neutrinos and a scalar field. The presented matrix formulation and subsequent determination of the eigenmodes renders our analysis very transparent. The four dominant modes we have identified form a complete set of basis vectors in initial condition space. We find those four dominant modes and choose them as adiabatic,

CDM Isocurvature, Baryon Isocurvature and Neutrino Isocurvature. For the Neutrino Isocurvature mode it is interesting to note that quintessence is automatically forced to non-adiabaticity. Hence, we could have as well labeled the Neutrino Isocurvature mode as Quintessence Isocurvature. In particular, we find that due to the presence of tracking scalar quintessence no additional dominant mode is introduced by the scalar field because quintessence cannot be non-adiabatic if the other components are. With this decomposition into basis vectors we are able to analyze the CMB spectrum of any possible admixture of adiabatic and isocurvature initial conditions.

As was mentioned before, a neutrino velocity mode as a stable, non-decaying mode could not be found, contrary to the results of Bucher et al. [115]. This is due to the difference in formalism. Bucher et al. work in synchronous gauge and they argued in favor of the neutrino velocity mode because it has non-diverging potentials only in synchronous gauge. Such a neutrino velocity mode has diverging Newtonian potentials in longitudinal gauge or gauge-invariant formulation and is therefore absent in our discussion.

To analyze the possible contribution of isocurvature initial conditions towards the CMB we have calculated CMB spectra for the different isocurvature modes as well as for some admixtures of adiabatic and isocurvature initial conditions. We have not performed a full search of the parameter space to find the best fit mixture of isocurvature contributions but the presented results already show that pure isocurvature initial perturbations are excluded while admixtures are strongly constrained.

Following the discussion of initial conditions we focussed our work on the influence of early quintessence on the CMB spectrum. The WMAP collaboration introduced a ΛCDM model with a running spectral index to explain the WMAP first year data. This k-dependent spectral index introduces a tilt in the dark matter power spectrum. Noteworthy, a small contribution of quintessence towards the energy density at the time of last scattering $\Omega_q^{(ls)}$ or structure formation $\Omega_q^{(sf)}$ has the effect of suppressing the growth of structure for all dark matter modes that enter the horizon after matter radiation equality – a comparable effect to that of a running of the spectral index. We used LKT term quintessence models with non-negligible fractions of early quintessence to find cosmological models which fit the data and do not rely on a k-dependent spectral index. We presented two of those early quintessence models in Table 7.1. The WMAP data is the by far most accurate measurement of the CMB but did not have the discriminating power to rule out one of the cosmological models. Combining the WMAP result with other CMB experiments and large scale structure data does show an impressive agreement of various observations. The cosmological constant, despite being theoretically unsatisfying, does very well in explaining the data as do quintessence models. Tightening the constraints on the third peak in the CMB spectrum could increase the sensitivity in detecting early quintessence, as traces of non-negligible dark

energy contribution become discernable from a Λ dominated cosmological model.

A different aspect of an additional scalar field in cosmology was discussed in connection with the time variation of the fundamental couplings. Because a time evolution of the fundamental constants should be driven by a field it is natural to assume that this field can be identical with the quintessence field. Motivated by the slight discrepancies between theoretical predictions [139] and observational determination [86, 140] of the primordial helium abundance we studied the effects of a change of the fundamental couplings on the BBN predictions. The result we obtained is very useful in determining the effect of a change of the fundamental constants has on the predicted helium abundance. The evolution of the scalar field itself is of minor importance in this analysis as we have only compared the BBN epoch and today. To include the other bounds on a variation of α_{em} from the QSO absorption lines and the Oklo natural reactor one needs to calculate the time evolution of the quintessence field and find a model that incorporates the different constraints, as well as satisfying the other cosmological constraints the dark energy component has to obey. Indulging in the analysis of the interdependencies of the fundamental couplings in a GUT scheme was well justified. Our example shows that the dominant contribution to a change of the primordial helium abundance can be due to a change in the reduced Planck mass instead of the change in α_{em}. The provided treatment will hopefully encourage future researchers to include the relations among the different fundamental couplings when studying BBN predictions.

What can we expect from the proclaimed "decade of precision cosmology"? Maybe the answer to the nature of dark matter can be given by particle physics if the LHC is fully operational. The observation of dark matter decay products could guide this search for a dark matter particle candidate.

Concerning the cosmological model with all its parameters we depend on improving observational constraints to make progress. With the help of planned supernovae missions like SNAP we should be able to determine the equation of state very accurately. This should settle the question wether w is smaller , equal or larger than -1. Also, future CMB observations will be useful as ever, especially if some of these observations detect B-mode polarization confirming gravitational waves. Careful measurement of the E-mode and B-mode polarization and its cross-correlation with the temperature anisotropies can further constrain possible cosmological models. As was mentioned, scientists also discuss the possibility to use the SZ effect to gain more information on the surface of last scattering as seen by distant clusters. It will also be of great importance to combine the different observations to break the parameter degeneracies that exist.

Further improvements in the observational sector are already foreseeable. The theory of weak gravitational lensing and associated observations will hopefully provide excellent constraints on both the equation of state today and the dark matter distri-

bution in the universe. The direct probing of the dark matter power spectrum will also be able to rule out early dark energy as discussed in Chapter 7 and improve our knowledge of structure formation.

Putting it all together, with upcoming observational techniques, cosmologists have a good chance of making substantial progress in describing the universe. Whether the 'cosmological standard model' of the future will contain a scalar field, a cosmological constant or something entirely different only time can tell.

Acknowledgements

First of all I would like to thank Christof Wetterich, who gave me the chance of coming to Heidelberg without knowing anything about me. Since then he has been a great supervisor who enjoys the discussion among the research group and never refuses to give advise and to explain. In addition he provides an abundance of interesting ideas and spreads a very welcoming and positive atmosphere in the institute. A better support for my PhD thesis would not have been possible. I also thank my co-supervisor Michael G. Schmidt for showing interest in my work over the past three years and for his open minded and genuine attitude.

The friendly and fruitful surrounding is not imaginable without the other members of the research group. Michael Doran, Christian Mueller and Joerg Jaeckel are great colleges and good friends. I enjoyed every minute of the numerous discussions we had about almost any field of theoretical physics. I have to thank all of them for helping me to become a theoretical physicist.

Furthermore, I would like to thank my room mates under the roof of the ITP for making it such a memorable place to me. Greetings go to Frank Steffen (remember that legendary snowboarding day?), Jan Schwindt, Juliane Behrend, Tobias Kleinschmidt, Sebastian Diehl and Armin Steinkasserer.

But how come the ITP in Heidelberg is such a friendly place? The institute would of course collapse without the guiding hand of Eduard Thommes, who (apart from running the institute) also provided helpful advise about various astrophysical questions.

I also would like to express my gratitude towards my family for making it possible that I could study physics and for supporting me all my life. They taught me the attitude that was needed to accomplish this work.

Last but not least I am grateful Claudia who I deeply love. She stayed with me all those years that I studied in England and in Heidelberg and always believed in me. She gave me strength and to her I dedicate this work.

Appendix A

Early Time Quintessence Field Fluctuations

While in Chapter 5, we describe quintessence perturbations by the variables $\{\Delta_q, V_q\}$, one could instead use the field fluctuation and its time derivative $\{X, \dot{X}\}$. We will give analytic expressions for X and $\dot{X}$ in the case of tracking quintessence for super-horizon modes. We will do so assuming that Ψ and Φ are at least almost constant. As this is not the case for CDM Isocurvature and Baryon Isocurvature(which have been described in Chapter 6), the following steps do not apply in these modes. Furthermore, we will assume that the universe expands as if radiation dominated during the time of interest. In this case, $\mathcal{H} = \tau^{-1}$, $\Omega_q \propto \tau^{1-3w_q}$ and hence by means of Equation (5.51) $\dot{\varphi} \propto \tau^{-\frac{1}{2}(1+3w_q)}$. Using this, we infer from Equation (5.53) that $V' \propto \tau^{-\frac{1}{2}(7+3w_q)}$. In addition, a straightforward calculation using (5.52) and (5.53) yields

$$a^2\tau^2 V'' = a^2\tau^2 \frac{\mathrm{d}V'}{\mathrm{d}\tau}\frac{\mathrm{d}\tau}{\mathrm{d}\varphi} = \frac{3}{4}(1-w_q)(7+3w_q). \tag{A1}$$

The Equation of motion for X (5.43) contains a term $\dot{\varphi}\left(\dot{\Psi} - 3\dot{\Phi}\right)$, which by assumption we may drop. In addition, we see from Equation (A1), that for super-horizon modes, $a^2 V'' \gg k^2$ (except for w_q very close to 1), and hence the Equation of motion reduces to

$$\ddot{X} = -2a^2 V' \Psi - a^2 V'' X - 2\frac{\dot{a}}{a}\dot{X}. \tag{A2}$$

Using the power law behaviour in τ of V', V'' and a, as well as Equations (5.53) (A1), one finds the particular solution

$$X(\tau) = \frac{\tau}{2}\Psi\,\dot{\varphi}, \tag{A3}$$

as well as two complementary solutions that may be added to obtain the general solution

$$X(\tau) = \frac{\tau}{2}\Psi\,\dot{\varphi} + c_1\,\tau^{-\frac{1}{2}\left(1-\sqrt{1-4a^2\tau^2 V''}\right)} + c_2\,\tau^{-\frac{1}{2}\left(1+\sqrt{1-4a^2\tau^2 V''}\right)}. \tag{A4}$$

The mode proportional to c_2 is at least as rapidly decaying as the one proportional to c_1. Using the explicit form of $4a^2\tau^2 V''$, Equation (A1), we find that $\sqrt{1-4a^2\tau^2 V''}$ is

imaginary if $w_q \in [-\frac{2}{3}(1 + \sqrt{6}), -\frac{2}{3}(1 - \sqrt{6})]$, which holds for all scalar quintessence models of current interest. Hence, the complementary modes decay $\propto 1/\sqrt{\tau}$ in an oscillating manner.

Coming back to the dominating particular solution (A3), Figure 6.1 shows that the accuracy of this analytic result is indeed high at early times, when compared to numerical simulations.

Inserting the solution (A3) and its time derivative into Equation (5.47), we find the simple expression

$$\Delta_q = 3(1 + w_q) \left(\Phi - \frac{1}{2}\Psi \right), \tag{A5}$$

which is just a restatement of eqn. (6.31) and (6.32). Hence, the energy density contrast in tracking quintessence models remains constant on super horizon scales, provided the gravitational potentials are constant to good approximation.

Appendix B

Conventions

Throughout this thesis we use units in which $c = \hbar = 1$. Latin indices denote space dimensions $i = 1..3$ whereas Greek indices run from $\mu = 0..3$. A dot denotes the derivative with respect to time. In Chapter 2 we used normal time (to keep the standard notation used in most textbooks) while in Chapter 5 and following we use conformal time τ.

Symbols and their Meanings

Symbol	
$g_{\mu\nu}$	metric with signature $(-1, +1, +1, +1)$
$M_{\bar{P}}$	reduced Planck mass $(8\pi G)^{-1/2}$
a	cosmic scale factor
t	normal time
τ	conformal time $\mathrm{d}\tau = \mathrm{d}t/a$
w	equation of state ρ/p
Ω_α	fraction of total energy density of species α
H	Hubble's constant $\dot{a}/a$

Table 9.1: Short reference for symbols: general

Symbol	
Ψ, Φ	Bardeen potentials
$\bar{\varphi}$	background quintessence field
χ	quintessence field perturbation
Δ_α	gauge-inv. density contrast of species α
V_α	gauge-invariant velocity of species α
Π	shear
Γ	entropy perturbation
$\tilde{V}$	reduced velocity: $\tilde{V} = x^{-1}V$
$\tilde{\Pi}$	reduced shear: $\tilde{\Pi} = x^{-2}\Pi$

Table 9.2: Short reference for symbols: Chapter 5

Symbol	
η	baryon to photon ratio
Y_{He}	helium abundance in terms of mass fraction
Y_{d}	deuterium abundance in terms of mass fraction
Y_{t}	tritium abundance in terms of mass fraction
Y_3	^{3}He abundance in terms of mass fraction
τ_n	neutron lifetime
Q	proton neutron mass difference
B_d	deuterium binding energy
m_u	mass of the up quark
m_d	mass of the down quark
m_q	$(m_u + m_d)/2$
Δm	$m_d - m_u$

Table 9.3: Short reference for symbols: Chapter 8

Bibliography

[1] Albert Einstein. The formal foundation of the general theory of relativity. *Sitzungsber. Preuss. Akad. Wiss. Berlin (Math. Phys.)*, 1914:1030–1085, 1914.

[2] Albert Einstein. The field equations of gravitation. *Sitzungsber. Preuss. Akad. Wiss. Berlin (Math. Phys.)*, 1915:844–847, 1915.

[3] Albert Einstein. Cosmological considerations in the general theory of relativity. *Sitzungsber. Preuss. Akad. Wiss. Berlin (Math. Phys.)*, 1917:142–152, 1917.

[4] Arno A. Penzias and Robert Woodrow Wilson. A measurement of excess antenna temperature at 4080-mc/s. *Astrophys. J.*, 142:419–421, 1965.

[5] Alan H. Guth. The inflationary universe: A possible solution to the horizon and flatness problems. *Phys. Rev.*, D23:347–356, 1981.

[6] K. Sato. First order phase transition of a vacuum and expansion of the universe. *Mon. Not. Roy. Astron. Soc.*, 195:467–479, 1981.

[7] Andrei D. Linde. A new inflationary universe scenario: A possible solution of the horizon, flatness, homogeneity, isotropy and primordial monopole problems. *Phys. Lett.*, B108:389–393, 1982.

[8] C. Wetterich. Cosmology and the fate of dilatation symmetry. *Nucl. Phys.*, B302:668, 1988.

[9] Bharat Ratra and P. J. E. Peebles. Cosmological consequences of a rolling homogeneous scalar field. *Phys. Rev.*, D37:3406, 1988.

[10] F. Zwicky. Spectral displacement of extra galactic nebulae. *Helv. Phys. Acta*, 6:110, 1933.

[11] Massimo Persic, Paolo Salucci, and Fulvio Stel. The universal rotation curve of spiral galaxies: 1. the dark matter connection. *Mon. Not. Roy. Astron. Soc.*, 281:27, 1996, astro-ph/9506004.

[12] C. Alcock et al. The macho project: Microlensing results from 5.7 years of lmc observations. *Astrophys. J.*, 542:281–307, 2000, astro-ph/0001272.

[13] C. Afonso et al. Limits on galactic dark matter with 5 years of eros smc data. *Astron. Astrophys.*, 400:951–956, 2003, astro-ph/0212176.

[14] Eduard Masso. Axions and axion-like particles. *Nucl. Phys. Proc. Suppl.*, 114:67–73, 2003, hep-ph/0209132.

[15] Arnd Brandenburg and Frank Daniel Steffen. Axino dark matter from thermal production. 2004, hep-ph/0405158.

[16] R. Bernabei et al. Dark matter search. *Riv. Nuovo Cim.*, 26N1:1–73, 2003, astro-ph/0307403.

[17] D. S. Akerib et al. First results from the cryogenic dark matter search in the soudan underground lab. 2004, astro-ph/0405033.

[18] A. Benoit et al. Improved exclusion limits from the edelweiss wimp search. *Phys. Lett.*, B545:43–49, 2002, astro-ph/0206271.

[19] Adam G. Riess et al. Type ia supernova discoveries at z¿1 from the hubble space telescope: Evidence for past deceleration and constraints on dark energy evolution. 2004, astro-ph/0402512.

[20] A. Vilenkin. Cosmic strings and other topological defects. In *Kyoto 1985, Proceedings, Quantum Gravity and Cosmology*, 269-302.

[21] Richard A. Battye, Martin Bucher, and David Spergel. Domain wall dominated universes. 1999, astro-ph/9908047.

[22] C. Brans and R. H. Dicke. Mach's principle and a relativistic theory of gravitation. *Phys. Rev.*, 124:925–935, 1961.

[23] L. Perivolaropoulos. Equation of state of oscillating brans-dicke scalar and extra dimensions. *Phys. Rev.*, D67:123516, 2003, hep-ph/0301237.

[24] Ivaylo Zlatev, Li-Min Wang, and Paul J. Steinhardt. Quintessence, cosmic coincidence, and the cosmological constant. *Phys. Rev. Lett.*, 82:896–899, 1999, astro-ph/9807002.

[25] Paul J. Steinhardt, Li-Min Wang, and Ivaylo Zlatev. Cosmological tracking solutions. *Phys. Rev.*, D59:123504, 1999, astro-ph/9812313.

[26] Christof Wetterich. The cosmon model for an asymptotically vanishing time dependent cosmological 'constant'. *Astron. Astrophys.*, 301:321–328, 1995, hep-th/9408025.

[27] Varun Sahni and Li-Min Wang. A new class of cosmological quintessence models. *Phys. Rev.*, D62:103517, 2000, astro-ph/9910097.

[28] Philippe Brax and Jerome Martin. Quintessence and supergravity. *Phys. Lett.*, B468:40–45, 1999, astro-ph/9905040.

[29] T. Barreiro, Edmund J. Copeland, and N. J. Nunes. Quintessence arising from exponential potentials. *Phys. Rev.*, D61:127301, 2000, astro-ph/9910214.

[30] Edmund J. Copeland, N. J. Nunes, and F. Rosati. Quintessence models in supergravity. *Phys. Rev.*, D62:123503, 2000, hep-ph/0005222.

[31] Andreas Albrecht and Constantinos Skordis. Phenomenology of a realistic accelerating universe using only planck-scale physics. *Phys. Rev. Lett.*, 84:2076–2079, 2000, astro-ph/9908085.

[32] Constantinos Skordis and Andreas Albrecht. Planck-scale quintessence and the physics of structure formation. *Phys. Rev.*, D66:043523, 2002, astro-ph/0012195.

[33] S. C. C. Ng, N. J. Nunes, and F. Rosati. Applications of scalar attractor solutions to cosmology. *Phys. Rev.*, D64:083510, 2001, astro-ph/0107321.

[34] A. Hebecker and C. Wetterich. Natural quintessence? *Phys. Lett.*, B497:281–288, 2001, hep-ph/0008205.

[35] Christof Wetterich. Probing quintessence with time variation of couplings. *JCAP*, 0310:002, 2003, hep-ph/0203266.

[36] C. Wetterich. Crossover quintessence and cosmological history of fundamental 'constants'. *Phys. Lett.*, B561:10–16, 2003, hep-ph/0301261.

[37] Luca Amendola. Coupled quintessence. *Phys. Rev.*, D62:043511, 2000, astro-ph/9908023.

[38] Michael Doran and Joerg Jaeckel. Loop corrections to scalar quintessence potentials. *Phys. Rev.*, D66:043519, 2002, astro-ph/0203018.

[39] C. Armendariz-Picon, V. Mukhanov, and Paul J. Steinhardt. Essentials of k-essence. *Phys. Rev.*, D63:103510, 2001, astro-ph/0006373.

[40] Theodor Kaluza. Zum unitätsproblem der physik. *Sitzungsber. Preuss. Akad. Wiss. Berlin (Math. Phys.)*, K1:966, 1921.

[41] David Langlois. Brane cosmology: An introduction. *Prog. Theor. Phys. Suppl.*, 148:181–212, 2003, hep-th/0209261.

[42] Philippe Brax, Carsten van de Bruck, and Anne-Christine Davis. Brane world cosmology. 2004, hep-th/0404011.

[43] Alexander Yu. Kamenshchik, Ugo Moschella, and Vincent Pasquier. An alternative to quintessence. *Phys. Lett.*, B511:265–268, 2001, gr-qc/0103004.

[44] R. R. Caldwell. A phantom menace? *Phys. Lett.*, B545:23–29, 2002, astro-ph/9908168.

[45] G. F. Smoot et al. Structure in the cobe dmr first year maps. *Astrophys. J.*, 396:L1–L5, 1992.

[46] A. Balbi et al. Constraints on cosmological parameters from maxima-1. *Astrophys. J.*, 545:L1–L4, 2000, astro-ph/0005124.

[47] C. Pryke et al. Cosmological parameter extraction from the first season of observations with dasi. *Astrophys. J.*, 568:46–51, 2002, astro-ph/0104490.

[48] P. de Bernardis et al. A flat universe from high-resolution maps of the cosmic microwave background radiation. *Nature*, 404:955–959, 2000, astro-ph/0004404.

[49] C. L. Bennett et al. First year wilkinson microwave anisotropy probe (wmap) observations: Preliminary maps and basic results. *Astrophys. J. Suppl.*, 148:1, 2003, astro-ph/0302207.

[50] D. N. Spergel et al. First year wilkinson microwave anisotropy probe (wmap) observations: Determination of cosmological parameters. *Astrophys. J. Suppl.*, 148:175, 2003, astro-ph/0302209.

[51] Wayne Hu, Naoshi Sugiyama, and Joseph Silk. The physics of microwave background anisotropies. *Nature*, 386:37–43, 1997, astro-ph/9604166.

[52] Wayne Hu. Concepts in cmb anisotropy formation. *Lect. Notes Phys.*, 470:207, 1996, astro-ph/9511130.

[53] Ruth Durrer. The theory of cmb anisotropies. *J. Phys. Stud.*, 5:177–215, 2001, astro-ph/0109522.

[54] R. K. Sachs and A. M. Wolfe. Perturbations of a cosmological model and angular variations of the microwave background. *Astrophys. J.*, 147:73–90, 1967.

[55] R. A. Sunyaev and Ya. B. Zeldovich. The velocity of clusters of galaxies relative to the microwave background. the possibility of its measurement. *Mon. Not. Roy. Astron. Soc.*, 190:413–420, 1980.

[56] Marc Kamionkowski and Abraham Loeb. Getting around cosmic variance. *Phys. Rev.*, D56:4511–4513, 1997, astro-ph/9703118.

[57] Jamie Portsmouth. Beating cosmic variance with cmb polarization. 2004, astro-ph/0402173.

[58] A. Kogut et al. Wilkinson microwave anisotropy probe (wmap) first year observations: Te polarization. *Astrophys. J. Suppl.*, 148:161, 2003, astro-ph/0302213.

[59] Tom Theuns et al. Constraints on reionization from the thermal history of the intergalactic medium. *Astrophys. J.*, 567:L103, 2002, astro-ph/0201514.

[60] Steven Furlanetto and Abraham Loeb. Is double reionization physically plausible? 2004, astro-ph/0409656.

[61] Chao-lin Kuo et al. High resolution observations of the cmb power spectrum with acbar. *Astrophys. J.*, 600:32–51, 2004, astro-ph/0212289.

[62] B. S. Mason et al. The anisotropy of the microwave background to l = 3500: Deep field observations with the cosmic background imager. *Astrophys. J.*, 591:540–555, 2003, astro-ph/0205384.

[63] T. J. Pearson et al. The anisotropy of the microwave background to l = 3500: Mosaic observations with the cosmic background imager. *Astrophys. J.*, 591:556–574, 2003, astro-ph/0205388.

[64] Clive Dickinson et al. High sensitivity measurements of the cmb power spectrum with the extended very small array. 2004, astro-ph/0402498.

[65] Rafael Rebolo et al. Cosmological parameter estimation using very small array data out to l=1500. 2004, astro-ph/0402466.

[66] C. Barnes et al. First year wilkinson microwave anisotropy probe (wmap) observations: Galactic signal contamination from sidelobe pickup. *Astrophys. J. Suppl.*, 148:51, 2003, astro-ph/0302215.

[67] C. Bennett et al. First year wilkinson microwave anisotropy probe (wmap) observations: Foreground emission. *Astrophys. J. Suppl.*, 148:97, 2003, astro-ph/0302208.

[68] Will J. Percival et al. The 2df galaxy redshift survey: The power spectrum and the matter content of the universe. *Mon. Not. Roy. Astron. Soc.*, 327:1297, 2001, astro-ph/0105252.

[69] Rupert A. C. Croft et al. Towards a precise measurement of matter clustering: Lyman- alpha forest data at redshifts 2-4. *Astrophys. J.*, 581:20–52, 2002, astro-ph/0012324.

[70] Nickolay Y. Gnedin and Andrew J. S. Hamilton. Matter power spectrum from the lyman-alpha forest: Myth or reality? 2001, astro-ph/0111194.

[71] G. Franco, Pablo Fosalba, and J. A. Tauber. Systematic effects in the measurement of polarization by the planck telescope. *Astron. Astrophys.*, 405:349–366, 2003, astro-ph/0210109.

[72] A. C. Taylor et al. Clover: A new instrument for measuring the b-mode polarization of the cmb. 2004, astro-ph/0407148.

[73] N. Mandolesi, M. Bersanelli, C. Burigana, and F. Villa. The planck low frequency instrument. *AIP Conf. Proc.*, 616:193–201, 2002, astro-ph/9904135.

[74] Gianfranco De Zotti et al. The planck surveyor mission: Astrophysical prospects. 1998, astro-ph/9902103.

[75] Matthew Colless et al. The 2df galaxy redshift survey: Final data release. 2003, astro-ph/0306581.

[76] Kevork Abazajian et al. The first data release of the sloan digital sky survey. *Astron. J.*, 126:2081, 2003, astro-ph/0305492.

[77] Max Tegmark et al. The 3d power spectrum of galaxies from the sdss. *Astrophys. J.*, 606:702–740, 2004, astro-ph/0310725.

[78] Nick Kaiser and Gordon Squires. Mapping the dark matter with weak gravitational lensing. *Astrophys. J.*, 404:441–450, 1993.

[79] Matthias Bartelmann and Peter Schneider. Weak gravitational lensing. 1999, astro-ph/9912508.

[80] Henk Hoekstra, Howard Yee, and Mike Gladders. Constraints on ω_m and σ_8 from weak lensing in rcs fields. *Astrophys. J.*, 577:595–603, 2002, astro-ph/0204295.

[81] Andy N. Taylor et al. Mapping the 3-d dark matter with weak lensing in combo-17. 2004, astro-ph/0402095.

[82] Volker Springel, Naoki Yoshida, and Simon D. M. White. Gadget: A code for collisionless and gasdynamical cosmological simulations. 2000, astro-ph/0003162.

[83] Matias Zaldarriaga, Roman Scoccimarro, and Lam Hui. Inferring the linear power spectrum from the lyman-alpha forest. *Astrophys. J.*, 590:1–7, 2003, astro-ph/0111230.

[84] Patrick McDonald et al. The lyman-alpha forest power spectrum from the sloan digital sky survey. 2004, astro-ph/0405013.

[85] T. S. Kim, M. Viel, M. G. Haehnelt, R. F. Carswell, and S. Cristiani. The power spectrum of the flux distribution in the lyman- alpha forest of a large sample of uves qso absorption spectra (luqas). *Mon. Not. Roy. Astron. Soc.*, 347:355, 2004, astro-ph/0308103.

[86] Y. I. Izotov and T. X. Thuan. Systematic effects and a new determination of the primordial abundance of 4he and dy/dz from observations of blue compact galaxies. *Astrophys. J.*, 602:200–230, 2004, astro-ph/0310421.

[87] Edward W. Kolb, Sabino Matarrese, Alessio Notari, and Antonio Riotto. The effect of inhomogeneities on the expansion rate of the universe. 2004, hep-ph/0409038.

[88] Chung-Pei Ma and Edmund Bertschinger. Cosmological perturbation theory in the synchronous and conformal newtonian gauges. *Astrophys. J.*, 455:7–25, 1995, astro-ph/9506072.

[89] James M. Bardeen. Gauge invariant cosmological perturbations. *Phys. Rev.*, D22:1882–1905, 1980.

[90] Hideo Kodama and Misao Sasaki. Cosmological perturbation theory. *Prog. Theor. Phys. Suppl.*, 78:1–166, 1984.

[91] V. F. Mukhanov, H. A. Feldman, and Robert H. Brandenberger. Theory of cosmological perturbations. part 1. classical perturbations. part 2. quantum theory of perturbations. part 3. extensions. *Phys. Rept.*, 215:203–333, 1992.

[92] Michael Doran. Cmbeasy:: an object oriented code for the cosmic microwave background. 2003, astro-ph/0302138.

[93] R. Durrer. *Fund. Cosmic Phys.*, 15:209, 1994.

[94] P. J. E. Peebles and J. T. Yu. Primeval adiabatic perturbation in an expanding universe. *Astrophys. J.*, 162:815–836, 1970.

[95] V. F. Mukhanov and G. V. Chibisov. Quantum fluctuation and 'nonsingular' universe. (in russian). *JETP Lett.*, 33:532–535, 1981.

[96] James M. Bardeen, Paul J. Steinhardt, and Michael S. Turner. Spontaneous creation of almost scale - free density perturbations in an inflationary universe. *Phys. Rev.*, D28:679, 1983.

[97] A. R. Liddle and D. H. Lyth. Cosmological inflation and large-scale structure. Cambridge, UK: Univ. Pr. (2000) 400 p.

[98] David H. Lyth, Carlo Ungarelli, and David Wands. The primordial density perturbation in the curvaton scenario. *Phys. Rev.*, D67:023503, 2003, astro-ph/0208055.

[99] N Bartolo and Andrew R Liddle. The simplest curvaton model. *Phys. Rev.*, D65:121301, 2002, astro-ph/0203076.

[100] R. R. Caldwell, Rahul Dave, and Paul J. Steinhardt. Cosmological imprint of an energy component with general equation-of-state. *Phys. Rev. Lett.*, 80:1582–1585, 1998, astro-ph/9708069.

[101] Pedro T. P. Viana and Andrew R. Liddle. Perturbation evolution in cosmologies with a decaying cosmological constant. *Phys. Rev.*, D57:674–684, 1998, astro-ph/9708247.

[102] Rahul Dave, R. R. Caldwell, and Paul J. Steinhardt. Sensitivity of the cosmic microwave background anisotropy to initial conditions in quintessence cosmology. *Phys. Rev.*, D66:023516, 2002, astro-ph/0206372.

[103] Michael Malquarti and Andrew R. Liddle. Evolution of large-scale perturbations in quintessence models. *Phys. Rev.*, D66:123506, 2002, astro-ph/0208562.

[104] L. R. W. Abramo and F. Finelli. Attractors and isocurvature perturbations in quintessence models. *Phys. Rev.*, D64:083513, 2001, astro-ph/0101014.

[105] Masahiro Kawasaki, Takeo Moroi, and Tomo Takahashi. Isocurvature fluctuations in tracker quintessence models. *Phys. Lett.*, B533:294–301, 2002, astro-ph/0108081.

[106] Francesca Perrotta and Carlo Baccigalupi. Early time perturbations behaviour in scalar field cosmologies. *Phys. Rev.*, D59:123508, 1999, astro-ph/9811156.

[107] Robert R. Caldwell, Michael Doran, Christian M. Mueller, Gregor Schaefer, and Christof Wetterich. Early quintessence in light of wmap. *Astrophys. J.*, 591:L75–L78, 2003, astro-ph/0302505.

[108] Anton K. Rebhan and Dominik J. Schwarz. Kinetic versus thermal field theory approach to cosmological perturbations. *Phys. Rev.*, D50:2541–2559, 1994, gr-qc/9403032.

[109] David Wands, Karim A. Malik, David H. Lyth, and Andrew R. Liddle. A new approach to the evolution of cosmological perturbations on large scales. *Phys. Rev.*, D62:043527, 2000, astro-ph/0003278.

[110] Jerome Martin and Dominik J. Schwarz. The influence of cosmological transitions on the evolution of density perturbations. *Phys. Rev.*, D57:3302–3316, 1998, gr-qc/9704049.

[111] Kari Enqvist, Hannu Kurki-Suonio, and Jussi Valiviita. Limits on isocurvature fluctuations from boomerang and maxima. *Phys. Rev.*, D62:103003, 2000, astro-ph/0006429.

[112] Roberto Trotta, A. Riazuelo, and R. Durrer. The cosmological constant and general isocurvature initial conditions. *Phys. Rev.*, D67:063520, 2003, astro-ph/0211600.

[113] Christopher Gordon and Antony Lewis. Observational constraints on the curvaton model of inflation. *Phys. Rev.*, D67:123513, 2003, astro-ph/0212248.

[114] Uros Seljak and Matias Zaldarriaga. A line of sight approach to cosmic microwave background anisotropies. *Astrophys. J.*, 469:437–444, 1996, astro-ph/9603033.

[115] Martin Bucher, Kavilan Moodley, and Neil Turok. Constraining isocurvature perturbations with cmb polarization. *Phys. Rev. Lett.*, 87:191301, 2001, astro-ph/0012141.

[116] David Langlois and Alain Riazuelo. Correlated mixtures of adiabatic and isocurvature cosmological perturbations. *Phys. Rev.*, D62:043504, 2000, astro-ph/9912497.

[117] Luca Amendola, Christopher Gordon, David Wands, and Misao Sasaki. Correlated perturbations from inflation and the cosmic microwave background. *Phys. Rev. Lett.*, 88:211302, 2002, astro-ph/0107089.

[118] G. Hinshaw et al. First year wilkinson microwave anisotropy probe (wmap) observations: Angular power spectrum. *Astrophys. J. Suppl.*, 148:135, 2003, astro-ph/0302217.

[119] L. Verde et al. First year wilkinson microwave anisotropy probe (wmap) observations: Parameter estimation methodology. *Astrophys. J. Suppl.*, 148:195, 2003, astro-ph/0302218.

[120] L. Page et al. First year wilkinson microwave anisotropy probe (wmap) observations: Interpretation of the tt and te angular power spectrum peaks. *Astrophys. J. Suppl.*, 148:233, 2003, astro-ph/0302220.

[121] C. Armendariz-Picon, V. Mukhanov, and Paul J. Steinhardt. A dynamical solution to the problem of a small cosmological constant and late-time cosmic acceleration. *Phys. Rev. Lett.*, 85:4438–4441, 2000, astro-ph/0004134.

[122] C. Wetterich. Cosmology with varying scales and couplings. 2003, hep-ph/0302116.

[123] Christof Wetterich. Conformal fixed point, cosmological constant and quintessence. *Phys. Rev. Lett.*, 90:231302, 2003, hep-th/0210156.

[124] Michael Doran, Jan-Markus Schwindt, and Christof Wetterich. Structure formation and the time dependence of quintessence. *Phys. Rev.*, D64:123520, 2001, astro-ph/0107525.

[125] Pedro G. Ferreira and Michael Joyce. Cosmology with a primordial scaling field. *Phys. Rev.*, D58:023503, 1998, astro-ph/9711102.

[126] Michael Doran, Matthew J. Lilley, Jan Schwindt, and Christof Wetterich. Quintessence and the separation of cmb peaks. *Astrophys. J.*, 559:501–506, 2001, astro-ph/0012139.

[127] Greg Huey, Li-Min Wang, Rahul Dave, R. R. Caldwell, and Paul J. Steinhardt. Resolving the cosmological missing energy problem. *Phys. Rev.*, D59:063005, 1999, astro-ph/9804285.

[128] Saul Perlmutter, Michael S. Turner, and Martin J. White. Constraining dark energy with sne ia and large-scale structure. *Phys. Rev. Lett.*, 83:670–673, 1999, astro-ph/9901052.

[129] Licia Verde et al. The 2df galaxy redshift survey: The bias of galaxies and the density of the universe. *Mon. Not. Roy. Astron. Soc.*, 335:432, 2002, astro-ph/0112161.

[130] J. A. Peacock et al. A measurement of the cosmological mass density from clustering in the 2df galaxy redshift survey. *Nature*, 410:169–173, 2001, astro-ph/0103143.

[131] Wayne Hu, Masataka Fukugita, Matias Zaldarriaga, and Max Tegmark. Cmb observables and their cosmological implications. *Astrophys. J.*, 549:669, 2001, astro-ph/0006436.

[132] Michael Doran and Matthew Lilley. The location of cmb peaks in a universe with dark energy. *Mon. Not. Roy. Astron. Soc.*, 330:965–970, 2002, astro-ph/0104486.

[133] E. L. Wright, C. L. Bennett, K. Gorski, G. Hinshaw, and G. F. Smoot. Angular power spectrum of the microwave background anisotropy seen by the cobe differential microwave radiometer. 1996, astro-ph/9601059.

[134] G. Hinshaw et al. 2-point correlations in the cobe dmr 4-year anisotropy maps. 1996, astro-ph/9601061.

[135] Brian P. Schmidt et al. The high-z supernova search: Measuring cosmic deceleration and global cur vature of the universe using type ia supernovae. *Astrophys. J.*, 507:46–63, 1998, astro-ph/9805200.

[136] Adam G. Riess et al. Observational evidence from supernovae for an accelerating universe and a cosmological constant. *Astron. J.*, 116:1009–1038, 1998, astro-ph/9805201.

[137] Peter M. Garnavich et al. Supernova limits on the cosmic equation of state. *Astrophys. J.*, 509:74–79, 1998, astro-ph/9806396.

[138] S. Perlmutter et al. Measurements of omega and lambda from 42 high-redshift supernovae. *Astrophys. J.*, 517:565–586, 1999, astro-ph/9812133.

[139] Richard H. Cyburt, Brian D. Fields, and Keith A. Olive. Primordial nucleosynthesis in light of wmap. *Phys. Lett.*, B567:227–234, 2003, astro-ph/0302431.

[140] Brian D. Fields and Keith A. Olive. On the evolution of helium in blue compact galaxies. 1998, astro-ph/9803297.

[141] John K. Webb, Victor V. Flambaum, Christopher W. Churchill, Michael J. Drinkwater, and John D. Barrow. Evidence for time variation of the fine structure constant. *Phys. Rev. Lett.*, 82:884–887, 1999, astro-ph/9803165.

[142] Alexander I. Shlyakhter. Direct test of the time-independence of fundamental nuclear constants using the oklo natural reactor. 1982, physics/0307023.

[143] Thibault Damour and Freeman Dyson. The oklo bound on the time variation of the fine-structure constant revisited. *Nucl. Phys.*, B480:37–54, 1996, hep-ph/9606486.

[144] Yasunori Fujii and Akira Iwamoto. Re/os constraint on the time-variability of the fine- structure constant. *Phys. Rev. Lett.*, 91:261101, 2003, hep-ph/0309087.

[145] Raghunathan Srianand, Hum Chand, Patrick Petitjean, and Bastien Aracil. Limits on the time variation of the electromagnetic fine- structure constant in the low energy limit from absorption lines in the spectra of distant quasars. *Phys. Rev. Lett.*, 92:121302, 2004, astro-ph/0402177.

[146] Hum Chand, Raghunathan Srianand, Patrick Petitjean, and Bastien Aracil. Probing the cosmological variation of the fine-structure constant: Results based on vlt-uves sample. *Astron. Astrophys.*, 417:853, 2004, astro-ph/0401094.

[147] Ralf Quast, Dieter Reimers, and Sergei A. Levshakov. Probing the variability of the fine-structure constant with the vlt uves. 2003, astro-ph/0311280.

[148] John N. Bahcall, Charles L. Steinhardt, and David Schlegel. Does the fine-structure constant vary with cosmological epoch? *Astrophys. J.*, 600:520, 2004, astro-ph/0301507.

[149] Rahim Esmailzadeh, Glenn D. Starkman, and Savas Dimopoulos. Primordial nucleosynthesis without a computer. *Astrophys. J.*, 378:504–512, 1991. CFPA-TH-90-023.

[150] S. Weinberg. Gravitation and cosmology. 1972. New York, USA: John Wiley and Sons.

[151] Michael S. Smith, Lawrence H. Kawano, and Robert A. Malaney. Experimental, computational, and observational analysis of primordial nucleosynthesis. *Astrophys. J. Suppl.*, 85:219–247, 1993.

[152] E. W. Kolb and Michael S. Turner. The early universe. Redwood City, USA: Addison-Wesley (1990) 547 p. (Frontiers in physics, 69).

[153] L. Bergstrom, S. Iguri, and H. Rubinstein. Constraints on the variation of the fine structure constant from big bang nucleosynthesis. *Phys. Rev.*, D60:045005, 1999, astro-ph/9902157.

[154] Kenneth M. Nollett and Robert E. Lopez. Primordial nucleosynthesis with a varying fine structure constant: An improved estimate. *Phys. Rev.*, D66:063507, 2002, astro-ph/0204325.

[155] C. Angulo. A compilation of charged-particle induced thermonuclear reaction rates. *Nucl. Phys. A*, 656, 1999.

[156] Richard H. Cyburt, Brian D. Fields, and Keith A. Olive. The nacre thermonuclear reaction compilation and big bang nucleosynthesis. *New Astron.*, 6:215–238, 2001, astro-ph/0102179.

[157] J. Gasser and H. Leutwyler. Quark masses. *Phys. Rept.*, 87:77–169, 1982.

[158] B. S. Pudliner, V. R. Pandharipande, J. Carlson, Steven C. Pieper, and R. B. Wiringa. Quantum monte carlo calculations of nuclei with $a \leq 7$. *Phys. Rev.*, C56:1720–1750, 1997, nucl-th/9705009.

[159] Jerry Jaiyul Yoo and Robert J. Scherrer. Big bang nucleosynthesis and cosmic microwave background constraints on the time variation of the higgs vacuum expectation value. *Phys. Rev.*, D67:043517, 2003, astro-ph/0211545.

[160] C. Wetterich. Cosmologies with variable newton's 'constant'. *Nucl. Phys.*, B302:645, 1988.

[161] Michael Doran, Christian M. Muller, Gregor Schafer, and Christof Wetterich. Gauge-invariant initial conditions and early time perturbations in quintessence universes. *Phys. Rev.*, D68:063505, 2003, astro-ph/0304212.

[162] Christian M. Mueller, Gregor Schaefer, and Christof Wetterich. Nucleosynthesis and the variation of fundamental couplings. 2004, astro-ph/0405373.